UNIVERSIDAD DE CÓRDOBA

Programa de doctorado: Química Fina

Título de la tesis (español e inglés):

Perspectivas Estructurales y Valorización de las Huminas: Un Enfoque Catalítico

/

Structural Insights and Valorization of Humins: A Catalytic Approach

Directores: Rafael Luque, Alina M. Balu, Ed de Jong

Autor de la tesis: Layla Filiciotto

Fecha de depósito tesis en el Idep: 27 Septiembre de 2019

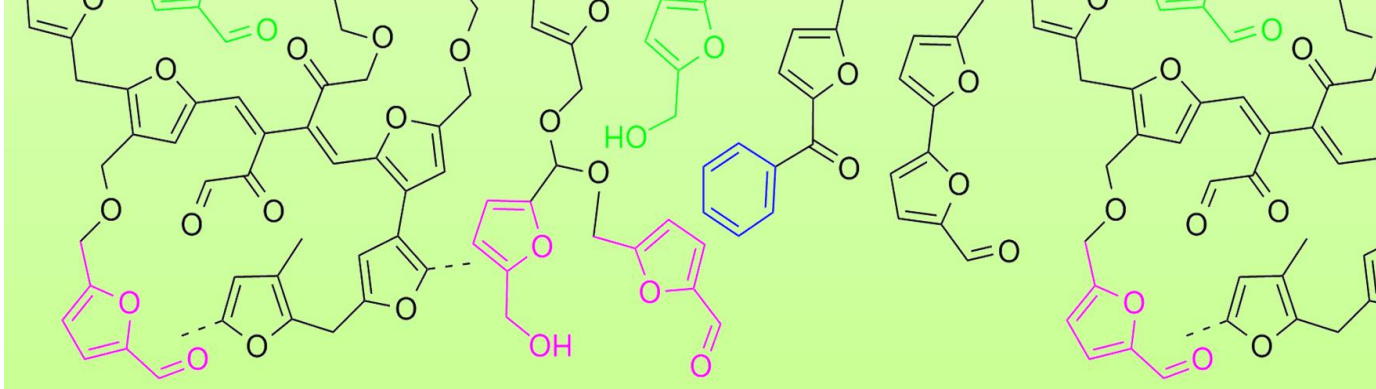TITULO: *Structural Insights and Valorization of Humins: A Catalytic Approach*

AUTOR: *Layla Filiciotto*

Structural Insights and Valorization of Humins: A Catalytic Approach.

Perspectivas Estructurales y Valorización de las Huminas: Un Enfoque Catalítico

Layla Filiciotto

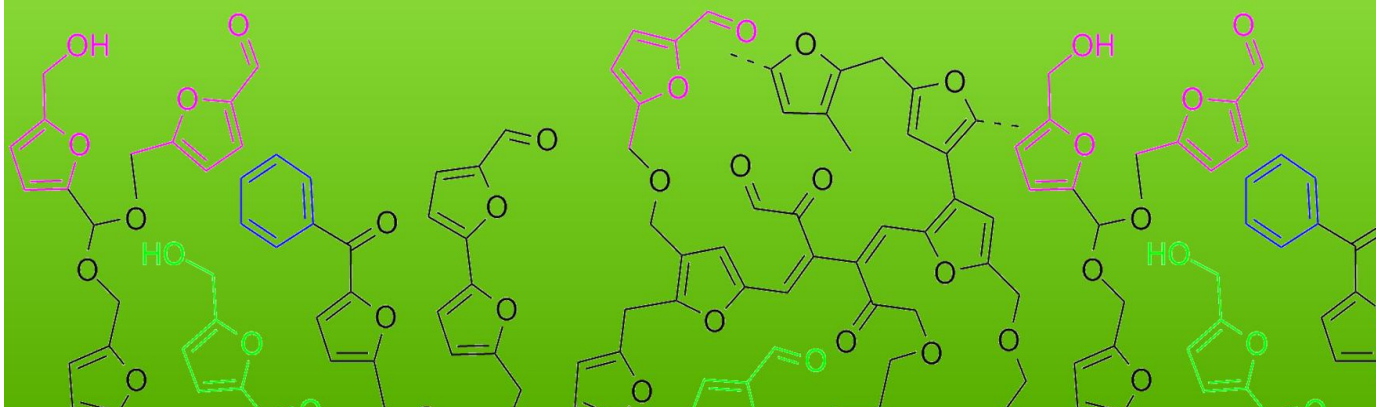*PhD Thesis*

Universidad de Córdoba

Structural Insights and Valorization of Humins:
A Catalytic Approach.

Perspectivas Estructurales y Valorización de las Huminas:
Un Enfoque Catalítico

Layla Filiciotto, PhD Thesis

Supervirsors

Rafael Luque
Álvarez de
Sotomayor

Alina M. Balu
Balu

Ed de Jong

To those who imperfectly make the world perfect,

To my family,

"[When combustion occurs,] one body, at least, is oxygenated, and another restored, at the same time, to its combustible state... This view of combustion may serve to show how nature is always the same, and maintains her equilibrium by preserving the same quantities of air and water on the surface of our globe: for as fast as these are consumed in the various processes of combustion, equal quantities are formed, and rise regenerated like the Phoenix from her ashes."

Elizabeth Fulhame on the first evidences of catalysis

"An essay on combustion with a view to a new art of dyeing and painting. Wherein the phlogistic and antiphlogistic hypotheses are proven erroneous"

Printed for the author by J. Cooper, London, 1794.

MSCA ID: 675325

TÍTULO DE LA TESIS: Perspectivas Estructurales y Valorización de las Huminas: Un Enfoque Catalítico

DOCTORANDA: Layla Filiciotto

INFORME RAZONADO DEL/DE LOS DIRECTOR/ES DE LA TESIS
(se hará mención a la evolución y desarrollo de la tesis, así como a trabajos y publicaciones derivados de la misma).

Los objetivos de la tesis están relacionados con la valorización por vías catalíticas de subproductos de biorefinería, las huminas. En particular, se han desarrollado la descomposición de las huminas a moléculas de alto valor añadido y la utilización de las mismas como material catalítico. Layla abordó el trabajo de tesis con gran entusiasmo, estudiando diferentes aspectos de las huminas, algunos no incluidos en esta tesis. En totalidad, el trabajo de tesis ofrece técnicas innovadoras en el entendimiento y la valorización de estos biocompuestos no bien conocidos.

En primer lugar, estudiando la solubilidad de las huminas en diferentes disolventes, se observaron una serie de propiedades de fluorescencia de las huminas que han sido investigadas en colaboración con el Departamento de Química Física de la Universidad de Córdoba. Estos resultados muestran la complejidad estructural de las huminas así como su potencial en varias aplicaciones prácticas de fluorescencia. Esta parte del trabajo se publicó en *Chem. Commun.* **2017**, *53*, 7015 7017.

Sucesivamente, Layla abordó la descomposición de las huminas mediante varias metodologías (en *batch*, flujo continuo, bajo irradiación asistida por microondas) con la intención de obtener productos de alto valor añadido, como por ejemplo el nombrado compuesto plataforma, 5 hidroximetilfurfural. Al observar que se obtuvieron un sinfin de productos con difícil separación, el trabajo fue visto como una nueva técnica de identificación estructural. De este modo, existe una tendencia consistente en las diferentes clases de productos independientemente de la técnica de descomposición aplicada, sugiriendo que las huminas se forman por diferentes reacciones paralelas de compuestos de partida y (sub)productos de la conversión catalizada por

ácidos de bio-azúcares. Estos hallazgos han sido publicados en *Mol. Catal.* **2019**, *479*, 110564.

Finalmente, con los conocimientos adquiridos sobre las huminas desde el punto de vista estructural y de mecanismo, Layla ha investigado el empleo de las huminas como materiales catalíticos. En particular, combinando las huminas con óxidos de hierro, se han sintetizado catalizadores activos en reacciones de oxidación selectiva en presencia de peróxido de hidrogeno. Este trabajo muestra como las huminas se pueden emplear como fuente de carbono para la producción de nanohíbridos órganicos-inorgánicos activos en reacciones de oxidación selectiva. El resultado del trabajo fue publicado en *Green Chem.* **2017**, *19*, 4423-4434.

En total, Layla ha generado 6 publicaciones de primer autor incluyendo artículos de revisión y capítulos de libro en varios campos (biomasa, nanocatálisis, química verde/sostenible). Conjuntamente, Layla ha asistido a 12 conferencias (8 internacionales) donde ha ganado el premio al mejor poster en la conferencia internacional sobre la química verde (ISGC) en Francia. También, Layla ha participado en 3 actividades de divulgación científica y más de 20 cursos, actividades y seminarios profesionales.

En general, Layla ha demostrado grandes capacidades en varios campos profesionales. Layla ha ganado experiencia industrial relevante realizando una estancia de 18 meses (no seguidos) en el Departamento de Química Renovable de la empresa de desarrollo tecnológico, Avantium (Amsterdam, Países Bajos). Layla ha también ayudado a mejorar la seguridad y sostenibilidad en los laboratorios con pequeñas iniciativas (por ejemplo, poner límites máximos de apertura de las campanas extractoras) y contribuyendo activamente a obtener el certificado de nivel 2 del programa Trébol del Servicio de Protección Ambiental (SEPA) de la Universidad de Córdoba al grupo FQM-383. Además, Layla ha iniciado reuniones de intercambio de ideas en el grupo de investigación (BrainSesh).

Por todo ello, se autoriza la presentación de la tesis doctoral.

Córdoba, 25 de Septiembre de 2019

Firma de los directores

Fdo.:Rafael Luque   Fdo.: Alina M. Balu   Fdo.: Ed de Jong

Mediante la defensa de esta memoria se pretende optar a la mención de "Doctorado Internacional", habida cuenta que el doctorando reúne los requisitos exigidos por dicha mención:

- Se cuenta con los informes favorables de dos doctores expertos internacionales, con experiencia investigadora acreditada, pertenecientes a instituciones de educación o de investigación extranjeras.

- Existe un miembro en el Tribunal, que ha de evaluar la Tesis, perteneciente a una institución de educación superior o instituto de investigación del extranjero.

- Parte de la redacción y defensa de esta Memoria se realizará en una de las lenguas habituales para la comunicación científica y distinta a cualquiera de las lenguas oficiales en España.

- El doctorando ha realizado una estancia de investigación en la empresa holandesa Avantium Chemicals B.V. con objeto de obtener el Doctorado con Mención Internacional, concedido por la Universidad de Córdoba.

Además, debido a la estancia de investigación en la empresa Avantium de 18 meses obligatoria por el proyecto Europeo MSCA-ITN-EID-675325 se pretende optar a la mención de "Doctorado Industrial"

Table of Contents

Summary

In the framework of an industrial European doctorate (*MSCA-ITN-EID-675325*), the work described in this thesis was aimed to improve the sustainability of the chemical industry by implementing a circular economy in biomass conversion processes, particularly by gaining deeper knowledge on the formation of the so-called *humin by-products* and their applications e.g. as advanced catalytic systems.

The dark color of humin by-products indicates a strong absorption of visible light which could arise from overlapping of emitting species in the electromagnetic spectrum given by conjugated π bonds within the furanic network. In fact, by applying fluorescence spectroscopy to a solution of humins in acetonitrile (**Chapter 2**), three different fluorophores (one in the UV spectrum and two in the visible region) were identified. This result suggests the presence of three species of different structural complexity, depending on the length of the conjugated system. Since isolated fluorophores can find various applications (i.e. bioimaging or organic light-emitting diodes), simple biphasic solvent extractions were carried out on the humins solution. A pentane and water mixture was able to separate the UV-emitting fluorophore (organic fraction) from the two visible-emitting fluorophores (aqueous fraction). A small shift from 330 to 375 nm of the emission band was observed for the short-wavelength fluorophore (organic fraction), indicating a polarity-dependent deactivation process. Thus, careful solvent choice is needed to maximize the fluorescent properties of humins. Time-resolved fluorescence spectroscopy was then applied to further confirm the presence of three distinctive emitting species. Lifetimes

of *ca.* 2 ns were observed for the three species, comparable to common fluorescent probes. In the case of the long wavelength emitting fluorophore (530 nm) a bi-exponential fitting was required, hinting at the presence of different polymeric chain lengths within the same emission band. Overall, this study shows that humins are comprised of a broad molecular weigth distribution, indicating a certain structural complexity which could lead to variations during valorization processes. Nonetheless, separation of the different macromolecules can be achieved with biphasic solvent systems, if a narrow molecular weight distribution is required.

Generally, humins are considered to be derived from condensation reactions between HMF and/or sugar molecules in the acid-catalyzed hydrolysis of bio-based compounds. Based on this assumption and solid-state analyses of as-synthesized humins, a furanic-rich structure has been postulated. In **Chapter 3**, a novel approach in structural identification is proposed. By decomposing the humins macromolecules with or without a catalyst in continuous flow under non-acidic conditions, a wide variety of compounds was obtained with consistent reaction products. Independently whether hydrogenation or transfer hydrogenolysis was employed, five major classes of products were identified by GC-MS analyses: sugar-derived molecules, furanics, levulinates, aromatics, and small oxygenated molecules (including organic acids). The concomitant presence of these five classes demonstrates that humins possess a more heterogeneous structure than those present in literature. Interestingly, the presence of aromatics suggests Diels-Alder type of reactivity of the furanic moieties and alkenyl functionalities. By knowing the occurrence of this reactivity, an aromatized system can be imagined for humin by-products upon thermal treatments. In this case, materials similar to graphene oxide

may be anticipated, possessing electron and conduction transfer properties and hence potential catalytic activity.

Compounding the further knowledge acquired on humins during this thesis work, valorization of humins was attempted. As selective conversion of humins to a single product by decomposition may not be feasible with high resource efficiency, seeing humins as potential carbon materials may improve valorization by *i)* reducing molecular weight distribution *via* heat-induced cross-linking of oligomers/macromolecules, and *ii)* aromatization towards a graphene oxide-like material with improved catalytic performances. Addition of metal oxides to humins may lead to a more stable carbon-based catalytic system, due to anchoring through the oxygen functionalities. Thus, in **Chapter 4**, humins were combined with a cheap and environmentally-friendly metal: iron (as a precursor, *i.e.* ferrous chloride or ferric nitrate). Thermally treated humins, *alias* carbon macroporous systems (*i.e.* foams), were also investigated as heat may induce Diels-Alder of furanic moieties and decomposition products of humins, thus leading to a more aromatic carbon material with improved thermal properties. The resulting nanocomposites were tested in the selective oxidation of plant-based isoeugenol to the popular flavoring agent, vanillin. Enhanced catalytic activities were observed for all catalysts with the addition of hydrogen peroxide, gaining vanillin yields up to 57% under microwave irradiation. Compared to humins foams and commercial iron oxides, humins-containing iron oxides performed better under the investigated conditions. This study opens a valorization pathway to humin by-products, finding a potential application as a catalytic material.

Overall, humins present undiscovered potential for use in a variety of applications, such as their utilization as catalytic materials demonstrated herein. Furthermore, their fluorescent properties justify their investigation for other imaging techniques. Exploitation of the reactive oxygen and furanic groups can bring innovative applications ranging from chemistry to materials science. More research is required to find high-end humin-based products, thus improving sustainability as well as the process economics of biomass conversion strategies.

Resumen

En el marco de un doctorado europeo industrial (*MSCA-ITN-EID-675325*), el trabajo descrito en esta tesis tuvo como objetivo mejorar la sostenibilidad de la industria química mediante la implementación de una economía circular en los procesos de conversión de biomasa, particularmente obteniendo un conocimiento más profundo de los subproductos llamados *huminas* y encontrar una aplicación tangible, como en sistemas catalíticos más activos.

El color oscuro de las huminas indica una fuerte absorción de la luz visible que podría surgir de la superposición de especies emisoras en el espectro electromagnético dado por enlaces-π conjugados dentro una estructura furánica. De hecho, al aplicar espectroscopia de fluorescencia a una solución de huminas en acetonitrilo (***Capítulo 2***), se identificaron tres fluoróforos diferentes (uno en el espectro UV y dos en la región visible). Este resultado sugiere la presencia de tres especies de diferente complejidad estructural, dependiendo de la longitud del sistema conjugado. Dado que los fluoróforos aislados pueden encontrar varias aplicaciones, tales como en bioimagen o diodos orgánicos emisores de luz, se llevaron a cabo simples extracciones con disolventes bifásicos en la solución de huminas. Una mezcla de pentano y agua fue capaz de separar el fluoróforo emisor en el UV (fracción orgánica) de los dos fluoróforos emisores en el visible (fracción acuosa). Se observó un pequeño cambio de 330 a 375 nm de la banda de emisión para el fluoróforo de longitud de onda corta (fracción orgánica), lo que indica un proceso de desactivación dependiente de la polaridad. Por lo tanto, se necesita una elección cuidadosa del disolvente para maximizar las propiedades fluorescentes de las huminas. La

espectroscopia de fluorescencia resuelta en el tiempo se empleó sucesivamente para confirmar aún más la presencia de las tres especies emisoras. Tiempos de vida de 2 ns se observaron para las tres especies, comparables a las sondas fluorescentes comunes. En el caso del fluoróforo emisor de longitud de onda larga (530 nm), se requirió un ajuste biexponencial que sugiere la presencia de diferentes longitudes de cadena polimérica dentro de la misma banda de emisión. En general, este estudio muestra que las huminas poseen una amplia distribución de peso molecular, lo que indica una cierta complejidad estructural que podría conducir a variaciones en los procesos de valorización. No obstante, la separación de las diferentes macromoléculas se puede lograr con sistemas de disolventes bifásicos, si se requiere una distribución estrecha de pesos moleculares.

En general, se considera que las huminas derivan de reacciones de condensación entre HMF y/o moléculas de azúcar en la hidrólisis de compuestos de base biológica catalizada por ácidos. Sobre la base de este supuesto y los análisis de estado sólido de la huminas sintetizadas en bibliografía, se ha postulado una estructura rica en furanos. En el ***Capítulo 3,*** se propone un nuevo enfoque en la identificación estructural. En particular, la descomposición de las macromoléculas de huminas en ausencia o presencia de un catalizador (en flujo continuo en condiciones no ácidas) dio lugar a una amplia variedad de compuestos. Independientemente si se emplean procesos de hidrogenación o hidrogenólisis por transferencia, se identificaron cinco clases principales de productos mediante análisis pro cromatografía de gases acoplada a espectrometría de masas (CG-MS): moléculas derivadas de azúcares, furanos, levulinatos, compuestos aromáticos y pequeñas moléculas oxigenadas (incluidos ácidos orgánicos). La

presencia concomitante de estas cinco clases demuestra que las huminas poseen una estructura más heterogénea que las descritas en la bibliografía. Curiosamente, la presencia de compuestos aromáticos sugiere reactividad de tipo Diels-Alder de los grupos furánicos y funcionalidades de tipo alquenilo. Al conocer esta reactividad, se puede imaginar un sistema aromatizado para materiales tipo humina, obtenidos tras tratamientos térmicos a temperaturas moderadas. En este caso, se pueden anticipar materiales similares al óxido de grafeno que poseen propiedades de transferencia de electrones y conducción, por lo tanto actividad catalítica.

Finalmente, y tras entender la estructura de las huminas durante este trabajo de tesis, se intentó la valorización de las huminas. Dado que la conversión selectiva de huminas en un solo producto por descomposición puede no ser factible con una alta eficiencia, ver a las huminas como posibles materiales de carbono puede mejorar la valorización *i)* reduciendo la distribución del peso molecular mediante reticulación de oligómeros/macromoléculas inducida por la temperatura, y *ii)* aromatización hacia un material similar al óxido de grafeno con mejores rendimientos catalíticos. La adición de óxidos metálicos a las huminas puede conducir a un sistema catalítico basado en carbón más estable, debido al anclaje a través de las funcionalidades de oxígeno. Así, en el ***Capítulo 4***, las huminas se combinaron con un metal barato y ecológico: el hierro (como precursor, es decir cloruro ferroso o nitrato férrico). Las huminas tratadas térmicamente, *alias* sistemas macroporosos de carbono (es decir, espumas), también se investigaron, ya que el calor puede inducir reacciones de tipo Diels-Alder de grupos furánicos y productos de descomposición de las huminas, así conduciendo a un material de carbono más aromático con propiedades térmicas

mejoradas. Los nanocompuestos resultantes se comprobaron en la oxidación selectiva de isoeugenol derivado de plantas al agente saborizante popular, la vainillina. Se observaron actividades catalíticas mejoradas para todos los catalizadores con la adición de peróxido de hidrógeno, con rendimientos de vainillina hasta el 57% en reacciones asistidas mediante irradiación por microondas. En comparación con las espumas de huminas y los óxidos de hierro comerciales, los óxidos de hierro que contienen huminas presentaron mejor desempeño catalítico en las condiciones investigadas, encontrando una aplicación potencial como material catalítico.

En general, las huminas presentan un potencial no descubierto para una variedad de aplicaciones, donde aquí demostramos su uso como materiales catalíticos. Además, sus propiedades fluorescentes justifican su investigación para otras tecnicas de bioimagen. La explotación de los grupos reactivos con oxígeno y los furanos puede derivar aplicaciones innovadoras que van desde la catálisis a la ciencia de los materiales. Se necesita más investigación para encontrar productos de alta calidad basados en huminas, así como para mejorar la sostenibilidad y la economía de proceso de las estrategias de conversión de biomasa.

Hypotheses & Objectives

Humin by-products are inevitably formed during the acid-catalyzed hydrolysis of lignocellulosic carbohydrates (both cellulosic and hemicellulosic sugars), *i.e.* the key reaction for the production of bio-based platform chemicals and products (*e.g.* furfural, 5-hydroxymethylfurfural). In order to improve process economics, as well as to establish a circular economy, application development of humins is required. Also, a better understanding of the structure and mechanism of formation of humin by-products will also aid the minimization of such products at the source or the identification of well-suited valorization routes. In this thesis, the structural identification and valorization of humins *via* catalytic pathways will be presented.

Previous studies on humins showed the presence of a conjugated furanic network with oxygenated linkages. Conjugated systems generally possess fluorescence activity which was investigated in **Chapter 2**. In fact, by employing absorbance, emission and excitation spectra of a solution of humins, the structural complexity of these by-products was evidenced. In particular, three distinct fluorophores of different chain length were identified, showing a polydisperse macromolecular network. This project was performed in collaboration with the Physical Chemistry department of the University of Córdoba and finalized with a publication in *Chem. Commun. 2017, 53, 7015-7017*.

The structure of humin by-products has been investigated through a variety of spectroscopic techniques (*e.g.* NMR, IR) on as-synthesized humins. Generally, humins are believed to be derived from aldol condensation, acetalization, or ring-opening hydrolysis reactions with the formation of highly reactive intermediates;

however, up to date state of the art has not clearly identified the governing mechanism of humins formation. In **Chapter 3**, a novel approach in the identification of key molecules and mechanisms involved in the formation of humins is discussed. In particular, by applying (catalytic) hydrogenation and hydrogenolysis reactions on industrial humins, the identification of the decomposition products by GC-MS could hint to the coexistence of different formation mechanisms. Also, the observance of different classes of molecules, *i.e.* starting materials and (by-)products of the acid-catalyzed hydrolysis of sugars, suggests a higher complexity of the humins structure as compared to those previously reported in literature. These findings were published in *Mol. Catal. 2019, 479, 110564.*

Based on the knowledge obtained on the structural complexity of humins, valorization *via* the synthesis of catalytic materials was carried out. Humins are known to possess a variety of oxygen functionalities which may act as anchoring points to metal precursors in the production of nanomaterials. By using abundant and inexpensive precursors, along with *green* procedures (*i.e.* solventless, mechanochemical), humin-containing iron oxides were investigated in **Chapter 4**. Given the presence of expected superficial oxygen functionalities, the nanomaterials were tested in oxidation reactions. In particular, challenging hydrogen peroxide-assisted oxidative cleavage of a lignin-derived molecule isoeugenol to high-end flavoring agent vanillin was carried out. High activity and selectivity (up to 57% yield) in less than 5 minutes of reaction time under microwave irradiation was observed, which was not possible with the sole use of iron oxides. Also, the humin-containing materials showed satisfactory stability when recycled. These findings demonstrate the employability of humin by-products as carbon source for inorganic-organic nanohybrid

materials with improved catalytic performance. The results of this chapter were published in *Green Chem. 2017, 19, 4423-4434.*

Hipótesis y Objetivos

Los subproductos denominados huminas se forman inevitablemente durante la hidrólisis catalizada por ácidos de los carbohidratos lignocelulósicos (azúcares celulósicos y hemicelulósicos), es decir, la reacción clave para la producción de productos químicos de base biológica (por ejemplo, furfural, 5-hidroximetilfurfural). Para mejorar la economía del proceso, así como para establecer una economía circular, se requiere el desarrollo de aplicaciones para las huminas. Además, una mejor comprensión de la estructura y del mecanismo de formación de las huminas ayudará a minimizar la formación de subproductos y la identificación de rutas de valorización adecuadas. En esta tesis, se ha estudiado la identificación estructural y la valorización de huminas a través de vías catalíticas.

Estudios previos sobre las huminas mostraron la presencia de una red furánica conjugada con enlaces oxigenados. Los sistemas conjugados generalmente poseen actividad de fluorescencia que se investigó en el *Capítulo 2*. De hecho, al emplear los espectros de absorción, emisión y excitación de una solución de huminas, se evidenció la complejidad estructural de estos subproductos. En particular, se identificaron tres fluoróforos distintos de diferente longitud de cadena que muestran una red macromolecular polidispersa. Este proyecto se realizó en colaboración con el departamento de Química Física de la Universidad de Córdoba y finalizó con una publicación en *Chem. Commun. 2017, 53, 7015-7017*.

La estructura de las huminas se ha investigado a través de una variedad de técnicas espectroscópicas (por ejemplo, RMN, IR) en

huminas sintetizadas en bibliografía. En general, se cree que las huminas se derivan de las reacciones de condensación aldólica, acetalización o apertura de anillo por hidrólisis con la formación de intermedios altamente reactivos; sin embargo, el estado del arte actual en el campo no ha permitido hasta la fecha la identificación inequívoca del mecanismo de formación de las huminas. En el **Capítulo 3**, se analiza un enfoque novedoso en la identificación de moléculas clave y mecanismos involucrados en la formación de las huminas. En particular, al emplear reacciones de hidrogenación e hidrogenólisis (catalíticas) en huminas industriales, la identificación por CG-MS de los productos de descomposición podría indicar la coexistencia de diferentes mecanismos de formación. Además, la observación de diferentes clases de moléculas, es decir, materiales de partida y (sub)productos de la hidrólisis catalizada por ácidos de los azúcares, sugiere una mayor complejidad de la estructura de las huminas en comparación con las descritas anteriormente en la bibliografía. Estos hallazgos fueron publicados en *Mol. Catal. 2019, 479,* 110564.

Sobre la base del conocimiento obtenido sobre la complejidad estructural de las huminas, se llevó a cabo la valorización a través de la síntesis de materiales catalíticos. Se sabe que las huminas poseen una variedad de grupos funcionales con oxígeno que pueden actuar como puntos de anclaje a los precursores metálicos en la producción de nanomateriales. Mediante el uso de precursores abundantes y económicos, junto con procedimientos ecológicos (es decir, sin disolventes, mecanoquímicos), en el **Capítulo 4** se investigaron óxidos de hierro que contienen huminas. Dada la esperada presencia de grupos funcionales superficiales con oxígeno, los nanomateriales se probaron en reacciones de oxidación. En particular, se llevó a cabo una desafiante ruptura oxidativa asistida

con peróxido de hidrógeno de la molécula derivada de lignina, isoeugenol, a agente aromatizante de alta gama, vainillina. En dicha reacción se obtuvo una alta actividad y selectividad (hasta un 57% de rendimiento) en menos de 5 minutos de tiempo de reacción utilizando la irradiación por microondas, lo cual no fue posible con el uso exclusivo de óxidos de hierro. Además, los materiales que contienen huminas mostraron una estabilidad satisfactoria cuando se reciclaron. Estos hallazgos demuestran la empleabilidad de las huminas como fuente de carbono para materiales nanohíbridos inorgánicos-orgánicos para un rendimiento catalítico mejorado. Los resultados de este proyecto fueron publicados en *Green Chem. 2017, 19, 4423-4434*.

Chapter 1

Introduction

Introduction

       Chemistry touches each part of our lives: it is inside us, in the products we manage every day and even in the food and drinks we ingest. The considerable impact of the chemical industry is reflected in the production of more than 95% of goods, accounting for *ca.* $6 trillion global generated sales with a stable growth and more than 20 million jobs world-wide.[1] Since the advent of catalytic cracking in the 19th century,[2] a plethora of chemical products are fossil-based, *e.g.* fuels, pharmaceutical, and plastics/textiles. Although significant technological and societal improvements have been achieved thanks to the *boom* of the petroleum industry, current environmental and economic concerns are driving new sustainable chemical practices forward.

       The overexploitation of fossil resources has prompted the development of a *disposable society*, where resources appeared to be infinite, cheap, and harmless. However, advances in chemistry also brought forth a certain awareness of the consequent detrimental effects that prompted innovation and new practices. For instance, synthetic plastics were developed in parallel to the technological progress of the petrol-based industry, and bloomed in the last century finding a vast variety of applications, from packaging (*e.g.* polystyrene, 1929) to textiles (*e.g.* polyester, 1930).[3] Slow degradation of polymeric substances (1—100+ years), erroneous and careless disposal of plastic waste, as well as daily life activities, has brought the world to alarming environmental conditions. In 2014, an oceanographic model of debris distribution estimated >5 trillion particles of (micro)plastics navigating our seas.[4] A 2018 Eunomia report identified automotive tires as the primary cause of plastics unintentionally leaching to the environment (*ca.* 500 kton), followed

by pre-application raw materials (*e.g.* PET pellets), and washing of synthetic textiles.[5] In addition, the dynamic character of our ecosphere causes each environmental compartment to be contaminated: plastics in our environment will accumulate in oceans sink, eaten by fish and entering the animal and human food chain.[6,7] Today, biodegradable and bio-based plastics can offer the opportunity to reduce the impact given by the broad use of petroleum resources. This widespread pollution has caused soaring of numerous environmental movements, urging the chemical industry to find solutions, such as adopting the Zero Pellet Loss (ZPL) initiative of the Operation Clean Sweep® program, aiming to reduce the raw materials losses along the production chain.[8]

Sadly, synthetic plastics are not the only cause of concern on our planet. Since the fossil-driven industrial revolution, other trends are influencing the economic and environmental political decisions, being:

- Depreciation and irreversible depletion of traditional feedstocks (*i.e.* oil and gas).[9,10]
- Climate change with higher worldwide average temperature due to green-house gases, including CO_2 reaching record levels.[11]
- Intensification of global population (+9 billion projected by 2050), thus incremented energy and food demands.[12]

Concomitance of these anthropological consequences calls for the implementation of a sustainable chemical industry, embracing the concepts of *Green Chemistry*, *circular* and *low-carbon economies*, and *resource efficiency*. For this, fields looking at the conversion of renewable feedstocks (*e.g.* biomass) through environmentally-friendly processes (*e.g.* catalytic) are advancing to

fully shift towards a self-sustaining chemical industry with reduced negative impacts on human, animal, or plant life.

Sustainability Concepts

The increasing environmental and political pressures for creating a society without intergenerational issues culminated in the internationally accepted *2030 Agenda for Sustainable Development*, where 17 tangible goals have been implemented to improve societal and economical disparities, conservation and management of resources and ecosystems, and international cooperation (Figure 1).[13,14]

Figure 1. The 17 Sustainable Development Goals of the United Nations for the 2030 Agenda.[14]

Because of the versatility of the chemical industry, any improvement can have a big impact on the UN Sustainable Development Goals. In fact, a 2017 report from the International Council of Chemical Associations (ICCA) gives concrete industrial examples of the positive direct impact some of the major chemical companies have imparted through their initiatives, donations, and business strategies to 80% of the SDGs (Figure 2).[15]

Area of Impact	Goals Affected and Approaches
Sustainable Economies	• SDGs 1, 8 • Industrialization, roads, safety, crop protection.
Health and Well-Being	• SDGs 2, 3, 6 • Sanitation, clean water, plant protection, crop enhancement, medical breakthroughs
Learning & Education	• SDGs 4, 5, 10 • Donations to schools, hosting events, workshops, aid pro-bono organizations
Energy, Environment & Sustainable Cities	• SDGs 7, 9, 11, 12, 13 • Resource- and energy-efficiency, long product lifecycle, innovation.
Sustainable Consumption & Production	• SDG 12 • Resource- and energy-efficiency, GHG* reduction, waste recyclability, sustainable materials and business
Partnerships & Capacity Building	• SDG 17 • Safety management, training on new techniques, revitalization of cultural and recreational spaces

*GHG: green-house gases

Figure 2. Impact of the chemical industry on the SDGs and approaches. Graphically adapted from reference.[15]

For the implementation of a sustainable chemical industry, 4 critical pillars were identified:[16]

1. **Low-Carbon Economy:** Reduction of carbon dioxide and green-house gases emissions with the use of clean and renewable technologies.

2. **Resource Efficiency:** Using less energy and material inputs with more efficient chemical processes.

3. **Circular Economy:** Recycling, repurposing, and valorization of traditionally considered waste materials.

4. **Care for People and Planet:** Full implementation of Health, Safety, Security and Environment (HSSE) practices from product development to end-use to minimize impacts.

With these concepts, the environmental impact is minimized while intensification of the process can be achieved, bringing economic benefits to industry. In fact, according to the last PACE survey, chemical manufacturing companies have the highest pollution abatement costs ($5.2 bn), followed by petroleum and coal industry ($3.7 bn), for a total of $20.7 billion of expenditures for all industrial sectors.[17] By applying the concept of a circular economy, the abatement costs would significantly drop and could be potentially converted into economic benefit.

Furthermore, a series of sustainability concepts were developed in the last decades as a tool for researchers to move towards sustainability with tangible measures of comparison. The efficiency of a process and the waste outflow of the same are interrelated concepts which can be calculated by using the *atom economy*[18] and *E-factor*[19] values, respectively. Where the former considers the mass of atoms in the desired product as opposed to the initial reactant's atoms, the latter considers the mass of waste over the mass of product, giving a straightforward indication of the environmental impact of manufacturing processes in different chemical sectors. These two indicators become *passive* tools of comparison for different already developed processes. However, as sustainability is becoming more and more imperative in the chemical industry, *active* tools for pollution prevention are required in the field.

In this sense, the concept of *benign-by-design* (development of synthetically efficient, economically viable, and environmentally benign processes),[20] culminated into formulation of specific guidelines for reaching a sustainable process: the *12 Green Chemistry principles*.[21] The 12 principles (Figure 3) can be embodied

in one general concept: *design.* Designing a chemical process from feedstocks to end-of-life product with one or more of the principles, several health, environmental, but also economical benefits can be achieved.

In particular, the environmental impact of a process can be drastically reduced (including noxious gas emissions), as well as the overall cost of a process, as it allows a simplified plant design, with less feedstocks and energy requirements, minimized waste production and minor risks and hazards not only for the environment, but also for people and animal life.

Figure 3. The 12 principles of Green Chemistry developed by P. T. Anastas and J. C. Warner. Adapted from reference.[21]

Peculiarly, the 9th principle of Green Chemistry (Catalysis) can improve greatly the sustainability of a chemical process by reducing the amount of energy and starting materials employed in an industrial production, as well as improve selectivity, thus minimizing waste, and increase process safety. In fact, *ca.* 90% of all chemical productions comprise of at least one catalytic step, being homogeneous or heterogeneous.[22]

Some key examples of improvements by catalysis are given as follows:

- Catalytic processes are often more selective, reducing the amount of by-products produced (which can be waste); also, the catalytic material has usually long life cycles and may be reused upon regeneration (if required and possible to do so).[23]

- Highly toxic stoichiometric reagents commonly used (*e.g.* chromium, carcinogen) may be substituted with a less hazardous catalyst,[24] and/or the catalyst may produce selectively a non-toxic isomer.[25]

- Catalytic processes often require less intensive operating conditions (*e.g.* temperature) thus requiring lower energy inputs;[26] catalysts may also allow to simplify multi-step procedures and work-ups reducing the amount of auxiliaries required.[27]

- For the production chemicals, (electro)catalysis can convert challenging renewable feedstocks such as carbon dioxide[28] or biomass,[29] both renewable resources.

With these tools in mind, including catalysis, a sustainable chemical industry can be evaluated and implemented. In particular, using renewable feedstocks is becoming crucial in order to achieve a

more sustainable chemical industry. In this sense, the conversion of *bio*-feedstocks is advancing as a green chemistry practice.

Biomass Valorization

The production of chemicals from renewable resources can be achieved *via* two valorization routes: (electro/photo)catalytic conversion of carbon dioxide, and conversion of biomass. Where CO_2 conversion strategies are still at a research level,[30,31] biomass is leading the way towards the sustainable production of chemicals.

Biomass is a broad concept that comprises plant-based resources (*e.g.* lignocelluloses, oilseed/sugar/starch crops, agricultural residues), biowastes (*e.g.* animal manure, sewage sludge), and aquatic organisms (*e.g.* algae). Depending on the source, biomass can be an optimum source of several compounds: carbohydrates, aromatics, terpenes, fatty esters, among others. Efficient isolation and conversion of each plant component could satisfy a wide range of applications. Also, various environmental benefits can be achieved with the valorization of these renewable feedstocks. In particular, the conversion of bio-sources can contribute to a sustainable chemistry by:

- **Reducing the CO_2 cycle through the process of photosynthesis.**
  Through photosynthesis, plants can transform CO_2 into flora in the scale of seconds/minutes, while the fossil fuels' carbon sink requires millions of years to be formed. Combined to intercropping, the short cycle of plants can lead to a low-carbon economy.[32]

- **Granting renewable and inherently safer feedstocks.**

Generally, biomass as a feedstock is nonhazardous to human life. Instead, the limited availability of cultivable land for both food and chemical/energy crops is of general public concern, especially due to the projected increase in global population. In lieu, a study on agro-ecological potential biomass production increase (PBPI) showed that biomass large-volume demands can be satisfied by implementation of polyculture and reallocation of crops for profit-maximization without any need for cropland expansion.[33] Furthermore, the development of high-output agricultural technologies can intensify harvests, yielding more available biomass.[34]

- **Having a better distribution across the globe compared to fossil fuels.**
  According to the 2017 OPEC Annual Statistical Bulletin, in 2016 >50% proven crude oil reserves are in the Middle East, followed by Latin America (22%), with Western Europe coming last (0.7%).[35] On the other hand, biomass is more ubiquitously distributed, although diversified, where C3-grasses/needleleaf trees dominate the northern hemisphere, and C4-grasses/broadleaf trees are favored in warmer climates in the southern hemisphere.[36]

- **Directly contributing to a circular economy.**
  Aside from microplastics and greenhouse gases, disposal of solid waste in landfills may pose significant threats to human health, as well as the environment.[37] Valorization of solid waste through various technologies (*e.g.* fermentation) allows reducing the negative effects.

General conversion strategies of biomass, however, come with low resource efficiency, causing higher production costs and limited

competitiveness with the well-established petroleum processing. In this sense, the use of lignocellulosic biomass may only offer a competitive option to the fossil-based industry in the long term.

1. Lignocellulosic Biomass

Lignocelluloses are the most abundant biomass on the planet, ranging from hardwood to grasses, including also agriculture and forestry waste (*e.g.* sugarcane bagasse, paper mill). Lignocellulosic biomass is comprised of two carbohydrate-based polymers, cellulose (40-50%) and hemicellulose (15-20%), and one aromatic polymer, lignin (25-35%). Cellulose confers tensile strength to the plant, being a crystalline and linear glucose-based polymer, thus being an optimum source of C6-sugars. Cellulose is cross-linked with hemicellulose, further strengthening the plant structure. Hemicellulose is a branched polymer made up of different C5-carbohydrates, uronic acids and C6-sugars including xylose, mannose, arabinose, and galactose. Lignin is an irregular polyaromatic macromolecule comprised of phenylpropane-type moieties, which confers the structural rigidity to lignocellulose.[38] Generally, lignocelluloses are comprised of highly oxygenated organic molecules with C5- and C6-moieties. The presence of these oxygen functionalities offers a completely different feedstock compared to petroleum-sources (*i.e.* hydrocarbon-like), thus changing the valorization routes as well as the range of obtainable products. Lignocellulose can be valorized *via* enzymatic and/or chemical pathways. Some examples of new platform chemicals arising from biomass valorization *via* the two routes are given in Figure 4.

Lignocellulose-based biorefinery developments of the past decades have focused on the production of *drop-in* energy solutions,

such as bio-ethanol as alternative transportation fuel. In particular, bio-ethanol comes from yeast fermentation (enzymatic) of C6-sugars. Nowadays bio-ethanol is produced in high volumes (>25 bn gallons worldwide) but mainly from starchy plants (*i.e.* sugar cane, corn), directly competing with the food market.[39] Furthermore, low product price and high production cost limits bio-fuel competitiveness with the petroleum market, especially in such high volumes.[40]
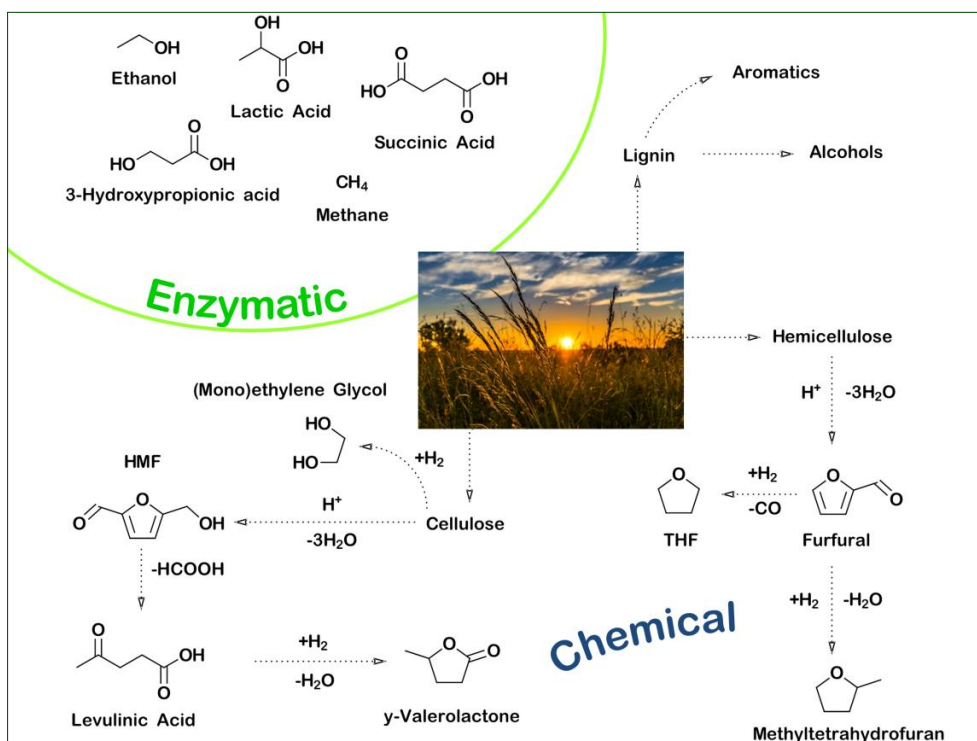
Figure 4. Examples of the enzymatic and chemical products obtainable from lignocelluloses.

Instead, different and innovative platform molecules can be obtained from lignocellulosic biomass, giving unique alternatives for the preparation of materials and chemicals. Such molecules would not have a direct competition with the petroleum market; in lieu, bio-products may offer cutting-edge market opportunities. Bio-products different from petrol-based were initially identified in a 2004 US Department of Energy report[41] and later updated by Bozell

and Petersen.[42] Products, state-of-the-art process, and current technical challenges are summarized in Table 1.

Table 1. Key examples of possible bio-based products, state-of-the-art processes, and challenges.[42]

Bio-product	Process	Technical Challenge
Ethanol	Aerobic fermentation	·Established market in competition with food (starch/sugar crops) ·Expensive pretreatment of lignocelluloses ·Seasonal changes in crop productivity
Furanics (Furfural, HMF, FDCA)	Acid-catalyzed dehydration of C-5 and C-6 sugars/Oxidation	·Low resource efficiency ·Process cost
Succinic acid	Anaerobic fermentation	·Separation/purification of products ·Process cost
Hydroxypropionic acid/ aldehyde	Aerobic fermentation	·Low resource efficiency ·Under research
Levulinates (Levulinic Acid, Alkyl Esters)	Acid-catalyzed dehydration of C-6 sugars	·Low yields ·Process cost
Biohydrocarbons (isoprene)	Aerobic fermentation	·Investment cost (reactors) ·High feedstock cost (high purity lignocellulosic sugars)
Lactic acid	Anaerobic fermentation	·Established market in competition with food (starch/sugar crops) ·High feedstock cost (high purity lignocellulosic sugars); ·Separation/purification of products
Xylitol/arabinitol	Hydrogenation of C-5 sugars/Biocatalysis	·Established hydrogenation ·Separation/purification of products ·Low product price

Sorbitol (hydrogenation of C6-sugars) and glycerol (by-product of biodiesel/soap production) were originally included in the list; however, the technologies for these two products are established, thus having low market price. Current challenges of these two economic bio-products lie in their further upgrading and valorization.

Challenges in biomass processing become particularly relevant when petrol-like molecules (*i.e.* no oxygen, aliphatics/aromatics/olefins) are the target chemical due to the reactivity of oxygen functionalities. Thus, new platform chemicals may be more appealing as well as giving innovative application products. Major focus has been given to the development of sustainable chemical routes for the production of furanics and levulinates *via* acid-catalyzed hydrolysis. The obtainable products can yield to a variety of high-added value applications (*e.g.* plastics, cosmetics). However, the production of these chemicals from whole lignocelluloses suffers from low yields, hence high process costs. In particular, differences in lignin content between lignocelluloses, for instance softwood *versus* hardwood, cause process variability. In fact, hydrogen bonding between the different biomass components reduces surface accessibility for raw lignocelluloses, preventing valorization routes. Also, metal salts present in natural biomass including K, Ca and Mg, may cause reactor fouling by precipitation of inorganic compounds,[43] or catalyst deactivation by ion-exchange.[44] In this sense, different pretreatment strategies for component separation have been developed. Peculiarly, separation of each of the macromolecular structures without further decomposition can contribute to the development of efficient conversion strategies for a competitive bio-economy.

1.1 Pretreatment of lignocelluloses

Due to the recalcitrant and chemical heterogeneous nature of lignin, a pretreatment step of the whole lignocellulosic biomass is considered essential for its cost-effective valorization.[45] An efficient pretreatment would separate the single lignocellulosic components (*i.e.* cellulose, hemicelluloses, lignin), allowing one standardized

process for each polymer, and reducing worldwide inequalities due to different types of biomass employed. It would also improve product yields and decrease overall process costs. For instance, in the case of biocatalytic routes, typical product yields are low (<20%) for untreated biomass; in this case, lignin acts as a physical barrier to enzymes for the hydrolysis of the digestible parts (carbohydrates).[46,47] Employing biological,[48] physical,[49] and/or chemical steps[45,50] (including physico chemical)[51,52] as pretreatments for lignocellulosic biomass would unleash the full potential of these feedstocks with higher resource efficiency. Ideally, an effective pretreatment allows the removal of lignin without degrading the desired carbohydrates, while being cost effective, *i.e.* low energy requirements, reactor capital costs and size, and production of waste.[53] The different pretreatment strategies, alongwith advantages and disadvantages, are illustrated in Table 2.

Overall, depending on the application one pretreatment method will be preferred. For instance, treatments with low production of toxic compounds (*i.e.* microbial inhibitors) will be favored in biological conversions (*e.g.* fermentation), while high sugar yields are preferred for chemical conversions. A good balance between cost and separation of each lignocellulosic component is of crucial importance for the development of selective bio-conversion processes. However, codependence of pretreatment with the type of biomass further complicates the process.[54] For instance, alkali treatments are inefficient for softwood-type of biomass and lignin-rich biomass cannot be processed by the ammonia fiber expansion process (AFEX). Overcoming these technical pretreatment challenges would furthely improve the economics of bio-processes towards the development of innovative products.

Table 2. Advantages and disadvantages of common lignocellulosic pretreatments

Strategy	Method	Advantages	Disadvantages
Biological	**Fungal**	·Low energy ·Degrades lignin/hemicellulose network	·Low hydrolysis rate
Physical	**Milling**	·Reduces cellulose crystallinity	·Energy-intensive
Chemical	**Ozonolysis**	·Lignin reduction ·Low production of microbial inhibitors	·Expensive ozone
	Organosolv	·Lignin and hemicellulose hydrolysis	·Big solvent volumes ·Solvent recycle
	Alkali treatment	·Lignin removal ·Partial degradation of hemicelluloses ·Reduces cellulose crystallinity	·Inefficient for softwoods ·Large amounts of water ·Long pretreatment times ·Base recycle
	Concentrated Acid	·High glucose yield ·Low energy	·Big acid volumes (cost) ·Acid recycle ·Reactor corrosion
	Diluted Acid	·Low production of microbial inhibitors ·Lower corrosion issues	·Low sugar yields ·Degradation products
	Ionic Liquids	·Reduces cellulose crystallinity ·Higher surface area ·Lignin removal ·Degrades lignin/hemicellulose network	·Expensive ionic liquids ·Difficult cellulose/hemicellulose recovery ·Toxicity and thermal instability of ionic liquids ·Difficult separation of sugars
Physico-chemical	**Steam Explosion**	·Lignin removal ·Hemicellulose solubilization ·Fair sugar yields ·Cost-effective	·Produces microbial inhibitors ·Partial hemicellulose degradation
	Ammonia Fiber Expansion (AFEX)	·Higher surface area ·Low production of microbial inhibitors	·Inefficient with lignin-rich biomass ·Big ammonia volumes (cost)
	CO_2 Explosion	·Higher surface area ·Low production of microbial inhibitors ·Cost-effective	·No effect on lignin and hemicelluloses ·High pressure (cost, reactor)
	Wet Oxidation	·Lignin removal ·Low production of microbial inhibitors ·Low energy	·Expensive oxygen and alkaline catalyst

Acid-assisted pretreatment may offer a low investment and efficient pretreatment method, especially if combined with catalyst recycling (typically, mineral acids). In fact, among all processes aiming at the separation of the bio-components, acid hydrolysis allows the release of most of the hemicellulose sugars as monomers while obtaining a solid glucose-rich fraction.[55] At the same time, acid hydrolysis allows the removal of inorganic salts and lignin,[56] increase of cellulose concentration/accessibility,[57] and pretreatment products can be directly employed for acid-catalyzed conversions, as ideally the same environment (*i.e.* acidic, aqueous) would be employed.[58]

Up to date, industrial conversions of non-food plants to single lignocellulosic components (*i.e.* sugars, lignin) are under development. In Europe, the Dutch company Avantium is developing a pilot plant where combination of high acid concentration and low temperature process allows the conversion of lignocelluloses into high purity glucose.[59] One-pot transformation of lignocelluloses *via* acid-catalyzed hydrolysis have been attempted;[58,60] however, dependency on solvent, catalyst (acid strength, loading), and operating conditions for each biomass type complicates the development of an efficient one-step process. In this sense, valorization of single bio-components (*i.e.* sugars) to target products is preferred for the commercialization and full implementation of biomass conversion strategies.

## 1.2 Acid-catalyzed conversion of lignocellulosic sugars

Biocatalytic routes have remarkable potential in the conversion of biomass,[61] although tailored to certain chemical products (*e.g.* methane, biohydrogen). According to the green chemistry principles, if a solvent is needed for a determined process,

the best would be water. However, the aqueous broth used in bioconversions originates higher purification costs.[62] In this sense, upgrading of lignocelluloses is being redirected to chemical valorization which can be economic, resource- and energy-efficient, as well as with a wide variety of obtainable products.

Although still under development, recent advances of lignocellulose valorization are bringing forward promising routes for a cost-competitive market. Particularly, catalytic pathways offer sustainable processes thanks to lower energy requirements, faster production lines, and recyclability when in the heterogeneous form. Significant focus has been given to acid-catalyzed hydrolysis for the synthesis of key platform chemicals thanks to the low process economics, drop-in feasibility, and high-added value obtainable platform chemicals. 5-Hydroxymethylfurfural (HMF), furfural, levulinic acid, and their alkyl derivatives have been major objects of focus of development thanks to their wide application potential. Some examples of products possibly derived from HMF and furfural are given in Figure 6.

Both homogeneous and heterogeneous catalytic pathways have been investigated in the conversion of lignocellulosic sugars, *i.e.* fructose,[63-76] glucose,[63,68,77-90] and xylose.[91-105] As levulinic acid is an extra hydrolysis step, similar conditions for HMF but with usual longer reaction times are employed, and will be not discussed herein. Key examples of catalysts and conditions employed for the production of HMF from the two hexoses (*i.e.* glucose and fructose) and furfural from xylose are given in Tables 3—5 for homogeneous catalytic systems and Tables 6—8 for heterogeneous catalyzed conversions. The values in the tables are adjusted of ±0.5% for clearer comparison. Overall, quantitative yields for acid-catalyzed

hydrolysis of carbohydrates are hard to achieve due to the occurrence of side-reactions. In particular, the formation of humin by-products is the predominant process reducing resource efficiency and increasing production costs.
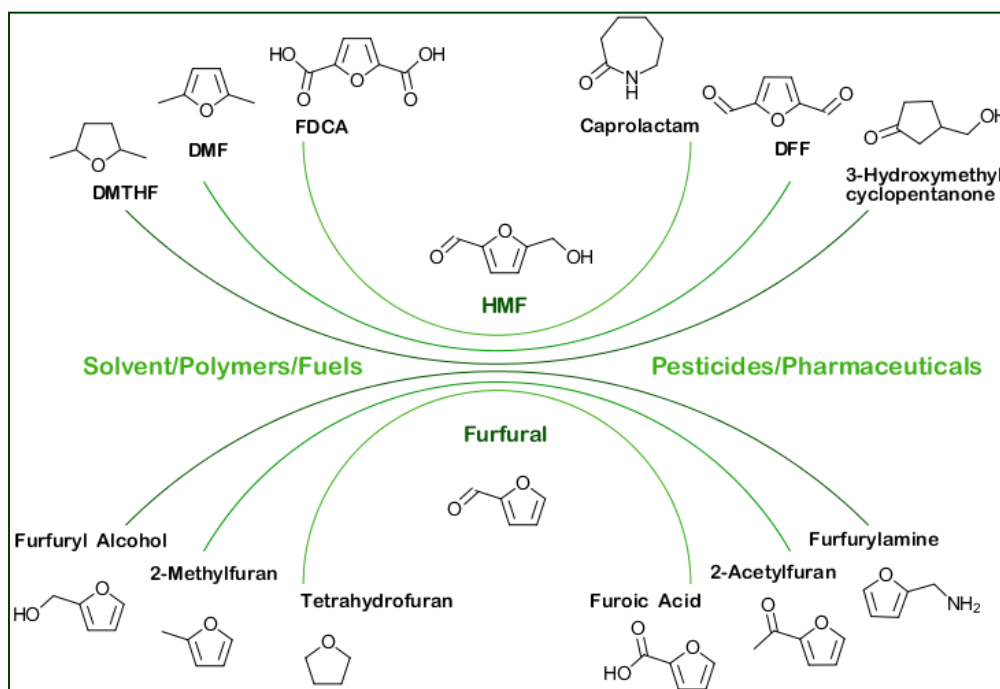
Figure 5. Products and applications of the conversion of HMF and furfural. *Legend:* **DMTHF**–2,5-dimethyltetrahydrofuran; **DMF**–2.5-dimethylfuran; **FDCA**–2,5-furandicarboxylic acid; **DFF**–2,5-diformyfuran.

1.2.1 Homogeneously-catalyzed conversion

Generally, homogeneous catalytic systems are more active than the heterogeneous counterparts due to the closer contact between the active sites (*e.g.* H+, metal centre) and the substrate molecule. In this sense, a variety of homogeneous catalysts have been investigated for the conversion of fructose (Table 3),[63-67] glucose (Table 4),[63,77-87] and xylose (Table 5).[91-93] Mineral acids are traditionally employed, however corrosion is always a matter of concern. Positively, higher acidic pH (*ca.* 5) gives higher HMF yields in the conversion of glucose.[64] The use of organic acids (*e.g.* maleic)

could also overcome reactors short life-time by reducing corrosion, but limited yields and relative higher price as compared to mineral acids favor the latter.

Table 3. Conversion of fructose to 5-hydroxymethylfurfural (HMF) with homogeneous catalysts.

Catalyst	C_F^a (wt/v%)	T (°C)	Time (min)	Solvent	Yield (%)	Ref.
None	8	140	60	DMSO	49	[63]
None	1	240	2	H_2O	18	[64]
H_2SO_4 (pH=1.5)	1	240	2	H_2O	15	[64]
H_2SO_4 (pH=5)	1	240	2	H_2O	41	[64]
H_3PO_4 (pH=5)	1	240	2	H_2O	65	[64]
Citric acid (pH=5)	1	240	2	H_2O	49	[64]
Maleic acid (pH=5)	1	240	2	H_2O	60	[64]
HCl (pH=1.5)	1	240	2	H_2O	15	[64]
HCl (pH=5)	1	240	2	H_2O	45	[64]
HCl (pH<1)	30	180	3	H_2O	25	[65]
HCl (pH<1)	30	180	3	H_2O:MIBK	55	[65]
HCl (pH<1)	30	180	3	(H_2O:DMSO:PVP)–(MIBK:2-BuOH)	76	[65]
HCl (pH<1)	50	180	3	(H_2O:DMSO:PVP)–(MIBK:2-BuOH)	71	[65]
$CrCl_3 \cdot 6H_2O$	142[b]	100	180	[C_4C_1im]Cl	96[c]	[67]

[a]Fructose concentration
[b]w/w% of substrate in ionic liquid
[c]Non-isolated yields

The use of Brønsted acid catalysts can efficiently dehydrate fructose into HMF,[64,65] whereas glucose requires the presence of a Lewis acid catalyst as its conversion to HMF is believed to go *via* sugar isomerization to fructose.[79-86] This extra step for glucose conversion renders the reaction generally less efficient. However, glucose is a more abundant and hence cheaper lignocellulosic sugar

compared to fructose, thus requiring further improvements to improve efficiency of the process.

Table 4. Conversion of glucose to 5-hydroxymethylfurfural (HMF) with homogeneous catalysts.

Catalyst	C_G[a] (wt/v%)	T (°C)	Time (min)	Solvent	Yield (%)	Ref.
None	8	140	1440	DMSO	8	[63]
H_2SO_4	9.1	200	5	H_2O	3	[77]
H_2SO_4	9.1	400[b]	1	[BMIM]Cl	49	[77]
CH_3SO_3H	8.3	120	180	[BMIM]Cl	58	[78]
HNO_3	8.3	120	180	[BMIM]Cl	43	[78]
HCl	8.3	393	180	[BMIM]Cl	33	[78]
$CrCl_3$	9.1	100	180	[EMIM]Cl	63	[79]
$CrCl_3 \cdot 6H_2O$	10	140	90	H_2O	18	[80]
$CrCl_3.6H_2O$	10	100	180	CPL[c]:LiCl	67	[81]
$CrCl_3 \cdot 6H_2O$	14[d]	120	30	$[C_4C_1im]Cl$	90[e]	[82]
$AlCl_3$	10	175	20	$(H_2O$:NaCl):CPME[f]	57	[83]
$AlCl_3$	10	175	20	$(H_2O$:NaCl):CPME[f]	46	[83]
$AlCl_3$	5	140	20	H_2O:DMSO	25	[84]
$AlCl_3$	2	170	10	H_2O:THF	43	[85]
$SnCl_4 \cdot 4H_2O$	10	100	180	CPL[b]:LiCl	42	[86]
$B(OH)_3$	10	120	60	[BMIM]Cl	1	[87]
$H_4SiW_{12}O_{40}$	10	120	60	[BMIM]Cl	22	[87]
$H_4SiW_{12}O_{40}$+$B(OH)_3$	10	120	60	[BMIM]Cl	41	[87]

[a]Glucose Concentration
[b]Microwave heating expressed in [W], no temperature specified
[c]Caprolactam
[d]w/w% of substrate in ionic liquid
[e]Non-isolated yield
[f]Cyclopentyl methyl ether

In this sense, the right combination of catalyst, operating conditions and solvent must be found. Lewis acid $CrCl_3$ was shown effective in its hydrated form in both conversions of fructose[67] and glucose[82] in ionic liquids. In the case of xylose, the presence of a Lewis acid would open the xylulose pathway which undergoes easier dehydration, although requiring biphasic or ionic liquid systems for high yields.[92,93] Also heteropolyacids (HPAs) have been investigated (*e.g.* $H_4SiW_{12}O_{40}$),[17-18,91] but no clear advantage can be drawn from using these catalytic systems as separation and recycling is severely hindered.

Table 5. Conversion of xylose to furfural with homogeneous catalysts.

Catalyst	Cx^a (wt/v%)	T (°C)	Time (min)	Solvent	Yield (%)	Ref.
None	3	140	240	DMSO	0.7	[91]
H_2SO_4	3	140	240	DMSO	58	[91]
PTSA	3	140	240	DMSO	67	[91]
$H_3PW_{12}O_{40}$	3	140	240	DMSO	63	[91]
$H_4SiW_{12}O_{40}$	3	140	240	DMSO	58	[91]
$CrCl_3$+HCl	1	140	120	H_2O:Toluene	76	[92]
$SnCl_4$	20^b	130	60	[EMIM]Br	71	[93]

[a]Xylose concentration

[b]w/w% of substrate in ionic liquid

Aqueous media would be generally favored due to the higher solubility of highly oxygenated bio-based feedstocks, as well as the lower price and environmental impact. However, yields of up to 65% of the desired product (being HMF or furfural) can be obtained in the aqueous systems due to the occurrence of side-reactions (*i.e.* decomposition, polymerization).[64,65,77,80] In this sense, the use of polar aprotic solvents, *e.g.* dimethyl sulfoxide (DMSO), has shown higher yields of the desired products compared to aqueous systems

due to high sugar solubility and suppression of side-reactions.[63,91] However, the high boiling point of DMSO complicates product separation, requiring tailored techniques which greatly increase production costs.

Ionic liquids (*e.g.* [C$_4$C$_1$im]Cl)[67,77-79,82,87,93] or similar (*e.g.* Caprolactam:LiCl)[81,86] in combination with metal halides provided satisfactory product yields, and these systems are a major field of study in biomass conversion. Although the catalytic system and ionic liquid can be recycled, separation of furanic products from ionic liquids is actually difficult and cost-ineffective.[106] Furthermore, ionic liquids are generally considered extremely stable and safe; however, their physico-chemical properties are not always well-defined.[107]

The use of biphasic systems has also been investigated, where the aqueous phase would act as reaction media, and an extracting organic phase for product separation.[65,83-85,92] In particular, hydrophobic extracting phases (*e.g.* cyclopentyl methyl ether, CPME) in the presence of a chloride salt (*e.g.* NaCl) can enhance the partitioning coefficient of the organic solvent, favoring extraction.[83] Otherwise, polar solvents with low water solubility (*e.g.* methyl isobutyl ketone, MIBK) can be used in the sugar conversions. A particularly successful example of a multiphase system is given by an aqueous phase containing DMSO and poly(1-vinyl-2-pyrrolidinone) (PVP), and an extractive phase based on MIBK and 2-butanol as partitioning enhancer, which gave satisfactory yields with HCl as catalyst and up to 50 wt% of substrate concentration.[65] However, it can be clear as the use of multiple solvents can greatly increase the process costs and complicate the purification step.

Combination of high temperatures (180-240 °C) and low residence times (<5 min) is advantageous for the conversion of carbohydrates into furanics, whereas the production of levulinates would be favored at lower temperatures and longer residence times.[108] Diluted feeds (typically <10 wt%) are preferred in order to suppress polymerization reactions. Only with the addition of several co-solvents and/or partitioning salts higher feed concentrations can be employed.[65,83] The requirement of such dilution factors is one of the main drawbacks of biomass processing which yet requires a clear solution. In this sense, catalyst, solvent and unreacted feed recycle can reduce process costs, allowing competition with the petroleum market. In the case of homogeneous catalysts, their separation often requires the use of biphasic systems, generating copious amounts of liquid waste as well as being inefficient.[109] Using heterogeneous catalysts would remarkably improve catalyst recyclability, thus sustainability and process economics.

1.2.2 Heterogeneously-catalyzed conversion of lignocellulosic sugars

The presence of plenty of oxygen functionalities, tendency towards decomposition at high temperature and low volatility of bio-based feedstocks requires catalytic systems active at lower temperatures and in polar media. As mentioned before, water would represent the *greenest* solvent; however, side-reactions are favored in aqueous media and water can chemisorb on acid sites, deactivating them. Thus, also in heterogeneous conversions of fructose (Table 6),[63,67-76] glucose (Table 7),[63,68,87-90] and xylose (Table 8),[94-105] the use of different solvents (*e.g.* DMSO, DMF, ionic liquids) or biphasic systems (water/toluene) have been investigated with significant advances. The use of a polymeric water adsorbent (*e.g.* PVP-K30)[72] can be used as efficient strategy to reduce

hydrolysis-driven side reactions.[72] Also, the temperature and concentration trends observed in the homogeneous transformation of bio-sugars are valid for heterogeneous catalytic systems.

Table 6. Conversion of fructose to 5-hydroxymethylfurfural (HMF) with heterogeneous catalysts.

Catalyst	C_F[a] (wt/v%)	T (°C)	Time (min)	Solvent	Yield (%)	Ref.
Amberlyst-70	8	140	60	DMSO	93	[63]
WO$_3$/RGO[b]	5[c]	120	120	DMSO	65	[67]
WO$_3$/RGO[b]	5[c]	120	120	[BMIM]Cl	84	[67]
TiO$_2$	2	200	5	H$_2$O	38	[68]
WO$_3$/ZrO$_2$	3	120	120	DMSO	94	[69]
Amberlyst-15-P[d]	3	120	120	DMSO	100	[69]
Nafion	3	120	120	DMSO	94	[69]
Nafion/SiO$_2$	3	90	120	DMSO	75	[70]
KIT-5-SO$_3$H	6	125	45	DMSO	90	[71]
Ethylene Tar-SO$_3$H (C-catalyst)	7	130	140	i-PrOH	52	[72]
Ethylene Tar-SO$_3$H (C-catalyst)	7	130	140	i-PrOH:PVP-K30	88	[72]
ZSM-5	10	190	80	H$_2$O:MIBK	75	[73]
MCM-41-SO$_3$H	10	190	80	H$_2$O:MIBK	84	[73]
MIL-101(Cr)-SO$_3$H	10	120	60	DMSO	90	[74]
IL[e]-HSO$_4$-SiO$_2$	10	130	30	DMSO	63	[75]
CrCl$_3$·6H$_2$O-[FPIL][f]	10	120	60	DMSO	91	[76]

[a]Fructose Concentration
[b]Reduced Graphene Oxide
[c]w/w% of substrate in ionic liquid
[d]Powder (<0.15 mm)
[e]Ionic liquid, 3-Sulfobutyl-1-(3-propyktriethoxysilane)
[f]Functional polymeric ionic liquid, 1-vinyl-3-propane sulfonate imidazolium

Generally, homogeneous catalysts have higher activities than their heterogeneous counterparts given the different mechanism of

action: the former coordinates the substrate through the metal center (*intimate contact*), and the latter adsorbs the reactant through active sites on its surface (*superficial activity*). In this sense, immobilization of homogeneous catalysts on heterogeneous supports may allow high conversion and selectivity coupled to simple recyclability.

Table 7. Conversion of glucose to 5-hydroxymethylfurfural (HMF) with heterogeneous catalysts.

Catalyst	C_G[a] (wt/v%)	T (°C)	Time (min)	Solvent	Yield (%)	Ref.
Amberlyst-70	8	140	1440	DMSO	33	[63]
WO_3/RGO[b]	5[c]	120	120	[BMIM]Cl	36	[67]
TiO_2	2	200	5	H_2O	8	[68]
TiO_2	2	175	105	H_2O:THF	73	[87]
P-TiO_2	2	175	105	H_2O:THF	83	[87]
P-TiO_2	5	175	105	H_2O:THF	63	[87]
H-ZSM-5	10	120	60	[BMIM]Cl	3	[88]
MCM-41	15	150	24	H_2O	15	[89]
MCM-20	15	150	23	H_2O	19	[89]
Amberlyst-15+HT[d]	3	100	180	DMF	41	[90]

[a]Glucose Concentration
[b]Reduced Graphene Oxide
[c]w/w% of substrate in ionic liquid
[d]Hydrotalcite, layered clay

Moderate activity and stability were obtained employing silica-supported ionic liquid as catalyst.[75] Higher yields were instead obtained with the functionalization of a polymeric ionic liquid with a Lewis acid in the conversion of fructose.[76] However, gradual loss of activity was observed upon recycling of the catalysts. Furthermore, immobilization of homogeneous catalysts would translate into higher synthesis cost, lower turnovers, and increased chance of leaching.[110]

Table 8. Conversion of xylose to furfural with heterogeneous catalysts.

Catalyst	C_X[a] (wt/v%)	T (°C)	Time (min)	Solvent	Yield (%)	Ref.
ZSM-5	2	190	15	H_2O:GVL	70	[94]
Amberlyst-70	2	190	15	H_2O:GVL	67	[94]
SAPO-34	2	190	360	H_2O:GVL	40	[94]
H-Mordenite	12	260	3	H_2O:Toluene	97	[95]
H-Mordenite	3	140	240	DMSO	24	[96]
H-ZSM-5	3	140	240	H_2O	19	[96]
H-ZSM-5	3	140	240	DMSO	20	[96]
H-ZSM-5	3	140	240	H_2O:Toluene	43	[96]
H-β(25[b])	3	140	240	H_2O:Toluene	25	[96]
Del-Nu-6[c]	3	170	240	H_2O:Toluene	47	[97]
SAPO-11	3	180	240	H_2O:Toluene	51	[98]
H-MCM-22(24[b])	3	170	960	H_2O:Toluene	70	[99]
ITQ-2[c]	3	170	960	H_2O:Toluene	66	[99]
SBA-15-SO_3H	3	160	240	H_2O:Toluene	68	[100]
MCM-41	3	170	120	H_2O:1-BuOH	39	[101]
MCM-41+NaCl	3	170	120	H_2O:1-BuOH	48	[101]
MCM-41-SO_3H	3	140	1440	DMSO	75	[102]
Propylsulfonic-SBA	2	170	1200	H_2O:Toluene	82	[103]
Arenesulfonic-SBA	2	160	1200	H_2O:Toluene	86	[104]
Carbon-SO_3H	1	200	90	H_2O	55	[105]

[a]Xylose Concentration
[b]Si/Al ratio
[c]Dealuminated zeolites

Especially when already expensive ionic liquids are employed, these catalytic systems would require quantitative performances for their industrial implementation. Typical petroleum catalysts, zeolites

(*e.g.* H-ZSM-5, H-Mordenite) and mesoporous (alumino)silicates (*e.g.* MCM-41, SBA-15), have been investigated in the conversion of sugars given their tunable acidity and shape selectivity.[73,88-89,94-104] Where significant coke formation hindered the activity of MCM catalysts in glucose conversion,[89] these catalysts were found more active in the conversion of both fructose[73] and xylose.[99,102]

In particular, the surface modification with sulfonic groups would provide these catalysts with the necessary Brønsted acid sites for the dehydration of sugars. However, leaching of these functional groups is typical in polar acidic systems. Despite the high activity of aluminosilicates,[73,94-95] significant deactivations were observed, attributed either to active site leaching,[94] or severe coke (or humins) formation in the small pores of zeolites.[73] Among all, H-modernite was found to be more resistant, however deactivation due to coking was observed at the first recycle and regeneration of the catalysts via acid treatment could not be achieved.[95] In fact, higher Si/Al are believed to reduce site accessibility,[96] causing pore blockage. Dealumination to improve surface area was attempted on zeolites;[97,99] however, no relevant improvement in activity and stability was observed. Mesoporous silica with low diffusion limitations, KIT-5, was found active at mild temperatures and fair fructose concentration upon superficial sulfonation.[71] However, the catalyst was not stable probably due to both humins adsorption on the active sites and leaching of –SO$_3$H groups.

Metal organic frameworks (MOF) such as MIL-101 are advancing as alternative catalysts to zeolites.[74] However, superficial modification with leaching-prone sulfonic groups is also required to improve activity. Thus, leaching can be expected. For these reasons,

new catalytic systems are being investigated with higher stability and recyclability.

Particularly, cheap catalytic systems resistant to leaching and/or fouling should be implemented in order to compete with the petroleum market. In this sense, hydrothermally stable metal oxides such as titania or zirconia have been investigated in the acid-catalyzed hydrolysis of bio-sugars.[67-69,87] These oxides, presenting Lewis acidity, may be peculiarly active for glucose transformation.

Modification of these oxides, however, is necessary for reaching significant activities in biomass conversion strategies. In particular, phosphate-TiO_2 was found efficient in the conversion of glucose thanks to enhanced acidity and superficial area, although up to a 2 wt% feed concentration.[87] P-TiO_2 catalyst was postulated to convert directly glucose to HMF through the formation of 3-deoxyglucosone rather than isomerization to fructose. Acidic tungsten trioxide (WO_3) was also investigated with reduced graphene oxide (RGO) or zirconia supports.[67,69] The acidity of the oxide was found efficient only for fructose conversion, rather than glucose, and suffering catalyst deactivation upon recycling.[67] A reduced pressure to continuously remove water from the reaction media enhanced the activity of zirconia-supported tungsten trioxide.[69] However, in the same work, cheaper and more environmental-friendly catalyst, Amberlyst-15, was found more active in the dehydration of fructose under vacuum.

In fact, sulfonated polymer and carbon catalysts may offer improved stability, peculiarly to hydrothermal conditions, as well as resistance to acidic and chelating environments. However, these catalysts present only Brønsted-type of functionalities, thus active

only in fructose and xylose conversions.[63,69,70,72,94,105] Combination of a layered hydrotalcite as a base catalyst with Amberlyst-15 can be a strategy for the one-pot conversion of glucose without the use of a Lewis acid.[90] Nonetheless, leaching was also observed in these catalytic systems due to the liability of the sulfonic groups. Significant leaching was observed for Amberlyst-70 in the synthesis of furfural[94]; however, the work was also conducted at the maximum operating temperature of the resin (190 °C) and aqueous environment. The use of other polar but aprotic solvents may benefit the use of ion-exchange resins in the conversion of bio-sugars. In fact, remarkable activity was observed for fructose-to-HMF in DMSO with Amberlyst-70, although only a third of the activity could be obtained for glucose.[63] In DMSO, however, leaching was suppressed and deactivation was only attributed to carbon deposition, hence the formation of humins. Other carbon-based catalysts were investigated in the acid-hydrolysis of sugars, *e.g.* ethylene tar-based.[72,105] Nevertheless, further improvements are required in carbon catalysis as in terms of synthetic reproducibility and stability of surface groups added upon functionalization.

Overall, despite great advances in the conversion of bio-based sugars, quantitative yields of the desired platform molecules with a long-lasting catalytic system are yet to be achieved. The main issue in both homogeneous and heterogeneous systems is the formation of polymeric by-products (known as humins) which decrease resource efficiency as well as deactivate solid acid catalysts. These by-products are generally considered undesired; however, their valorization, instead, can greatly increase the economics of acid-catalyzed hydrolyses of bio-sugars, but also open a new class of chemical products and/or materials following the principles of a circular economy.

In particular, the valorization of humins is becoming relevant at the industrial level given significant advances in the synthesis of bio-based products. For instance, chemical technology development company Avantium is moving towards the commercialization of bio-plastic PEF, deriving from oxidized HMF product, 2,5-furandicarboxylic acid (FDCA), and monoethylene glycol (MEG).[111] In particular, the technology relies on the use of alcoholic solvents (*e.g.* methanol) which protect the functional groups of the reactive intermediates through etherification. Yet, given the bigger volumes of an industrial level, the occurrence of side-reactions is almost unavoidable. Thus, humin by-products can play a new role in the biomass strategies if suitable applications can be found.

2. Humin by-products

Acid-catalyzed hydrolysis of lignocellulosic-derived carbohydrates is limited by the formation of humin by-products (Figure 7). Both structurally and mechanistically, the nature of these dark and viscous-to-solid (depending on process conditions) by-products is still a matter of debate. Generally, humins studies are aimed at minimizing their formation (*e.g.* by using ionic liquids, biphasic systems, *vide supra*) due to the following reasons:

1. State-of-the-art sugar conversion processes, peculiarly acid-catalyzed hydrolyses, suffer from low resource efficiency. In fact, humins can have yields up to 40 wt%,[112-114] severely affecting process economics. For instance, the Biofine process for levulinic acid manufacture can have as much as 30 wt% yield of humins.[115]

2. Humins, similar to the petroleum-based coke, can adsorb on heterogeneous catalysts active sites causing deactivation and reactor fouling.[116] This phenomenon would lead to increased

costs in catalyst regeneration/substitution, as well as unsafe situations due to increased pressure drop in continuous flow systems.

3. Humins can act as adsorbents of both catalysts (*e.g.* H_2SO_4)[117] or desired (by-)products (*e.g.* levulinic acid),[118] thus further reducing the process resource efficiency.

Overall, the mechanism of humins formation, structure and yields is influenced by process conditions including temperature, residence time, feedstock nature and concentration, solvent and catalyst.[119-121]
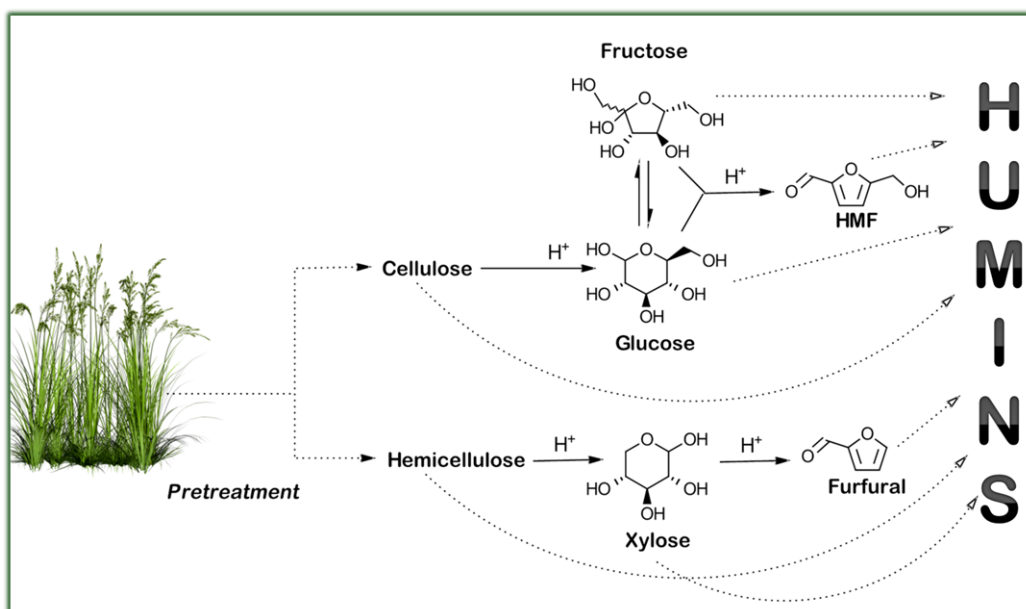
Figure 6. Schematic formation of humins from different lignocellulosic components, including cellulose, hemicelluloses, derived sugars and products.

2.1 Kinetics of formation of humins

The thermodynamics of the acid-catalyzed hydrolysis of sugars suggest that the formation of humins is unavoidable. Particularly, the sugar-to-levulinic acid pathway shows lower free energies (5-10 kJ mol^{-1}) for condensation reactions between carbohydrates and HMF as compared to hydrolysis to the final

product (*ca.* 60 kJ mol^{-1}).[122] This particular phenomenon is also reflected in the fractional reaction orders obtained for the kinetics of humins formation (1.2-2) with higher values compared to glucose and HMF conversions/production.[118,123,124] Fractional reaction orders higher than 1 signal a strong dependence on feedstock concentration with a complex mechanism of humins formation involving multiple species. In fact, dilute carbohydrate feeds were found to limit side reactions to humins,[124,125] as was also observed in the previous paragraph.

The nature of feedstock also influences the occurrence of polymerization reactions. A higher incorporation of the desired product, HMF, was observed in fructose-derived humins as opposed to glucose and HMF itself.[126,127] The latter, in fact, is considered key intermediate in the formation of humins. When considering HMF conversion, favorable activation energies for humins formation have been estimated (85-130 kJ mol^{-1}), stressing the reactivity of such a platform chemical.[126-129] Experimentally, humins formation yields follow the order fructose>xylose>glucose.[119] Moreover, the co-presence of desired product and starting materials appear to favor the formation of humins. For example, lower activation energies were extrapolated when furfural was in the presence of a carbohydrate (*i.e.* glucose or xylose).[130-132] In fact, lower yields of humins are obtained when the desired product is extracted from the reaction media (*e.g.* with the use of biphasic systems).

Process conditions also influence humins formation. In fact, a linear correlation between temperature and reaction rates of humins condensation was observed in the dehydration of xylose to furfural, as well as lower activation energies.[133] A fairly high activation energy for the formation of humins (165 kJ mol^{-1}) was reported for the

glucose to levulinic acid reaction when lower temperatures were considered (<150 °C).[124] Residence time is another parameter in sugar dehydration pathways. In fact, high temperatures (180-200 °C) with short reaction times (<1 min) favor the formation of HMF, while lower temperatures (140-160 °C) with longer residence times (>100 min) favor the formation of levulinic acid.[108] High temperatures and long reactions times will in turn bring higher humins yields.

The acid concentration or type (*i.e.* Lewis or Brønsted) can also trigger the formation of humins. Higher acid concentrations were found to favor the formation of levulinic acid rather than humins due to higher fractional orders (*ca.* 1.4 as opposed to 1.1), particularly at low substrate concentrations.[134] The presence of a Lewis acid, on the other hand, appears to open new pathways for the formation of humins, giving >50% yields from fructose and 25-40% from glucose, whereas Brønsted acids favor sugar degradation to levulinic acid.[135] This was also observed in the case of heterogeneous catalysts where higher concentrations of Lewis acid sites favors the formation of humins.[136]

2.2 Structure of humins

A univocal structure of humin by-products is yet to be established due to a possible dependence between the kinetics of condensation and the co-existence of parallel reaction mechanisms. Several spectroscopical (*i.e.* FT/ATR IR, ^{1}H/^{13}C/2D NMR, Raman, pyrolysis GC-MS) and elemental analyses have been carried out on as-synthesized humins from different sources (*i.e.* fructose, glucose, xylose, HMF, cellobiose, mixtures thereof).[120,121,126,127,137-141] Due to fast kinetics, fructose-derived humins present higher incorporation of HMF.[126] On the other hand, the free C5-position of furfural

(*i.e.* where HMF would have a –CH$_2$OH group) allows xylose-derived humins to present a more conjugated structure.[142]

Combination of the bulk analyses hints to a polyfuranic structure with a variety of oxygen functionalities (*i.e.* carbonyl, ether, hydroxyl) and short aliphatic chains (Figure 8), although differences on the relative concentrations of functional groups exist between studies.[119,121,126,127,141] For instance, Sumerskii *et al.* suggested that humins are a combination of furanic rings (*ca.* 60%) and ether or acetal groups (*ca.* 20%),[143] whereas acetal groups were disregarded in another work.[144] A highly conjugated network of furanics with aldehyde and/or ketone groups was deduced from IR analysis.[127] A recent work on industrially-obtained humins quantified carbonyl groups at *ca.* 7 wt%, in both aliphatic and conjugated forms.[145]
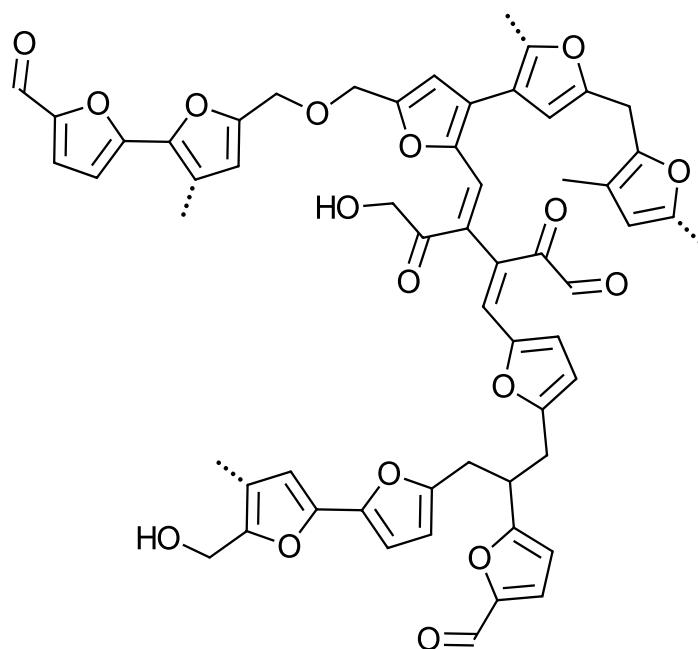
Figure 7. Example of humins structure, adapted from references.[119,141]

By using ^{13}C-labeled humins, ssNMR analyses showed a higher tendency for condensation through the side-groups

functionalities (C_α, carbonyl) rather than branching through the C_β position (alkenyl), which occurs to a lower extent.[141] Similar findings were observed upon IR analysis of acid-catalyzed hydrothermal carbon,[146] and Brønsted acid-catalyzed degradation of HMF.[128] The two positions are susceptible to nucleophilic attacks which can be suppressed by the presence of aprotic polar solvents, *e.g.* DMSO, due to the solvation effect on the C_α position, the most prone to condensation reactions.[147]

Humins also present a dynamic structure which is susceptible to further modifications. For instance, alkaline solubilization of humins yield a more aromatic structure (*i.e.* arenes).[141,144] In fact, an increase of *ca.* 10% of the C content in NaOH-treated humins (from *ca.* 65 to 72 wt%) at the expense of oxygen (from *ca.* 30 to 23 wt%) suggests the possible existence of Diels-Alder type of reactions.[144] Simple thermal treatment of humins to macroporous structures (*i.e.* foams) also showed an extensive polyaromatic structure at high temperatures and under inert atmospheres.[148]

2.3 Mechanism of humins formation

As with their structure, the mechanism of formation of humins is still largely undefined and a matter of debate. Different mechanisms have been proposed focusing on HMF, as the latter is considered the key intermediate in the polymerization to humins (Figure 9). Depending on whether the first step involves protonation (Figure 9, A—B) or hydrolysis (Figure 9, C—D), different reactive intermediates were proposed in the formation of humins. These intermediates can maintain the furanic ring central structure by undergoing side-group substitution reactions (Figure 9, A—B) or be a ring-opening product forming a linear intermediate (Figure 9, C—D).
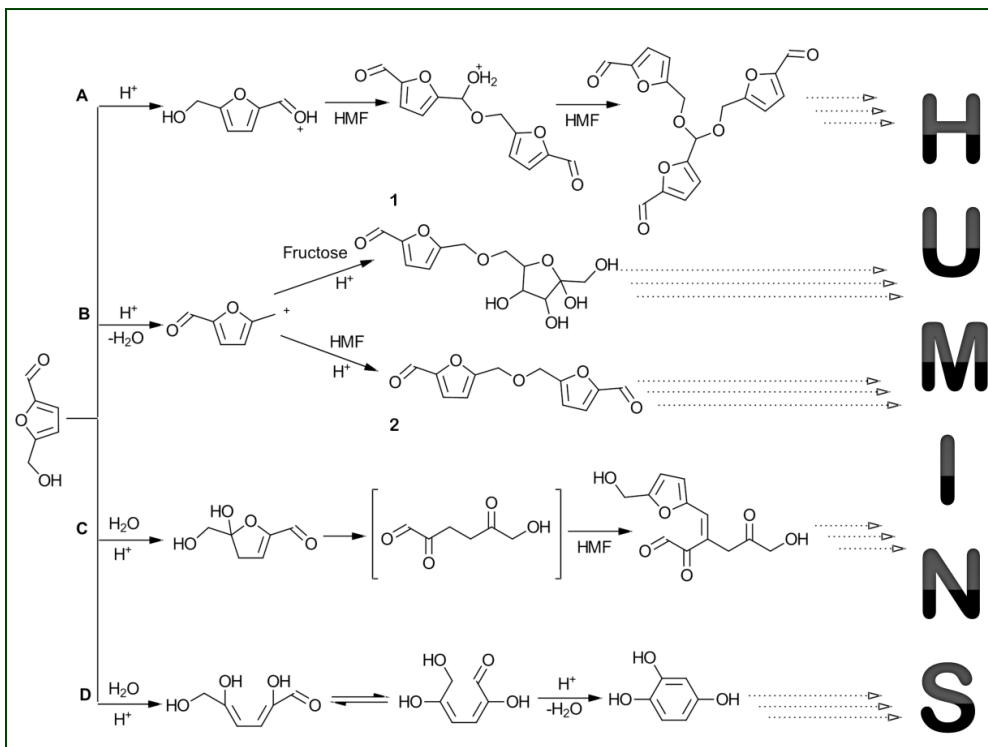
Figure 8. Mechanism of formation of key intermediates from HMF for the synthesis of humins identified in literature.[126,143,144,152-155]

The traditional use of mineral acids allows the presence of protons in the reaction media that can create electrophilic centers that can undergo a series of substitutions to form humins (Figure 9, A-B). Based on ^{13}C NMR studies on humins derived from a variety of C5- and C6-sugars, different parallel mechanisms were proposed.[143] It was observed that humins with furfural as intermediate (*i.e.* C5-derived) tend to form more C—C bonds between furan rings; on the other hand, C6-derived humins (*i.e.* HMF as intermediate) favor the formation of ether and/or acetal bonds.

With these findings, Sumerskii *et al.* proposed a series of mechanisms involving the formation of reactive cationic intermediates from HMF, furfural and levulinic acid. In the case of C6-derived humins, HMF was proposed to be prone to

polymerization *via* electrophilic attack of the carbonyl oxygen to form acetals (Figure 9, A), or *via* carbocation formation to ether intermediates (Figure 9, B2).[143] Acetalization has been disregarded by others, although not fully excluded as the observed signal could be ascribed to either ether or acetal linkages.[144] The formation of a carbocation *via* demethoxylation was proposed also by Yang *et al.*, considering both reaction with another HMF molecule or a sugar molecule (Figure 9, B). The reaction of an HMF-derived carbocation with fructose (Figure 9, B2) was found to be energetically favorable compared to a reaction with another HMF molecule. Nevertheless, activation energies are very low compared those observed for the formation of the desired products,[122] thus both pathways may occur simultaneously. Further, the absence of a hydrogen atom on the C_α position of HMF hints to cross-polymerizations between HMF, HMF derivatives, and/or sugars[129,138,149,150] rather than self-condensation.[151]

By studying *in situ*–NMR and ^{13}C-labeled fructose, it was proposed that pyranose-type molecules (hexose form) are responsible for humins formation rather than furanoses (pentose form).[149] The pyranose route, in particular, requires linearization and rearrangement of fructose to hexose prior to a series of dehydrations leading to humins. Although this could be plausible, the observation of prevalent furanic moieties in the structure suggests the occurrence of such mechanism only to a small extent. Linear levulinic acid, on the other hand, is considered stable towards the formation of humins; however, it was experimentally observed that the presence of levulinic acid in the reaction media increases humins yields.[118] According to Sumerskii *et al.*, levulinic acid undergoes protonation at the ketone functionality forming a reactive carbocation.[143]

Lignocellulosic sugars are highly soluble in water; hence, the latter is often used as reaction media. Otherwise, the presence of water in azeotropic mineral acids, the release of water molecules in the sugars-to-chemicals dehydrations, or simply adsorbed humidity on a catalyst surface (if heterogeneous) can prompt hydrolysis reaction catalyzed by the acidic media. Due to the importance of water, various hydrolysis/hydration mechanisms were proposed in the formation of humins (Figure 9, C—D).[126,143,152-155] Hydrolysis of HMF was proposed to undergo *via* the formation of a reactive ring-opening product. The formation of the hexanal known as DHH (in square brackets, Figure 9, C) has been brought forth although the intermediate has never been identified spectroscopically, while the formation of a benzenetriol (Figure 9, D) was observed at a smaller extent. Recent studies on the polymerization of model compounds suggest also the key role of α-carbonyl aldehydes, carboxylic acids and α,β-unsaturated aldehydes, although under hydrothermal conditions (*i.e.* non-acidic).[156,157] Nevertheless, it can be concluded that aldehyde functionalities play a role in the formation of humins.

In general, the presence of water and protons in the reaction media is a key trigger to the formation of humins, hence the use of biphasic systems/ionic liquids/anhydrous conditions to minimize polymerization. Yet, humins form inevitably, thus requiring their valorization.

2.4 General considerations on humins application potential

Maximization of HMF and/or furfural yields, hence minimization of humins formation, has been the main research focus to improve bio-processes economics in lignocellulosics conversion to furanics. However, as seen in the previous paragraphs,

humins will form in such acidic conditions, thus requiring valorization solutions.

Traditionally, humins are used as a fuel source as for instance in the Biofine process.[158] However, this solution is not valuable given the fairly low energy content of humins. In fact, thermal and fire behavior of humins showed heating values comparable to dry wood (*ca.* 20 kJ g^{-1}).[159] On the other hand, these results also show that humins can be safely stored against fire hazards with the same precautions used for woody materials. Short-term fish immunomarker tests showed that humins do not pose significant ecotoxicological threats, making these by-products potentially environmentally-friendly chemicals.[160] These safety properties make humins an attractive *green* product for new applications.

Thermal treatment of humins has also shown promising behavior for further upgrading to materials applications. In particular, low-temperature treatment (120-140 °C) was found to initiate crosslinking between furanic moieties and/or possible physisorbed monomers (*e.g.* HMF), increasing the glass transition of the initially viscous material.[161] At higher temperatures (180-900 °C) humins undergo decomposition and auto-crosslinking to form macroporous structures known as foams.[148,162] The more severe the thermal treatment, the more humins lose oxygen-containing groups, leading to a more aromatized compound, especially under inert gas. These thermal properties can be exploited for the production of thermoset materials with variable porosity and electron-transfer ability, depending on the application.

Furthermore, the presence of highly oxygenated functionalities in humin by-products suggests possibilities for

surface modification, as well as use as anchoring groups for adsorption and/or catalyst support applications. On the other hand, the observance of alkyl linkages in the humins structure hints to recalcitrant behavior towards decomposition to small molecules (*e.g.* furanics, levulinates), which under certain conditions (heat, catalyst) would lead to coke/char formation. Nevertheless, few valorization studies have been conducted so far on humin by-products, which are mainly focused on high temperature treatments (*e.g.* pyrolysis) and materials studies (*e.g.* composites).

2.5 Valorization routes for humin-based products

Thermal (catalytic) treatments of humins to hydrogen and/or oils have been investigated. Catalytic steam reforming of humins can be a sustainable pathway in the formation of hydrogen from natural resources. With a base catalyst, Na_2CO_3, a H_2/CO ratio of *ca.* 2 could be obtained from humins.[112,163] However, significant amounts of humins (*ca.* 45 wt%) are lost as volatiles, predominantly at high temperatures (700-1000 °C).[163] Lower temperature treatments (300-600 °C) such as (catalytic) pyrolysis and hydrothermal liquefaction have also been carried out, in particular for the production of biofuels. Generally, conversions of up to 70% were obtained with low specific product selectivities. Micropyrolysis gave only a 30 wt% yield cumulative of gas and liquid products.[164] The use of a catalyst for the same process decreased the char formation by *ca.* 15-45% depending on humins source (char: 38 wt% for industrial humins, 58 wt% for synthetic humins).[165] Up to 14 wt% oil yield could be achieved with H-ZSM-5 catalyst against other (alumino)silicates. Similar concentrations of alkyl phenolics with biofuel potential were obtained *via* catalytic hydrotreatment of humins.[166,167] In the presence of 2-propanol and an hydrogen

source, either H_2 or formic acid, up to 70% conversions were obtained for carbon-supported metal catalysts, *i.e.* Ru[166] or Pt.[167] Although promising, more suitable substrates (*e.g.* lignin) with higher aromatic concentrations may be preferred over using humins. Degradation to other products (*e.g.* organic acids) may offer higher resource efficiency in the process as deoxygenation reactions could occur only at very small extents. The production of acetic acid *via* H_2O_2-assisted wet oxidation yielded *ca.* 26% of the desired product.[168] However, the process relies on the alkaline-solubilization of humins as well as requiring an acidification step to pH ~1. The low yields combined with multiple auxiliary components make the process expensive. A more sustainable approach has been shown by using polyoxometalate catalysts in water under oxygen.[169] However, the process gave up to *ca.* 6% acetic acid yields, along with formic acid (up to 6%), and carbon oxides, with CO_2 being the main product. In general, the decomposition of humins will give a range of products which may be difficult to separate (*e.g.* similar boiling points) or which present in low yields. In this sense, taking advantage of humins as produced may be more promising and contribute directly to a circular economy.

Improvement of overall physical properties (*e.g.* tensile strength, water resistance) upon addition of humins to synthetic or natural fibers has been achieved.[170,171] In fact, humins can confer hydrophobic properties to flax fibers,[170] and decrease the brittleness of polyfurfuryl alcohol resins.[171] Alkaline-solubilized humins monomers were reacted with phenol and formaldehyde for the synthesis of adhesive resins.[172] An interesting approach for the one-pot conversion of bio-sugars and valorization of humins was given recently by Kang *et al.* whereby glucose is converted into levulinic acid in the presence of high concentrations of

para-toluenesulfonic acid (PTSA).[173] The use of PTSA allowed the double synthesis of levulinic acid (50 mol% yield) and sulfonated humins (25 wt%) to be used as a carbon-based catalyst. The final sulfonated carbon was then tested in the esterification of levulinic acid giving high activities.

The overall work on humin by-products valorization, however, requires further research to find economical and high added-value applications. Furthermore, deeper insights into the humins structure and mechanism of formation are still required in order to fully utilize these by-products. In this sense, we have studied different types of approaches to understand further the humins structure, mechanism of formation, and valorization. In particular:

- Photophysical studies were employed to understand the macromolecular complexity of humins;
- An innovative *down-up* approach *via* catalytic decompositions was used to gain insights into the mechanism and structure of humins;
- A valorization route is proposed taking advantage of the humins' oxygen functionalities for the synthesis of metal-organic nanocomposites.

References

[1] International Council of Chemical Associations, Sustainable Development, The chemistry of economic growth and propesperity, https://www.icca-chem.org/sustainable-development/ (accessed Jan 08, 2019).

[2] Vassilious, M. S. Historical dictionary of the petroleum industry. In *Historical dictionaries of professions and industries*; Woronoff, J. Ed.; Rowman & Littlefield: Lanham, 2018; 2nd Edition, pp 1-18.

[3] Landes, D. S. *The unbound Prometheus: Technological change and industrial development in Western Europe from 1750 to the present*; Cambridge University Press: Cambridge, 2003; 2nd Edition, Chapter 2, pp 41-123.

[4] Eriksen, M.; Lebreton, L. C. M.; Carson, H. S.; Thiel, M.; Moore, C. J.; Borerro, J. C.; Galgani, F.; Ryan, P. G.; Reisser, J. Plastic pollution in the world's oceans: More than 5 trillion plastic pieces weighing over 250,000 tons afloat at sea. *PLoS ONE* **2014**, *9*(12), e111913.

[5] Hann. S.; Sherrington, C.; Jamieson, O.; Hickman, M.; Kershaw, P.; Bapasola, A.; Cole, G. Investigating options for reducing releases in the aquatic environment of microplastics emitted by (but not intentionally added in) products. *Report for DG Environment of the European Commission*; Eunomia Research & Consulting and ICF; London, 2018; pp 1-100.

[6] Eerkes-Medrano, D.; Thompson, R. C.; Aldridge, D. C. Microplastics in freshwater systems: A review of the emerging threats, identification of knowledge gaps and prioritisation of research needs. *Water Res.* **2015**, *75*, 63–82.

[7] Law, K. L.; Thompson, R. C. Microplastics in the seas. *Science* **2014**, *345*(6193), 144-145.

[8] PlasticsEurope Operation Clean Sweep®. *Association of Plastics Manufactures Report*; PlasticsEurope AISBL; Brussels, 2018; pp 8-34.

[9] Aboudah, M. Dealing with economic sustainability challenges evolving from declining oil production in Saudi Arabia. M.Sc. Thesis, Michigan Technological University, November 2015.

[10] Campbell, C. J. *Campbell's atlas of oil and gas depletion*; Springer-Verlag: New York, 2013; 2nd Edition, pp 3-9.

[11] Global Climate Change: Vital signs of the planet, NASA. https://climate.nasa.gov/ (accessed Jan 08, 2019).

[12] World population projected to reach 9.8 billion in 2050, and 11.2 billion in 2100, Department of economic and social affairs, United Nations. https://www.un.org/development/desa/en/news/population/world-population-prospects-2017.html (accessed Jan 08, 2019).

[13] Sustainable Development knowledge platform, Sustainable Development Goals, United Nations. https://sustainabledevelopment.un.org/sdgs (accessed Jan 08, 2019).

[14] Sustainable Development Goals, Communications Material, United Nations. https://www.un.org/sustainabledevelopment/news/communications-material/ (accessed Jan 08, 2019).

[15] Global chemical industry contributions to the sustainable development goals. *International Council of Chemical Association (ICCA) Report*; September, 2017, pp 2-20. https://www.icca-chem.org/wp-content/uploads/2017/02/Global-Chemical-Industry-Contributions-to-the-UN-Sustainable-Development-Goals.pdf (accessed Jan 08, 2019).

[16] Chemistry can. Accelerating Europe towards a sustainable future. *Cefic sustainability report*; European Chemical Industry Council, Cefic; 2017, pp 1-29. https://chemistrycan.com/app/uploads/2017/10/SD-Report2017.pdf (accessed Jan 08, 2019).

[17] Pollution abatement costs and expenditures: 2005. *Current Industrial Reports*; Department of Commerce–Economics and Statistics Administration–U.S. Census Bureau; April 2008, pp 1-2. https://www.census.gov/prod/2008pubs/ma200-05.pdf (accessed Jan 08, 2019).

[18] Trost, B. M. The atom economy—A search for synthetic efficiency. *Science* **1991**, *254*, 1471-1477.

[19] Sheldon, R. A. The E Factor: fifteen years on. *Green Chem.* **2007**, *9*(12), 1273-1283.

[20] Anastas, P. T. Benign by Design Chemistry. In *Benign by Design: Alternative synthetic design for pollution prevention*; Anastas, P. T., Farris, C. A., Eds.; ACS Symposium Series: Washington, DC, 1994; pp 2-22.

[21] Anastas, P. T.; Warner, J. C. Green chemistry: Theory and practice. Oxford University Press: New York, 1998; pp 10-55.

[22] de Vries, J. G.; Jackson, S. D. Homogeneous and heterogeneous catalysis in industry. *Catal. Sci. Technol.* **2012**, *2*(10), 2009-2009.

[23] Sheldon, R. A. Catalysis: The key to waste minimization. *J. Chem. Tech. Biotechnol.* **1997**, *68*, 381-388.

[24] Anastas, P. T.; Kirchhoff, M. M.; Williamson, T. C. Catalysis as a foundational pillar of green chemistry. *Appl. Catal. A.* **2001**, *221*(1-2), 3-13.

[25] Smith, S. W. Chiral Toxicology: It's the Same Thing...Only Different. *Toxicol. Sci.* **2009**, *110*(1), 4-30.

[26] Judai, K.; Abbet, S.; Wörz, A. S.; Heiz, U.; Henry, C. R. Low-temperature cluster catalysis. *J. Am. Chem. Soc.* **2004**, *126*(9), 2732-2737.

[27] The Presidential Green Chemistry Challenge Awards Program, Summary of 1999 Award Entries and Recipients; *United States Environmental Protection Agency (EPA) Report*; EPA744-R-00-001; US Environmental Protection Agency, Office of Pollution Prevention and Toxics; Washington, DC, 2000; pp 5.

[28] Centi, G.; Quadrelli, E. A.; Perathoner, S. Catalysis for CO_2 conversion: a key technology for rapid introduction of renewable energy in the value chain of chemical industries. *Energy Environ. Sci.* **2013**, *6*(6), 1711-1731.

[29] Luque, R.; De, S.; Balu, A. M. Catalytic Conversion of Biomass. *Catalysts* **2016**, *6*, 148-149.

[30] Sun, Y.; Lin, Z.; Peng, S. H.; Sage, V.; Sun, Z. A critical perspective on CO_2 conversions into chemicals and fuels. *J. Nanosci. Nanotechnol.* **2019**, *19*(6), 3097-3109.

[31] Kondratenko, E. V.; Mul, G.; Baltrusaitis, J.; Larrazábal, G. O.; Pérez-Ramírez, J. Status and perspectives of CO_2 conversion into fuels and chemicals by catalytic, photocatalytic and electrocatalytic processes. *Energy Environ. Sci.* **2013**, *6*, 3112-3135.

[32] Cong, W.-F.; Jing, J.; Rasmussen, J.; Søegaard, K.; Eriksen, J. Forbs enhance productivity of unfertilised grass clover leys and support low carbon bioenergy. *Sci. Rep.* **2017**, *7*, 1422.

[33] Mauser, W.; Klepper, G.; Zabel, F.; Delzeit, R.; Hank, T.; Putzenlechner, B.; Calzadilla, A. Global biomass production potentials exceed expected future demand without the need for cropland expansion. *Nat. Commun.* **2015**, *6*, 8946.

[34] Wu, L.; Moteki, T.; Gokhale, A.A.; Flaherty, D.W.; Toste, F.D. Production of fuels and chemicals from biomass: Condensation reactions and beyond. *Chem* **2016**, *1*(1), 32-58.

[35] OPEC Annual Statistical Bulletin 2017. *Organization of the Petroleum Exporting Countries Report*; 0475-0608; OPEC; Vienna, 2017; pp 26.

[36] Woodward, F. I.; Lomas, M. R.; Kelly, C. K. Global climate and the distribution of plant biomes. *Phil. Trans. R. Soc. Lond. B* **2004**, *359*, 1465-1476.

[37] Abdel-Shafy, H. I.; Mansour, M. S. M. Solid waste issue: Sources, composition, disposal, recycling, and valorization. *Egypt. J. Petrol.* **2018**, *27*(4), 1275-1290.

[38] Ragauskas, A. J.; Williams, C. K.; Davison, B. H.; Britovsek, G.; Cairney, J.; Eckert, C. A.; Frederick Jr., W. J.; Hallet, J. P.; Leak, D. J.; Liotta, C. L.; Mielenz, J. R.; Murphy, R.; Templer, R.; Tschaplinski, T. The path forward for biofuels and biomaterials. *Science* **2006**, *311*, 484-489.

[39] Zabed, H.; Sahu, J. N.; Suely, A.; Boyce, A. N.; Faruq, G., Bioethanol production from renewable sources: Current perspectives and technological progress. *Renew. Sust. Energ. Rev.* **2017**, *71*, 475-501.

[40] Bruyn, M. D.; Fan, J.; Budarin, V. L.; Macquarrie, D. J.; Gomez, L. D.; Simister, R.; Farmer, T. J.; Raverty, W. D.; Mcqueen-Mason, S. J.; Clark, J. H., A new perspective in bio-refining: Levoglucosenone and cleaner lignin from waste biorefinery hydrolysis lignin by selective conversion of residual saccharides. *Energy Environ. Sci.* **2016**, *9*(8), 2571-2574.

[41] Werpy, T. A.; Petersen, G. Top value added chemicals from biomass: Volume I. Results of screening for potential candidates from sugars and synthesis gas. *US Department of Energy Report*; PNNL, NREL, EERE; Washington, DC, 2004; pp 1-66.

[42] Bozell, J. J.; Petersen, G. R. Technology development for the production of biobased products from biorefinery carbohydrates—the US Department of Energy's "Top 10" revisited. *Green Chem.* **2010**, *12*(4), 539-554.

[43] Girisuta, B. Levulinic acid from lignocellulosic biomass. Ph.D. Thesis, University of Groningen, November 2007.

[44] Tang, P.; Yu, J. Kinetic analysis on deactivation of a solid Brønsted acid catalyst in conversion of sucrose to levulinic acid. *Ind. Eng. Chem. Res.* **2014**, *53*(29), 11629-11637.

[45] Den, W.; Sharma, V. K.; Lee, M.; Nadadur, G.; Varma, R. S. Lignocellulosic biomass transformations via greener oxidative pretreatment processes: Access to energy and value-added chemicals. *Front. Chem.* **2018**, *6*, 141.

[46] Satari, B.; Karimi, K.; Kumar, R. Cellulose solvent-based pretreatment for enhanced second-generation biofuel production: A review. *Sustainable Energy Fuels* **2019**, *3*, 11-62.

[47] Mosier, N.; Wyman, C.; Dale, B.; Elander, E.; Lee, Y.Y.; Holtzapple, M.; Ladisch, M. Features of promising technologies for pretreatment of lignocellulosic biomass. *Bioresour. Technol.* **2005**, *96*(6), 673-686.

[48] Wagner, A. O.; Lackner, N.; Mutschlechner, M.; Prem, E. M.; Markt, R.; Illmer, P. Biological pretreatment strategies for second generation lignocellulosic resources to enhance biogas production. *Energies* **2018**, *11*(7), 1797.

[49] Kucharska, K.; Rybarczyk, P.; Hołowacz, I.; Łukajtis, R.; Glinka, M.; Kamiński, M. Pretreatment of lignocellulosic materials as substrates for fermentation processes. *Molecules* **2018**, *23*, 2937.

[50] Hou, Q.; Ju, M.; Li, W.; Liu, L.; Chen, Y.; Yang, Q. Pretreatment of lignocellulosic biomass with ionic liquids and ionic liquid based solvent systems. *Molecules* **2017**, *22*(3), 490.

[51] Kumar, G.; Dharmaraja, J.; Arvindnarayan, S.; Shaban, S.; Bakonyi, P.; Saratale, G. D.; Nemestóthy, N.; Bélafi–Bakó, K.; Yoong, J.-J.; Kim, S.-H. A comprehensive review on thermochemical, biological, biochemical and hybrid conversion methods of bio-derived lignocellulosic molecules into renewable fuels. *Fuel* **2019**, *251*, 352-367.

[52] Bensah, E. C.; Mensah, M. Y. Emerging physico-chemical methods for biomass pretreatment. In *Fuel ethanol production from sugarcane*; Basso, T. P., Basso, L. C., Eds.; IntechOpen Limited: London, 2018; Chapter 3, pp 41-62.

[53] Alvira, P.; Tomás-Pejó, E.; Ballesteros, M.; Negro M. J. Pretreatment technologies for an efficient bioethanol production process based on enzymatic hydrolysis: A review. *Bioresour. Technol.* **2010**, *101*, 4851-4861.

[54] Guragain, Y. N.; Vadlani, P. V. Importance of biomass-specific pretreatment methods for effective and sustainable utilization of renewable resources. In *Biotechnology and Biochemical Engineering*; Prasanna, B. D., Gummadi, S. N., Vadlani P. V., Eds.; Springer Science+Business Media: Singapore; pp 207-215.

[55] Yang, B.; Wyman, C. E. Pretreatment: the key to unlocking low-cost cellulosic ethanol. *Biofuels Bioprod. Technol.* **2007**, *2*(1), 26-40.

[56] Lloyd, T. A.; Wyman, C. E. Combined sugar yields for dilute sulfuric acid pretreatment of corn stover followed by enzymatic hydrolysis of the remaining solids. *Bioresour. Technol.* **2005**, *96*(18), 1967-1977.

[57] Heeres, H.; Handana, R.; Chunai, D.; Rasrendra, C. R.; Heeres, H. J. Combined dehydration/(transfer)-hydrogenation of C6-sugars (D-glucose

and D-fructose) to γ-valerolactone using ruthenium catalysts. *Green Chem.* **2009**, *11*, 1247-1255.

[58] Menegazzo, F.; Ghedini, E.; Michela, S. 5-Hydroxymethylfurfural (HMF) production from real biomasses. *Molecules* **2018**, *23*(9), 2201.

[59] DAWN Technology, Avantium. https://www.avantium.com/renewable-chemistries/dawn-technology/ (accessed May 10, 2019).

[60] Mirzaei, H. M.; Karimi, B. Sulphanilic acid as recyclable bifunctional organic catalyst in the selective conversion of lignocellulosic biomass to 5-HMF. *Green Chem.* **2016**, *18*, 2282-2286.

[61] Ferreira-Leitão, V. S.; Cammarota, M. C.; Gonçalves Aguieiras, E. C.; Vasconcelos de Sá, L. R.; Fernandez-Lafuente, R.; Guimarães Freire, D. M. The protagonism of biocatalysis in green chemistry and its environmental benefits. *Catalysts* **2017**, *7*, 9.

[62] Scott, E. L.; Bruins, M. E.; Sanders, J. P. M. Rules for the bio based production of bulk chemicals on a small scale. Can the production of bulk chemicals on small scale be competitive? *Wageningen UR/Biobased Commodity Chemistry Report*; BCH 2013/016; Agrotechnology and Food Sciences Group; Wageningen, 2013; pp 5-26.

[63] Morales, G.; Melero, J. A.; Paniagua, M.; Iglesias, J.; Hernández, B.; Sanz, M. Sulfonic acid heterogeneous catalysts for dehydration of C_6-monosaccharides to 5-hydroxymethylfurfural in dimethyl sulfoxide. *Chin. J. Catal.* **2014**, *35*(5), 644-655.

[64] Asghari, F. S.; Yoshida, H. Acid-catalyzed production of 5-hydroxymethyl furfural from d-Fructose in subcritical water. *Ind. Eng. Chem. Res.* **2006**, *45*(7), 2163-2173.

[65] Román-Leshkov, Y.; Chheda, J. N.; Dumesic, J. A. Phase modifiers promote efficient production of hydroxymethylfurfural from fructose. *Science* **2006**, *312*(5782), 1933-1937.

[66] Eminov, S.; Wilton-Ely, J. D. E. T.; Hallett, J. P. Highly selective and near-quantitative conversion of fructose to 5-hydroxymethyl furfural using mildly acidic ionic liquids. *ACS Sustainable Chem. Eng.* **2014**, *2*(4), 978-981.

[67] Han, H.; Zhao, H.; Liu, Y.; Li, Z.; Song, J.; Chu, W.; Sun, Z. Efficient conversion of fructose into 5-hydroxymethylfurfural over WO_3/reduced grapheme oxide catalysts. *RSC Adv.* **2017**, *7*, 3790-3795.

[68] Qi, X.; Watanabe, M.; Aida, T. M.; Smith Jr., R. L. Catalytic conversion of fructose and glucose into 5-hydroxymethylfurfural in hot compressed water by microwave heating. *Catal. Commun.* **2008**, *9*(13), 2244-2249.

[69] Shimizu, K.; Uozumi, R.; Satsuma, A. Enhanced production of hydroxymethylfurfural from fructose with solid acid catalysts by simple water removal methods. *Catal. Commun.* **2009**, *10*(14), 1849-1853.

[70] Huang, Z.; Pan, W.; Zhou, H.; Qin, F.; Xu, H.; Shen, W. Nafion-resin-modified mesocellular silica foam catalyst for 5-hydroxymethylfurfural production from D-fructose. *ChemSusChem* **2013**, *6*(6), 1063-1069.

[71] Chermahini, A. N.; Hafizi, H.; Andisheh, N.; Saraji, M.; Shahvar, A. The catalytic effect of Al-KIT-5 and KIT-5-So_3H on the conversion of fructose to 5-hydroxymethylfurfural. *Res. Chem. Intermed.* **2017**, *43*(10), 5507-5521.

[72] Zhang, S.; Zheng, Z.; Zhao, C.; Zhang, L. Fabrication of a novel and high-performance mesoporous ethylene tar-based solid acid catalyst for the dehydration of fructose into 5-hydroxymethylfurfural. *ACS Omega* **2017**, *2*(9), 6123-6130.

[73] Cheng, T.-Y.; Chao, P.-Y.; Huang, Y.-H.; Li, C.-C.; Hsu, H.-Y.; Chao, Y.-S.; Tsai, T.-C. Catalysis of ordered nanoporous materials for fructose dehydration through difructose anhydride intermediate. *Microporous Mesoporous Mater.*, **2016**, *233*, 148-153.

[74] Chen, J.; Li, K.; Chen, L.; Liu, R.; Huang, X.; Ye, D. Conversion of fructose into 5-hydroxymethylfurfural catalyzed by recyclable sulfonic acid-functionalized metal-organic frameworks. *Green Chem.* **2014**, *16*, 2490-2499.

[75] Sidhpuria, K. B.; Daniel-da-Silva, A. L.; Trindade, T.; Coutinho, J. A. Supported ionic liquid silica nanoparticles (SILnPs) as an efficient and recyclable heterogeneous catalyst for the dehydration of fructose to 5-hydroxymethylfurfural. *Green Chem.* **2011**, *13*(2), 340-349.

[76] Li, H.; Zhang, Q.; Liu, X.; Chang, F.; Zhang, Y.; Xue, W.; Yang, S. Immobilizing Cr^{3+} with SO_3H-functionalized solid polymeric ionic liquids as efficient and reusable catalysts for selective transformation of carbohydrates into 5-hydroxymethylfurfural. *Bioresour. Technol.* **2013**, *144*, 21-27.

[77] Watanabe, M.; Aizawa, Y.; Iida, T.; Aida, T. M., Levy, C.; Sue, K.; Inomata, H. Glucose reactions with acid and base catalysts in hot compressed water at 473 K. *Carbohydr. Res.* **2005**, *340*(12), 1925-1930.

[78] Chidambaram, M.; Bell, A. t. A two-step approach for the catalytic conversion of glucose to 2,5-dimethylfuran in ionic liquids. *Green Chem.* **2010**, *12*(7), 1253-1262.

[79] Zhang, Y.; Pidko, E. A.; Hensen, E. J. M. Molecular aspects of glucose dehydration by chromium chlorides in ionic liquids. *Chem.: Eur. J.* **2011**, *17*(19), 5281-5288.

[80] Choudhary, V.; Mushrif, S. H.; Ho, C.; Anderko, A.; Nikolakis, V.; Marinkovic, N. S.; Frenkel, A. I.; Sandler, S. I.; Vlachos, D. G. Insights into the interplay of Lewis and Brønsted acid catalysts in glucose and fructose conversion to 5-(hydroxymethyl)furfural and levulinic acid in aqueous media. *J. Am. Chem. Soc.* **2013**, *135*(10), 3997-4006.

[81] Chen, T.; Lin, L. Conversion of glucose in CPL-LiCl to 5-hydroxymethylfurfural. *Chin. J. Chem.* **2010**, *28*(9), 1773-1776.

[82] Eminov, S.; Brandt, A.; Wilton-Ely, J. D. E. T.; Hallett, J. P. The highly selective and near-quantitative conversion of glucose to 5-hydroxymethylfurfural using ionic liquids. *PLoS ONE* **2016**, *11*(10), e0163835.

[83] Wang, C.; Zhang, L.; Zhou, T.; Chen, J.; Xu, F. Synergy of Lewis and Brønsted acids on catalytic hydrothermal decomposition of carbohydrates and corncob acid hydrolysis residues to 5-hydroxymethylfurfural. *Sci. Rep.* **2017**, *7*, 40908.

[84] Yu, I. K. M.; Tsang, D. C. W.; Yip, A. C. K.; Chen, S. S.; Ok, Y. S.; Poon, C. S. Valorization of food waste into hydroxymethylfurfural: Dual role of metal ions in successive conversion steps. *Bioresour. Technol.* **2016**, *219*, 338-347.

[85] Cai, C. M.; Nagane, N.; Kumar, R.; Wyman, C. E. Coupling metal halides with a co-solvent to produce furfural and 5-HMF at high yields directly from lignocellulosic biomass as an integrated biofuels strategy. *Green Chem.* **2014**, *16*(8), 3819-3829.

[86] Hu, S.; Zhang, Z.; Song, J.; Zhou, Y.; Han, B. Efficient conversion of glucose into 5-hydroxymethylfurfural catalyzed by a common Lewis acid $SnCl_4$ in an ionic liquid. *Green Chem.* **2009**, *11*(11), 1746-1749.

[87] Atanda, L.; Mukundan, S.; Shrotri, A.; Ma, Q.; Beltramini, J. Catalytic conversion of glucose to 5-hydroxymethyl-furfural with a phosphated TiO_2 catalyst. *ChemCatChem* **2015**, *7*(5), 781-790.

[88] Hu, L.; Sun, Y.; Lin, L.; Liu, S. 12-Tungstophosphoric acid/boric acid as synergetic catalysts for the conversion of glucose into 5-hydroxymethylfurfural in ionic liquid. *Biomass Bioenergy* **2012**, *47*, 289-294.

[89] Lourvanij, K.; Rorrer, G. L. Reaction rates for the partial dehydration of glucose to organic acids in solid-acid, molecular-sieving catalysts powders. *J. Chem. Technol. Biotechnol.* **1997**, *69*(1), 35-44.

[90] Ohara, M.; Takagaki, A.; Nishimura, S.; Ebitani, K. Syntheses of 5-hydroxymethylfurfural and levoglucosan by selective dehydration of glucose using solid acid and base catalysts. *Appl. Catal. A* **2010**, *383*(1-2), 149-155.

[91] Dias, A. S.; Pillinger, M.; Valente, A. A. Liquid phase dehydration of D-xylose in the presence of Keggin-type heteropolyacids. *Appl. Catal. A* **2005**, *285*, 126-131.

[92] Choudhary, V.; Sandler, S. I.; Vlachos, D. G. Conversion of xylose to furfural using Lewis and Brønsted acid catalysts in aqueous media. *ACS Catal.* **2012**, *2*(9), 2022-2028.

[93] Nie, Y.; Hou, Q.; Li, W.; Bai, C.; Bai, X.; Ju, M. Efficient synthesis of furfural from biomass using $SnCl_4$ as catalyst in ionic liquid. *Molecules* **2019**, *24*, 549.

[94] Bruce, S. M.; Zong, Z.; Chatzidimitriou, A.; Avci, L. E.; Bond, J. Q.; Carreron, M. A.; Wettstein, S. G. Small pore zeolite catalysts for furfural synthesis from xylose and switchgrass in γ-valerolactone/water solvent. *J. Mol. Catal. A* **2016**, *422*, 18-22.

[95] Lessard, J.; Morin, J.-M.; Wehrung, J.-F.; Magnin, D.; Chornet, E. High yield conversion of residual pentoses into furfural via zeolite catalysis and catalytic hydrogenation of furfural to 2-methylfuran. *Top. Catal.* **2010**, *53*(15-18), 1231-1234.

[96] Kim, S. B.; You, S. J.; Kim, Y. T.; Lee, S.; Lee, H.; Park, K.; Park, E. D. Dehydration of D-xylose into furfural over H-zeolites. *Korean J. Chem. Eng.* **2011**, *28*(3), 710-716.

[97] Lima, S.; Pillinger, M.; Valente, A. A. Dehydration of D-xylose into furfural catalysed by solid acids derived from the layered zeolite Nu-6(1). *Catal. Commun.* **2008**, *9*(11-12), 2144-2148.

[98] Lima, S.; Fernandes, A.; Antunes, M. M.; Pillinger, M.; Ribeiro, F.; Valente, A. A. Dehydration of xylose into furfural in the presence of crystalline microporous silicoaluminophosphates. *Catal. Lett.* **2010**, *135*, 41-47.

[99] Antunes, M. M.; Lima, S.; Fernandes, A.; Pillinger, M.; Ribeiro, M. F.; Valente, A. A. Aqueous-phase dehydration of xylose to furfural in the

presence of MCM-22 and ITQ-2 solid acid catalysts. *Appl. Catal. A* **2010**, *417-418*, 243-252.

[100] Shi, X.; Wu, Y.; Yi, H.; Rui, G.; Li, P.; Yang, M.; Wang, G. Selective preparation of furfural from xylose over sulfonic acid functionalized mesoporous SBA-15 materials. *Energies* **2011**, *4*, 669-684.

[101] Zhang, J.; Zhuang, J.; Lin, L.; Liu, S.; Zhang, Z. Conversion of D-xylose into furfural with mesoporous molecular sieve MCM-41- as catalyst and butanol as the extraction phase. *Biomass Bioenergy* **2012**, *39*, 73-77.

[102] Dias, A. S.; Pillinger, M.; Valente, A. A. Dehydration of xylose into furfural over micro-mesoporous sulfonic acid catalysts. *J. Catal.* **2005**, *229*(2), 414-423.

[103] Agirrezabal-Telleria, I.; Requies, J.; Güemez, M. B.; Arias, P. L. Pore size tuning of functionalized SBA-15 catalysts for the selective production of furfural from xylose. *Appl. Catal. B.* **2012**, *115-116*, 169-178.

[104] Agirrezabal-Telleria, I.; Requies, J.; Güemez, M. B.; Arias, P. L. Dehydration of D-xylose to furfural using selective and hydrothermally stable arenesulfonic SBA-15 catalysts. *Appl. Catal. B.* **2014**, *145*, 34-42.

[105] Lin, Q.-X.; Zhang, C.-H.; Wang, X.; Cheng, B.-G.; Mai, N.; Ren, J.-L. Impact of activation on properties of carbon-based solid acid catalysts for the hydrothermal conversion of xylose and hemicelluloses. *Catal. Today* **2019**, *319*, 31-40.

[106] Wang, H.; Liu, S.; Zhao, Y.; Zhang, H.; Wang, J. Molecular origin for the difficulty in separation of 5-hydroxymethylfurfural from imidazolium based ionic liquids. *ACS Sustainable Chem. Eng.* **2016**, *4*(12), 6712-6721.

[107] Diallo, A.-O; Len, C.; Morgan, A. B.; Marlair, G. Revisiting physico-chemical hazards of ionic liquids. *Sep. Purif. Technol.* **2012**, *97*, 228-234.

[108] Weingarten, R.; Cho, J.; Xing, R.; Conner, W. C.; Huber, G. W. Kinetics and reaction engineering of levulinic acid production from aqueous glucose solutions. *ChemSusChem* **2012**, *5*(7), 1280-1290.

[109] Gürsel, I. V.; Noël, T.; Wang, Q.; Hessel, V. Separation/recycling methods for homogeneous transition metal catalysts in continuous flow. *Green Chem.* **2012**, *17*(4), 2012–2026

[110] Hübner, S.; de Vries, J. G.; Farina, V. Why does industry not use immobilized transition metal complexes as catalysts? *Adv. Synth. Catal.* **2016**, *358*(1), 3-25.

[111] YXY Technology, Avantium. https://www.avantium.com/yxy/ (accessed May 14, 2019).

[112] Hoang, T. M. C.; van Eck, E. R. H.; Bula, W. P.; Gardeniers, J. G. E.; Lefferts, L.; Seshan K. Humin based by-products from biomass processing as a potential carbonaceous source for synthesis gas production. *Green Chem.* **2015**, *17*(2), 959-972.

[113] Wang, S.; Lin, H.; Chen, J.; Zhao, Y.; Ru, B.; Qiu, K.; Zhou, J. Conversion of carbohydrates into 5-hydroxymethylfurfural in an advanced single-phase reaction system consisting of water and 1,2-dimethoxyethane. *RSC Adv.* **2015**, *5*(102), 84014-84021.

[114] Rice, F. A. H. Effect of aqueous sulfuric acid on reducing sugars. V. Infrared studies on the humins formed by the action of aqueous sulfuric acid on the aldopentoses and on the aldehydes derived from them. *J. Org. Chem.* **1958**, *23*(3), 465-468.

[115] Hayes, D. J.; Ross, J.; Hayes, M. H. B.; Fitzpatrick, S. W. The Biofine process—Production of levulinic acid, furfural, and formic acid from lignocellulosic feedstocks. In *Biorefineries-Industrial Processes and Products: Status Quo and Future Directions*; Kamm, B., Gruber, P. R., Kamm, M., Eds.; Wiley-VCH Verlag GmbH & Co.: Weinheim, 2006; Chapter 7, pp 139-164.

[116] Thapa, I.; Mullen, B.; Saleem, A.; Leibig, C.; Baker, R. T.; Giorgi, J. B. Efficient green catalysis for the conversion of fructose to levulinic acid. *Appl. Catal. A* **2017**, *539*, 70-79.

[117] Kang, S.; Yu, J. An intensified reaction technology for high levulinic acid concentration from lignocellulosic biomass. *Biomass Bioenergy* **2016**, *95*, 214-220.

[118] Tarabanko, V. E.; Smirnova, M. A.; Chernyak, M. Y.; Kondrasenko, A. A.; Tarabanko N. V. The nature and mechanism of selectivity decrease of the acid-catalyzed fructose conversion with increasing the carbohydrate concentration. *J. Sib. Fed. Univ. Chem.* **2015**, *8*(1), 6-18.

[119] van Zandvoort, I.; Wang, Y.; Rasrendra, C. B.; van Eck, E. R. H.; Bruijnincx, P. C. A.; Heeres, H. J.; Weckhuysen, B. M. Formation, molecular structure, and morphology of humins in biomass conversion: Influence of feedstock and processing conditions. *ChemSusChem* **2013**, *6*(9), 1745–1758.

[120] Sevilla, M.; Fuertes, A. B. Chemical and structural properties of carbonaceous products obtained by hydrothermal carbonization of saccharides. *Chem.: Eur. J.* **2009**, *15*(16), 4195–4203.

[121] Sevilla, M.; Fuertes, A. B. The production of carbon materials by hydrothermal carbonization of cellulose. *Carbon* **2009**, *47*(9), 2281–2289.

[122] Yang, G, Pidko, E. A.; Hensen, E. J. M. Mechanism of Brønsted acid-catalyzed conversion of carbohydrates. *J. Catal.* **2012**, *295*, 122–32.

[123] Girisuta, B.; Janssen, L. P. B. M.; Heeres, H. J. Kinetic study on the acid-catalyzed hydrolysis of cellulose to levulinic acid. *Ind. Eng. Chem. Res.* **2007**, *46*(6), 1696-1708.

[124] Girisuta, B.; Janssen, L. P. B. M.; Heeres, H. J. Green chemicals: a kinetic study on the conversion of glucose to levulinic acid. *Chem. Eng. Res. Des.* **2006**, *84*(5), 339-349.

[125] Kuster, B. F. M.; van der Baan, H. S. The influence of the initial and catalyst concentrations on the dehydration of D-fructose. *Carbohydr. Res.* **1977**, *54*(2), 165-176.

[126] Patil, S. K. R.; Heltzel, J.; Lund, C. R. F. Comparison of structural features of humins formed catalytically from glucose, fructose, and 5-hydroxymethylfurfuraldehyde. *Energy Fuels* **2012**, *26*(8), 5281-5293.

[127] Patil, S. K. R.; Lund, C. R. F. Formation and growth of humins via aldol addition and condensation during acid-catalyzed conversion of 5-hydroxymethylfurfural. *Energy Fuels* **2011**, *25*(10), 4745-4755.

[128] Tsilomelekis, G.; Orella, M. J.; Lin, Z.; Cheng, Z.; Zheng, W.; Nikolakis, V.; Vlachos, D. G. Molecular structure, morphology and growth mechanisms and rates of 5-hydroxymethyl furfural (HMF) derived humins. *Green Chem.* **2016**, *18*(7), 1983-1993.

[129] van Putten, R. -J.; van der Waal, J. C.; de Jong, E.; Rasrendra, C. B.; Heeres, H. J.; de Vries, J. G. Hydroxymethylfurfural, a versatile platform chemical made from renewable resources. *Chem. Rev.* **2013**, *113*(3), 1499-1597.

[130] Lamminpää, K.; Ahola, J.; Tanskanen, J. Kinetics of furfural destruction in a formic acid medium. *RSC Adv.* **2014**, *4*(104), 60243-60248.

[131] Danon, B.; van der Aa, L.; de Jong, W. Furfural degradation in a dilute acidic and saline solution in the presence of glucose. *Carbohydr. Res.* **2013**, *375*, 145-152.

[132] Weingarten, R.; Cho, J.; Conner, Jr., W. C.; Huber, G. W. Kinetics of furfural production by dehydration of xylose in a biphasic reactor with microwave heating. *Green Chem.* **2010**, *12*(8), 1423-1429.

[133] Eifert, T.; Liauw, M. A. Process analytical technology (PAT) applied to biomass valorisation: a kinetic study on the multiphase dehydration of xylose to furfural. *React. Chem. Eng.* **2016**, *1*(5), 521-532.

[134] Girisuta, B.; Janssen, L. P. B. M.; Heeres, H. J. A kinetic study on the decomposition of 5-hydroxymethylfurfural into levulinic acid. *Green Chem.* **2006**, *8*, 701-709.

[135] Swift, T. D.; Nguyen, H.; Anderko, A.; Nikolakis, V.; Vlachos, D. G. Tandem Lewis/Brønsted homogeneous acid catalysis: conversion of glucose to 5-hydroxymethylfurfural in an aqueous chromium(III) chloride and hydrochloric acid solution. *Green Chem.* **2015**, *17*(10), 4725-4735.

[136] Weingarten, R.; Kim, Y. T.; Tompsett, G. A.; Fernández, A.; Han, K. S.; Hagarman, E. W.; Conner Jr., W. C.; Dumesic, J. A.; Huber, G. W. Conversion of glucose into levulinic acid with solid metal(IV) phosphate catalysts. *J. Catal.* **2013**, *304*, 123-134.

[137] Heltzel, J.; Patil, S. K. R.; Lund, C.R.F. Humin Formation Pathways. In *Reaction Pathways and Mechanisms in Thermocatalytic Biomass Conversion II;* Schlaf, M., Zhang, Z., Eds.; Springer Science+Business Media: Singapore, 2016; Chapter 5, pp 105-118.

[138] Herzfeld, J.; Rand, D.; Matsuki, Y.; Daviso, E.; Makjurkauskas, M.; Mamajanov, I. Molecular structure of humin and melanoidin via solid state NMR. *J. Phys. Chem. B* **2011**, *115*(19), 5741-5745.

[139] Kang, S.; Li, X.; Fan, J.; Chang, J. A direct synthesis of adsorbable hydrochar by hydrothermal conversion of lignin. *Energ. Source Part A* **2016**, *38*(9), 1255-1261.

[140] Fuertes, A. B.; Camps Arbestain, M.; Sevilla, M.; Maciá-Agulló, J. A.; Fiol, S.; López, R.; Smernik, R. J.; Aitkenhead, W. P.; Arce, F.; Macias, F. Chemical and structural properties of carbonaceous products obtained by pyrolysis and hydrothermal carbonisation of corn stover. *Aust. J. Soil Res.* **2010**, *48*(7), 618-626.

[141] van Zandvoort, I.; Koers, E. J.; Weingarth, M.; Bruijnincx, P.C.A.; Baldus, M.; Weckhuysen, B.M. Structural characterization of ^{13}C-enriched humins and alkali-treated ^{13}C humins by 2D solid-state NMR. *Green Chem.* **2015**, *17*(8), 4383-4392.

[142] Gandini, A.; Belgacem, M. N. Furans in polymer chemistry. *Prog. Polym. Sci.* **1997**, *22*(6), 1203-1379.

[143] Sumerskii, I. V.; Krutov, S. M.; Zarubin, M. Y. Humin-like substances formed under conditions of industrial hydrolysis of wood. *Russ. J. Appl. Chem.* **2010**, *83*(2), 320-327.

[144] van Zandvoort, I.; van Eck, E. R. H.; de Peinder, P.; Heeres, H. J.; Bruijnincx, P. C. A.; Weckhuysen, B. M. Full, reactive solubilization of humin by-products by alkaline treatment and characterization of the alkali-treated humins formed. *ACS Sustainable Chem. Eng.* **2015**, *3*(3), 533-543.

[145] Constant, S.; Lancefield, C.S.; Weckhuysen, B.M.; Bruijnincx, P.C.A. Quantification and classification of carbonyls in industrial humins and lignins by ^{19}F NMR. *ACS Sustainable Chem. Eng.* **2016**, *5*(1), 965-972.

[146] Reiche, S.; Kowalew, N.; Schlögl, R. Influence of synthesis pH and oxidative strength of the catalyzing acid on the morphology and chemical structure of hydrothermal carbon. *ChemPhysChem* **2015**, *16*(3), 579-587.

[147] Tsilomelekis, G.; Josephson, T. R.; Nikolakis, V.; Caratzoulas, S. Origin of 5-hydroxymethylfurfural stability in water/dimethyl sulfoxide mixtures. *ChemSusChem* **2014**, *7*(1), 117-126.

[148] Tosi, P.; van Klink, G.P.M.; Celzard, A.; Fierro, V.; Vincent, L.; de Jong, E.; Mija, A. Auto-crosslinked rigid foams derived from biorefinery byproducts. *ChemSusChem* **2018**, *11*(16), 2797-2809.

[149] Akien, G. R.; Qi, L.; Horváth, I. T. Molecular mapping of the acid catalysed dehydration of fructose. *Chem. Commun.* **2012**, *48*(47), 5850-5852.

[150] Dee, S. J.; Bell, A. T. A study of the acid-catalyzed hydrolysis of cellulose dissolved in ionic liquids and the factors influencing the dehydration of glucose and the formation of humins. *ChemSusChem* **2011**, *4*(8), 1166-1173.

[151] Huber, G. W.; Dumesic, J. A. An overview of aqueous-phase catalytic processes for production of hydrogen and alkanes in a biorefinery. *Catal. Today* **2006**, *111*, 119-132.

[152] Horvat, J.; Klaić, B.; Metelko, B.; Šunjić, V. Mechanism of levulinic acid formation. *Tetrahedron Lett.* **1985**, *26*(17), 2111-2114.

[153] Hu, X.; Lievens, C.; Larcher, A.; Li, C.-Z. Reaction pathways of glucose during esterification: effects of reaction parameters on the formation of humin type polymer. *Bioresour. Technol.* **2011**, *102*(21), 10104-10113.

[154] Chuntanapum, A.; Matsumura, Y. Formation of tarry material from 5-HMF in subcritical and supercritical water. *Ind. Eng. Chem. Res.* **2009**, *48*(22), 9837-9846.

[155] Luijkx, G. C. A.; van Rantwijk, F.; van Bekkum, H. Hydrothermal formation of 1,2,4-benzenetriol from 5-hydroxymethyl-2-furaldehyde and D-fructose. *Carbohydr. Res.* **1993**, *242*, 131-139.

[156] Shi, N.; Liu, Q.; Cen, H.; Ju, R.; He, X.; Ma, L. Formation of humins during degradation of carbohydrates and furfural derivatives in various solvents. *Biomass Conv. Bioref.* [**2019**, 1-11.

[157] Shi, N.; Liu, Q.; Ju, R.; He, X.; Zhang, Y.; Tang, S.; Ma, L. Condensation of α carbonyl aldehydes leads to the formation of solid humins during the hydrothermal degradation of carbohydrates. *ACS Omega* **2019**, *4*, 7330-7343.

[158] Suganuma, S.; Nakajima, K.; Kitano, M.; Hayashi, S.; Michikazu, H. sp^3-Linked amorphous carbon with sulfonic acid groups as a heterogeneous acid catalyst. *ChemSusChem* **2012**, *5*(9), 1841-1846.

[159] Muralidhara, A.; Tosi, P.; Mija, A.; Sbirrazzuoli, N.; Len, C.; Engelen, V.; de Jong, D.; Marlair, G. Insights on the thermal and fire hazards of humins in support of their sustainable use in advanced biorefineries. *ACS Sustainable Chem. Eng.* **2018**, *6*(12), 16692-16701.

[160] Muralidhara, A.; Bado-Nilles, A.; Marlair, G.; Engelen, V.; Len, C.; Pandard, P. Humins in the environement: early stage insights on ecotoxicological aspects. *Biofuel Bioprod. Biorefin.,* **2019**, *13*(3), 464-470.

[161] Sangregorio, A.; Guigo, N.; van der Waal, J. C.; Sbirrazzuoli, N. Humins from biorefineries as thermoreactive macromolecular systems. *ChemSusChem* **2018**, *11*(24), 4246-4255.

[162] Mija, A. C.; de Jong, E.; van der Waal, J. C.; van Klink, G. P. M. Humins containing foam. WO Patent 2017074183A1, May 04, 2017.

[163] Hoang, T. M. C.; Lefferts, L.; Seshan, K. Valorization of humin-based byproducts from biomass processing—a route to sustainable hydrogen. *ChemSusChem* **2013**, *6*(9), 1651-1658.

[164] Rasrendra, C. B.; Windt, M.; Adisasmito, S.; Makertihartha, I. G. B. N.; van Eck, E. R. H.; Meier, D.; Heeres, H. J. Experimental studies on the pyrolysis of humins from the acid-catalysed dehydration of C6-sugars. *J. Anal. Appl. Pyrol.* **2013**, *104*, 299-307.

[165] Agarwal, S.; van Es, D.; Heeres, H. J. Catalytic pyrolysis of recalcitrant, insoluble humin byproducts from C6 sugar biorefineries. *J. Anal. Appl. Pyrol.* **2017**, *123*, 134-143.

[166] Wang, Y.; Agarwal, S.; Kloekhorst, A.; Heeres, H. J. Catalytic hydrotreatment of humins in mixtures of formic acid/2-propanol with supported Ruthenium catalysts. *ChemSusChem* **2016**, *9*(9), 951-961.

[167] Wang, Y.; Agarwal, S.; Heeres, H. J. Catalytic liquefaction of humin substances from sugar biorefineries with Pt/C in 2-propanol. *ACS Sustainable Chem. Eng.* **2017**, *5*(1), 469-480.

[168] Kang, S.; Zhang, G.; Yang, Q.; Tu, J.; Guo, X.; Qin, F. G. F.; Xu, Y. A new technology for utilization of biomass hydrolysis residual humins for acetic acid production. *Bioresources* **2016**, *11*(4), 9496-9505.

[169] Maerten, S. G.; Voß, D.; Liauw, M. A.; Albert, J. Selective catalytic oxidation of humins to low-chain carboxylic acids with tailor-made polyoxometalate catalysts. *ChemistrySelect* **2017**, *2*(24), 7296-7302.

[170] Sangregorio, A.; Guigo, N.; van der Waal, J. C.; Sbirrazzuoli, N. All 'green' composites comprising flax fibres and humins' resins. *Compos. Sci. Technol.* **2019**, *171*, 70-77.

[171] Pin, J.-M.; Guigo, N.; Mija, A.; Vincent, L.; Sbirrazzuoli, N.; van der Waal, J. C.; de Jong, E. Valorization of biorefinery side-stream products: Combination of humins with polyfurfuryl alcohol for composite elaboration. *ACS Sustainable Chem. Eng.* **2014**, *2*(9), 2182-2190.

[172] Kang, S.; Fu, J.; Zhang, G.; Zhang, W.; Yin, H.; Xu, Y. Synthesis of humin-phenol-formaldehyde adhesive. *Polymers* **2017**, *9*(8), 373-385.

[173] Kang, S.; Zhang, G.; Yang, X.; Yin, H.; Fu, X.; Liao, J.; Tu, J.; Huang, X.; Qin, F. G. F.; Xu, Y. Effects of *p*-toluenesulfonic acid in the conversion of glucose for levulinic acid and sulfonated carbon production. *Energy Fuels* **2017**, *31*(3), 2847-2854.

Chapter 2

Humins structural complexity *via* fluorescence

Abstract

Biomass conversion into chemicals, materials and fuels emerged in the past decade as the most promising alternative to the current petroleum-based industry. However, the chemocatalytic conversion of biomass and bio-derived sugars often leads to numerous side-products, such as humins. The limited characterization of humins materials restricts their study for possible future applications. Thus, herein photophysical studies on humins and separated humins fractions were carried out using steady-state and time-resolved fluorescence techniques. This paper aims to add to the literature important information for scientists involved in photophysical studies.

Introduction

The ongoing decrease of fossil feedstocks has pushed research towards the implementation of new technologies. Biomass conversion, for instance, has emerged in the past decade as an economically valid, environmentally-friendly, sustainable alternative to the petroleum-based industry, thanks to its abundance, potential fast renewability, and compatibility with the current refinery technologies. However, the conversion of biomass/sugars leads to numerous side-products, limiting overall product yields and thus gravely effecting process economy. In particular, side-production of humins with yields of up to 50 wt% causes a major concern for the implementation of biorefineries.[1-4] Reduction of humin formation, in fact, has been one of the focuses in biomass conversion;[5-7] however, these studies often resort to cost ineffective technologies, such as the use of ionic liquids, recently proposed by Eminov *et al.*[7] The authors of this manuscript, in contrast, believe in the potential valorization of humin by-products to high-end chemicals, such as platform molecules, additives, materials, *etc*. In order to fully understand the applicability of these dark and insoluble compounds in-depth characterization is required.

So far, the formation mechanism of humins and their structure have not yet been unequivocally established, also due to the random character of these polymeric compounds. Numerous characterization and mechanistic studies have been performed on humins by means of IR, ^{13}C NMR, and pyrolysis-GC-MS.[2,4,5,8-17] In general, a polymeric furanic-rich structure (270-650 g mol^{-1})[15] has been postulated, linked by short aliphatic chains, and acetal and/or ether functional group, leading to a highly oxygenated and possibly conjugated structure (Fig. 1). The conjugated structure of humins

suggests, therefore, possible fluorescence activity which could be applied to optical sciences. In fact, an organic π-conjugated system has attracted increasing attention thanks to its tunable optical and electronic properties, finding applications as organic photovoltaics, organic light-emitting devices, and organic field-effect transistors.[18-22] For this reason, fructose-derived humins (*ca.* 400 g mol^{-1})[15] solubilized in acetonitrile was investigated by means of steady-state and time-resolved fluorescence techniques. Moreover, these techniques have been applied to the separated organic and aqueous fractions of the said solution, as the isolation of humins oligomers might yield to highly fluorescent molecules. In general, the aim of this manuscript is to give the reader new information on humin by-products, and possibly the inspiration towards the valorization of these compounds to high-end products.
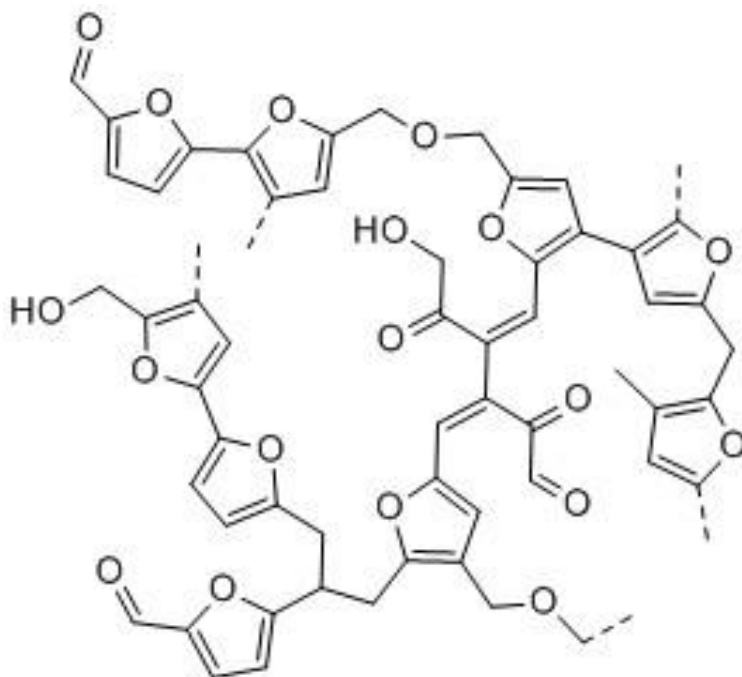
Figure 1. Humin structure adapted from ref. 16.

Results and Discussion

Fig. S1 (*vide* ESI†) displays the absorption spectrum (green line) of a dark solution of humins in a solvent with high polarity, *i.e.* acetonitrile (ACN). A featureless absorption signal with increasing values at the high-energy region is observed in the studied absorption range. Given the multicomponent character of the humins with the likely presence of different polymeric furan-rich species, the observed broad absorption signal can be explained as the overlapped contribution of different absorbing species. Fig. 2A shows the emission spectra of the humins in ACN at different excitation wavelengths (λ_{exc} = 250, 330 and 380 nm), revealing the presence of three emission peaks with maxima at 330, 405 and 500 nm. The emission peak at 500 nm is always detected regardless of the excitation wavelength, while the additional emission peaks at 330 and 405 nm appears exclusively upon excitation at 250 and 330 nm, respectively. Fig. 2B also exhibits the excitation spectra at selected emission wavelengths (λ_{em} = 325, 400 and 560 nm) indicating that three different absorption peaks are responsible for each emission signal. These results support our initial assumption that the absorption spectrum is composed of signals from different species. Thus, the overall fluorescence behavior can be easily accounted for the presence of three different fluorophores emitting at different wavelengths. The three species could be ascribed to different oligomeric fragments of the humins with varying length in the π-conjugated system including furan rings and double bonds.

With the aim of isolating each single fluorophore contained in the ACN solution, simple separations in biphasic systems have been performed in toluene/H_2O and in pentane/H_2O mixtures. When using toluene as the separating agent, all the aforementioned

emission peaks were observed indicating that the three fluorophores are soluble in both solvents, despite being reported that humins have poor solubility in H_2O (1.4 mg/mL).[23]
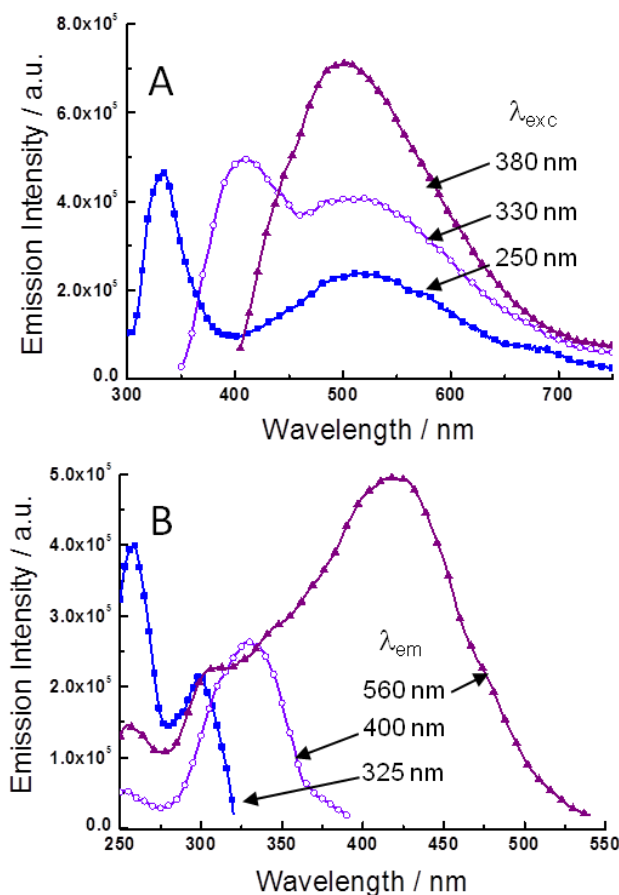
Figure 2. (A) Emission spectra of humins in ACN at different excitation wavelengths. λ_{exc} = 250 (full blue squares), 330 (empty violet circles) and 380 nm (full purple triangles). (B) Absorption and excitation spectra of the humins in ACN. λ_{em} = 330 (full blue squares), 400 (empty violet circles) and 560 nm (purple full triangles) in the excitation spectra.

The highly oxygenated (polar) and aromatic (non-polar) structure of humins denotes a certain amphiphilic character for these materials that certainly explains their solubility in the toluene/H_2O mixed solution. Regarding the pentane/H_2O solution, a partial separation of the components was observed in this case

based on the absorption and emission spectra for each phase. Thus, Fig. S1 (ESI†) shows the absorption spectra of the pentane and its aqueous fractions with again a featureless signal in the H_2O phase similar to that in ACN but with a more defined shape of the absorption signal in the organic phase. Thus, an apparent absorption band is visible at 365 nm with an additional signal around 325 nm in the pentane phase. Fig. 3A exhibits the excitation (λ_{em} = 385 nm) and emission (λ_{exc} = 310 nm) spectra of the organic fraction.

Excitation at different wavelengths was also performed giving no signal or the same emission spectrum as in λ_{exc} = 310 nm, which proves that only one fluorophore is found in the pentane phase (fluorophore **1**). The emission band is centered at around 375 nm with a vibrational progression at shorter wavelength. The position of this emission peak does not match with those measured in the ACN solution, which might be explained due to the different dielectric constant between both solvents (ACN *vs.* pentane) indicating a polarity-dependent deactivation process. Fig. 3B displays the emission spectra for the aqueous phase at two excitation wavelengths, λ_{exc} = 330 and 410 nm. The excitation with the longer wavelength (λ_{exc} = 410 nm) generates an intense emission peak with maximum at 530 nm, while pumping with a shorter wavelength (λ_{exc} = 330 nm) produces an emission peak at 415 nm and a shoulder at around 525 nm that matches well that obtained when exciting at a longer wavelength (λ_{exc} = 410 nm). This behavior is accounted for the presence of two emitting species in the aqueous phase, fluorophore **2** and **3** with λ_{em} = 415 and 530 nm, respectively. Moreover, the excitation spectra at λ_{em} = 410 and 560 nm (Fig. 3B) are almost identical to those observed in the ACN solution for the

same λ_{em} which indicates that the same two fluorophores **2** and **3** are present in both solutions.
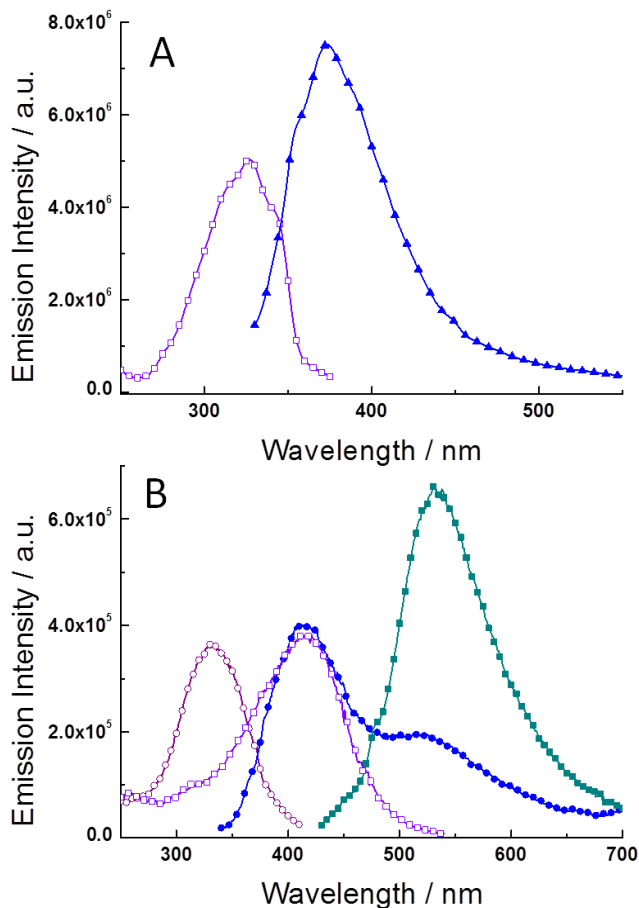
Figure 3. Excitation and emission spectra of the humins in the pentane phase (A) and in the aqueous phase (B). (A) λ_{em} = 385 (empty violet squares) in the excitation spectrum and λ_{exc} = 310 (full blue triangles) in the emission spectrum. (B) λ_{em} = 410 nm (empty purple circles) and λ_{em} = 560 nm (empty violet squares) in the excitation spectrum and λ_{exc} = 330 (full blue circles) and 410 nm (full green squares) in the emission spectrum.

The reported excitation and emission spectra of a highly concentrated ACN solution of furfural exhibits similar peaks to those presented in this work, greatly supporting the presence of furfural-based derivatives in our humin samples.[24] Finally, based on

the previous results we attribute the emission peak (λ_{em} = 375 nm) in the pentane fraction to the same species responsible for the emission peak at λ_{em} = 330 nm in the ACN solution (fluorophore **1**). These results prove the possibility of isolating the fluorophores with a simple mixture of water/pentane which could find application in organic electronics.

Time-resolved fluorescence measurements were also performed to shed light into the photophysical deactivation of the different components in the humins solutions. Table 1 shows the derived fluorescence lifetimes (τ) obtained from both mono- and bi-exponential fits of the emission signals. In the ACN solution, the lifetime derived at λ_{em} = 420 nm is 2.14 ns, which might attributed to fluorophore **2** since it is essentially the only species emitting at this wavelength. The latter value is in good agreement with that obtained for the aqueous fraction at the same wavelength (τ = 2.56 ns) indicating that both signals arise from the same fluorophore **2**. The experimental emission signal at λ_{em} = 530 nm of the ACN solution was fitted by using a bi-exponential function, with τ_1 = 0.10 ns and τ_2 = 2.17 ns. The origin of the double exponential behavior is unclear, but it might be tentatively assigned to the presence of a wide distribution of polymeric chains with different lengths that eventually produce a combination of emission lifetimes (fluorophore **3**). The same double exponential behavior was also detected in the aqueous fraction but with slightly lower lifetimes, τ_1 = 0.10 ns and τ_2 = 1.20 ns. Finally, the fit of the experimental emission signal of the pentane fraction gave a lifetime value of 1.70 ns, corresponding to the fluorophore **1** that is successfully separated in the organic phase.

Table 1. Lifetimes of the fluorophores derived from both mono- or bi-exponential fits of the experimental signals at λ_{exc} = 320 or 440 nm and λ_{em} = 370, 420 or 530 nm.

	λ_{exc} = 320 nm		λ_{exc} = 440 nm	
	λ_{em} = 370 nm	λ_{em} = 420 nm	λ_{em} = 530 nm	
	τ/ns	τ/ns	τ_1/ns	τ_2/ns
ACN solution		2.14	0.10 (0.30)	2.17 (0.70)
Pentane Fraction	1.70			
Aqueous Fraction		2.56	0.10 (0.15)	1.20 (0.85)

Conclusions

In summary, the results of the photophysical studies on humin by-products shows the presence of three distinctive fluorophores across the spectrum, of which one (fluorophore 1, emitting in the UV region), can be isolated by a simple separation of the starting solution with a water/pentane mixture. The time-resolved fluorescence studies showed both mono- and bi-exponential fits of the emission signals, with lifetimes of *ca.* 2 ns. In conclusion, a general elucidation of the photophysical properties of humin by-products in solution have been presented in the hopes of inspiring scientists in the investigation of these so-far waste materials for future optoelectronic applications.

References

[1] Filiciotto, L.; Balu, A. M.; van der Waal, J. C.; Luque, R. Catalytic insights into the production of biomass-derived side products methyl levulinate, furfural and humins. *Catal. Today* **2018**, *302,* 2-15.

[2] Rice, F. A. H. Effect of aqueous sulfuric acid on reducing sugars. V. Infrared studies on the humins formed by the action of aqueous sulfuric acid on the aldopentoses and on the aldehydes derived from them. *J. Org. Chem.* **1958**, *23*(3), 465–468.

[3] Hoang, T. M. C.; Lefferts, L.; Seshan, K. Valorization of humin-based byproducts from biomass processing—a route to sustainable hydrogen. *ChemSusChem* **2013**, *6,* 1651-1658.

[4] Sumerskii, I.V.; Krutov, S. M.; Zarubin, M. Y. Humin-like substances formed under conditions of industrial hydrolysis of wood. *Russ. J. Appl. Chem.* **2010**, *83*(2), 320–327.

[5] Wang, S.; Lin, H.; Zhao, Y.; Chen, J.; Zhou, J. Structural characterization and pyrolysis behavior of humin by-products from the acid-catalyzed conversion of C6 and C5 carbohydrates. *J. Anal. Appl. Pyrolysis* **2016**, *118*, 259-266.

[6] Tang, X.; Sun, Y.; Zeng, X.; Hao, W.; Lin, L.; Liu, S. Novel process for the extraction of ethyl levulinate by toluene with less humins from the ethanolysis products of carbohydrates. *Energy Fuels* **2014**, *28*(7), 4251-4255.

[7] Eminov, S.; Brandt, A.; Wilton-Ely, J. D. E. T.; Hallett, J. P. The highly selective and near-quantitative conversion of glucose to 5-hydroxymethylfurfural using ionic liquids. *PLoS ONE* **2016**, *11*(10), e0163835.

[8] van Putten, R. -J.**;** van der Waal, J. C.; de Jong, E.; Rasrendra, C. B.; Heeres, H. J.; de Vries, J. G. Hydroxymethylfurfural, A Versatile Platform Chemical Made from Renewable Resources. *Chem. Rev.* **2013**, *113*, 1499–1597.

[9] Stankovikj, F.; McDonald, A. G.; Helms, G. L.; Garcia-Perez, M. Quantification of bio-oil functional groups and evidences of the presence of pyrolytic humins. *Energy Fuels* **2016**, *30*(8), 6505-6524.

[10] Horvat, J.; Klaić, B.; Metelko, B.; Šunjić, V. Mechanism of levulinic acid formation. *Tetrahedron Lett.* **1985**, *26*(17), 2111-2114.

[11] Patil, S.K.R.; Heltzel, J.; Lund, C.R.F. Comparison of structural features of humins formed catalytically from glucose, fructose, and 5-hydroxymethylfurfuraldehyde. *Energy Fuels* **2012**, *26*(8), 5281-5293.

[12] Patil, S. K. R.; Lund, C. R. F. Formation and growth of humins via aldol addition and condensation during acid-catalyzed conversion of 5-hydroxymethylfurfural. *Energy Fuels* **2011**, *25*(10), 4745-4755.

[13] Herzfeld, J.; Rand, D.; Matsuki, Y.; Daviso, E.; Makjurkauskas, M.; Mamajanov, I. Molecular structure of humin and melanoidin via solid state NMR. *J. Phys. Chem. B* **2011**, *115*(19), 5741-5745.

[14] Akien, G.R.**;** Qi, L.; Horváth, I. T. Molecular mapping of the acid catalysed dehydration of fructose. *Chem. Commun.* **2012**, *48*(47), 5850-5852.

[15] van Zandvoort**,** I.; Wang, Y.; Rasrendra, C. B.; van Eck, E. R. H.; Bruijnincx, P. C. A.; Heeres, H. J.; Weckhuysen, B. M. Formation, molecular structure, and morphology of humins in biomass conversion: Influence of feedstock and processing conditions. *ChemSusChem* **2013**, *6*, 1745–1758.

[16] van Zandvoort, I.; van Eck, E. R. H.; de Peinder, P.; Heeres, H. J.; Bruijnincx, P. C. A.; Weckhuysen, B. M. Full, reactive solubilization of humin by-products by alkaline treatment and characterization of the alkali-treated humins formed. *ACS. Sustainable Chem. Eng.* **2015**, *3*(3), 533-543.

[17] Tsilomelekis**,** G.**;** Orella, M. J.; Lin, Z.; Cheng, Z.; Zheng, W.; Nikolakis, V.; Vlachos, D. G. Molecular structure, morphology and growth mechanisms and rates of 5-hydroxymethyl furfural (HMF) derived humins. *Green Chem.* **2016**, *18*(7), 1983–1993.

[18] Mazzio, K. A.; Luscombe, C. K. The future of organic photovoltaics. *Chem. Soc. Rev.* **2015**, *44*(1), 78-90.

[19] Zhong, C.; Duan, C.; Huang, F.; Wu, H.; Cao, Y. Materials and devices toward fully solution processable organic light-emitting diodes. *Chem. Mater.* **2011**, *23*(3), 326-340.

[20] Jou, J.-H.; Kumar, S.; Agrawal, A.; Li, T.-H.; Sahoo, S. Approaches for fabricating high efficiency organic light emitting diodes. *J. Mater. Chem. C* **2015**, *3*(13), 2974-3002.

[21] Wang. C.; Dong, H.; Hu, W.; Liu, Y.; Zhu, D. Semiconducting π-conjugated systems in field-effect transistors: A material odyssey of organic electronics. *Chem. Rev.* **2012**, *112*(4), 2208-2267.

[22] Zhang, C.l Chen, P.; Hu, W. Organic field-effect transistor-based gas sensors. *Chem. Soc. Rev.* **2015**, *44*(8), 2087-2107.

[23] Mija, A.; van der Waal, J. C.; Pin, J.-M.; Guigo, N.; de Jong, E. Humins as promising material for producing sustainable carbohydrate-derived building materials. *Constr. Build. Mater.* **2016**, *139*, 594-601.

[24] Gude, V.; Das, A.; Chatterjee, T.; Mandal, P. K. Molecular origin of photoluminescence of carbon dots: aggregation-induced orange-red emission. *Phys. Chem. Chem. Phys.* **2016**, *18*(40), 28247-28280.

Electronic Supplementary Information (ESI)

1. Experimental Section

1.1 Materials

Fructose-derived humin by-products were provided by Avantium (Netherlands) and used as received. Acetonitrile (99.9%), and toluene (99.8%) and pentane (≥99%) were purchased by PanReac and Sigma Aldrich, respectively, and employed without further purification.

1.2 Methods

Humins solutions in acetonitrile were prepared with a 0.1 g/mL ratio, whereas separations in the different fractions were performed by adding to the humins solution equal parts of water/organic solvent (*i.e.* toluene or pentane). UV-visible absorption spectra were measured on a Cary 100 Bio UV-visible spectrophotometer, by adjusting the concentration of the solution up to 0.5 a.u. of absorbance. Steady-state and time-resolved fluorescence measurements were performed on a FLS920 Fluorimeter (Edinburgh Instrument Ltd, Livingston, UK) with the same sample employed for the absorbance measurements.
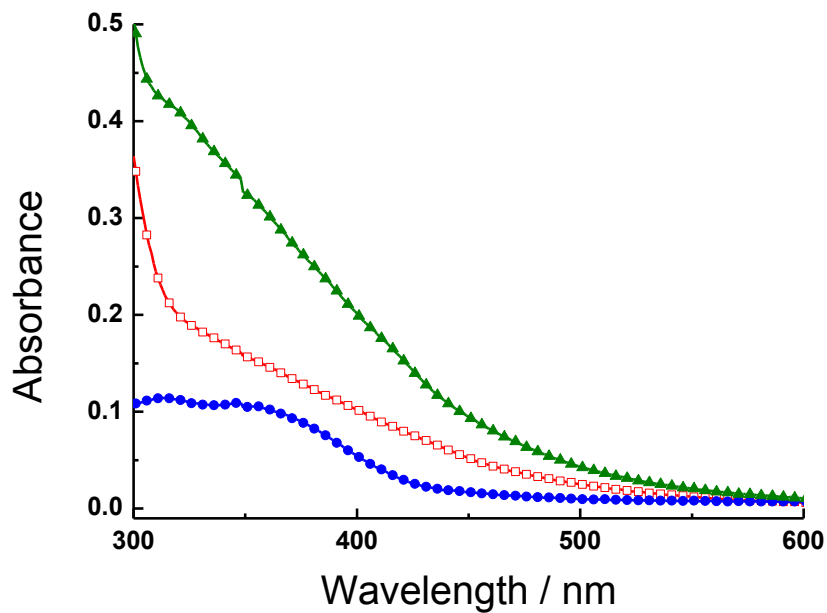
Figure S1. Absorption spectra of the humins in the ACN solution (full green triangles), and in the organic phase (full blue circles) and in the aqueous phase (empty red squares) of the pentane/water mixture.

Chapter 3

Humins structural complexity *via* decomposition

This chapter is based on: Filiciotto, L.; Balu, A. M., Romero, A. A.; Angelici, C.; van der Waal, J. C.; Luque, R. Reconstruction of humins formation mechanism from decomposition products: A GC-MS study based on catalytic continuous flow depolymerizations. *Mol. Catal.* 2019, *479,* 110564.

Abstract

Humins, a by-product of biomass chemical conversion technologies, still present controversies in their structural and mechanistic identification. Traditional studies of the structure and mechanism have focused so far on their syntheses from key molecules (sugars, HMF) and spectroscopic analyses of the as-synthesized oligomers/macromolecules. Herein, we propose structural and mechanism insights based on a novel down-up approach involving the decomposition of humins via catalytic reactions in continuous flow and interpretation of product molecules. The apparent co-existence of different mechanisms proposed in literature is observed upon product distribution analysis, and the key molecules taking part into humins formation are identified, including furanics, levulinates, sugar-derived molecules, and others. This work shows the complexity of humins formation, and their need of valorization.

Introduction

The continuous worldwide increase of population density (projected to 9.8 billion by 2050),[1] depletion of clean fossil-based resources (thus higher consumer price and more intensive purification technologies), and the importance of climate change mitigation by reducing green-house gases emissions (<2 °C global temperature increase),[2] call for the development of renewable and benign technologies, for instance biomass conversion.[3-8] Depending on the conversion technology (microbial fermentation vs chemical transformation), the transformation of lignocellulosic biomass (a complex structure comprised of lignin, cellulose, and hemicelluloses which does not compete with food-required biomass)[9] can yield a variety of important platform chemicals (Scheme 1). In particular, hydrolysis in alcoholic media (*e.g.* methanol, MeOH), yields to 5-methoxymethylfuran-2-carbaldehyde (MMF), the ether counterpart of important platform chemical, 5-hydroxymethylfurfural (HMF).
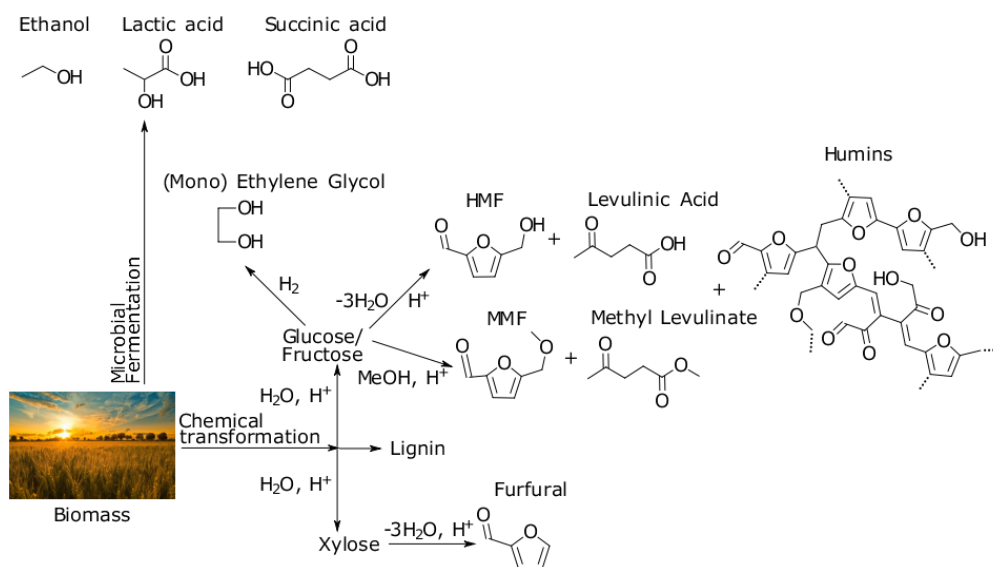
Scheme 1. Products and by-products of the biomass conversion technologies via microbial fermentation or chemical transformation, focused on acid-catalyzed hydrolysis.

An example of the advantage of biomass-conversion strategies lies in the production of bio-based plastics. In fact, a recent Life Cycle Assessment (LCA) on *traditional* bioplastics (*e.g.* bio-polyethylene, -polyamides, -polylactic acid) shows an astonishing possible reduction of up to 316 million tons of CO_2-eq. per year with the substitution of less than 66% of fossil-based plastics.[10] Parallel to traditional bio-plastics, the new platform chemicals that can be produced from biomass conversion (*e.g.* furanics as opposed to aromatics) can open new possibilities into the production of new bio-based plastics. For instance, polymerization of 2,5-furandicarboxylic acid (FDCA) and monoethylene glycol (MEG) yields PEF (polyethylene furanoate), a plastic with improved properties compared to PET (polyethylene terephthalate).[11,12] The production of FDCA relies on the acid-catalyzed hydrolysis of (lignocellulosic) biomass and consequent sugars (*i.e.* glucose, fructose) into HMF, and subsequent selective oxidation. However, the first conversion step into HMF favors the production of insoluble, black, oligomeric/macromolecular by-products denominated as humins with yields up to 30-40 wt%.[13-15] Minimization of humins can be achieved by utilizing biphasic solvent systems,[16-18] or by employing ionic liquids,[19] but their formation is unavoidable and is influenced by process conditions, including temperature, pH, residence time, substrate nature and concentrations, solvent systems, and catalysts. For this reason, humin by-products may not have a univocal structure and/or mechanism of formation. However, understanding the classes of products involved in their formation can aid their minimization by benign and economic strategies, and/or valorization to high-added value products.

So far, structural identification has been carried out with a variety of techniques comprising FT/ATR-IR; ^{1}H, ^{13}C and 2D NMR; elemental analysis; pyrolysis GC-MS; and Raman spectroscopy by synthesis of humins with either fructose, glucose, cellobiose, and/or HMF.[20-25] Higher incorporation of HMF was observed in the fructose-derived humins due to kinetics of formation.[26] Generally, humins are believed to display an oligo/macromeric furanic backbone with short aliphatic chains and ether bonds, given by a random polycondensation of the molecules involved in the carbohydrates acid hydrolysis (*e.g.* HMF).[24-28] In particular, 2D-NMR showed the presence of C_α and to a smaller extent C_β self- and aliphatic linkages,[28] also seen from IR analyses.[29] The α and β were in fact crucial nucleophilic centres in the formation of humins from HMF.[30] Ketone, hydroxyl, carboxylic, and/or aldehyde groups have been evidenced as functionalities in bulk structural analysis.[31] The overall elemental composition of humins is of the order of *ca.* 65wt% C, 30wt% O, and 5wt% H.[32] Recently, Constant *et al.* quantified the carbonyl concentration of industrial humins, setting it at 6.6wt%.[33] Traditional humins possess high and low molecular weight fractions, whose property is attributed to the length and complexity of the oligo/macromeric chains.[34] In fact, emission and excitation UV-Vis spectra of aqueous and organic fractions of humins show the presence of three fluorescent species, given by different conjugated chain lengths and complexity.[35] In general, we can consider humins as a complex matrix of different polymeric chains comprised of conjugated furanic rings, and oxygenated and aliphatic linkages, which resemble the structure of early hydrothermal carbons (HTC) from carbohydrates (Scheme 2).[36]
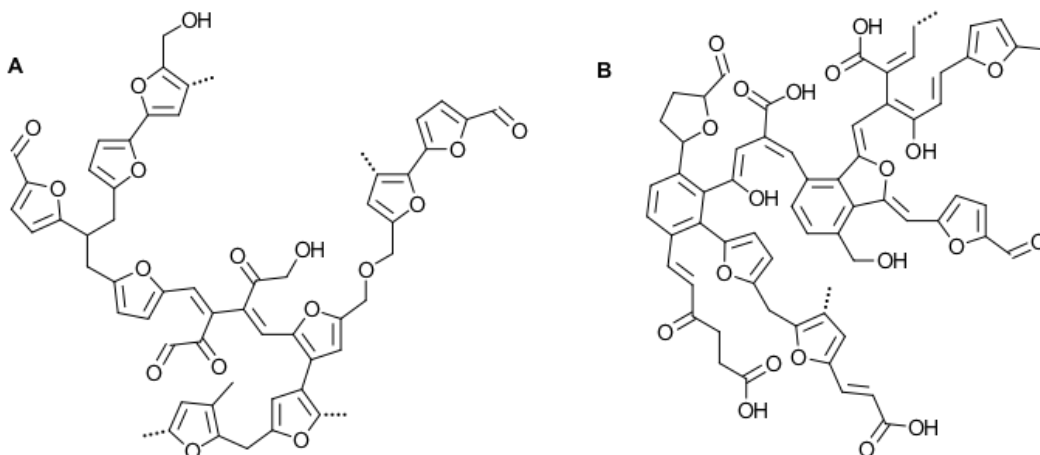
Scheme 2. Structures of humins (A, left)[25] and sugar-derived HTC (B, right).[36]

The mechanism of humins formation is still a matter of debate and controversy in the scientific community. In fact, due to the apparently random nature of the polycondensation network of reactions, different mechanisms have been proposed in literature mainly considering HMF as key trigger for humins formation. In fact, the presence of aromatic furanic C-bonds was detected in all fructose, glucose, and HMF-derived humins, suggesting the importance of the latter molecule.[30] Based on Gibbs free energy values for various HMF conversions, the formation of condensation products (HMF/HMF, HMF/fructose) is favored (5-10 kJ mol^{-1}) as opposed to levulinic acid formation (63 kJ mol^{-1}).[20] Sumerskii *et al.* proposed a series of parallel mechanisms involved in the formation of humins by-products, including aldol addition, incorporation of levulinic acid, and acetylization of furanic moieties.[34] In particular, it was proposed that carbonyl-containing intermediates would lead to a branched humins structure containing acetal bonds (Scheme 3). In contrast, acetal type of bonds were not incorporated in the model structure for humins proposed by van Zandvoort *et al.*, but not

excluded fully as a possibility due to the signal's attribution to either ether or acetal bonds.[32]
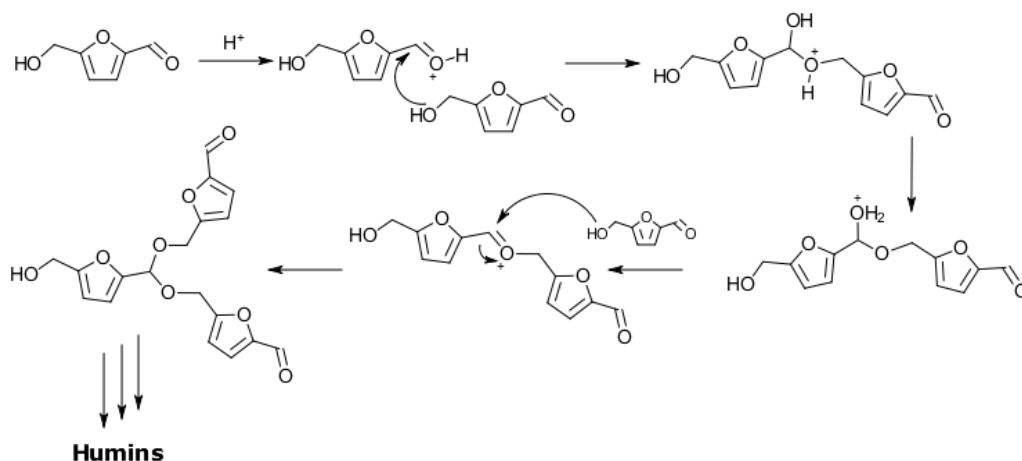
Scheme 3. Mechanism of humins formation proposed by Sumerskii et al. yielding branched HMF moieties with acetal bond.[34]

First proposed by Hovart in a ^{13}C NMR study of the levulinic acid formation mechanism, the 2,3-addition of water to HMF is believed to yield a highly reactive intermediate, 2,5-dioxo-6-hydroxyhexanal (DHH), which leads to polymerization products.[37] This theory was further developed by the work of Patil *et al.* where, although not detected spectroscopically, the humins formation proceeds *via* aldol condensation of DHH and HMF (Scheme 4), in competition with levulinic acid.[26,38] Another proposed intermediate involved in humins formation to a smaller extent has been identified as the 1,2,4-benzenetriol given by ring-opening of HMF by water addition, which polymerizes with other sugar-derived intermediates (Scheme 5).[39-41]

The further decomposition product of acid-catalyzed hydrolysis, levulinic acid, is usually believed to be stable and not reactive with regards the formation of humin by-products. However, it was found that addition of levulinic acid (desired product) results

in higher condensation, suggesting that levulinic acid is incorporated in the humins structure *via* carbocation formation.[42]
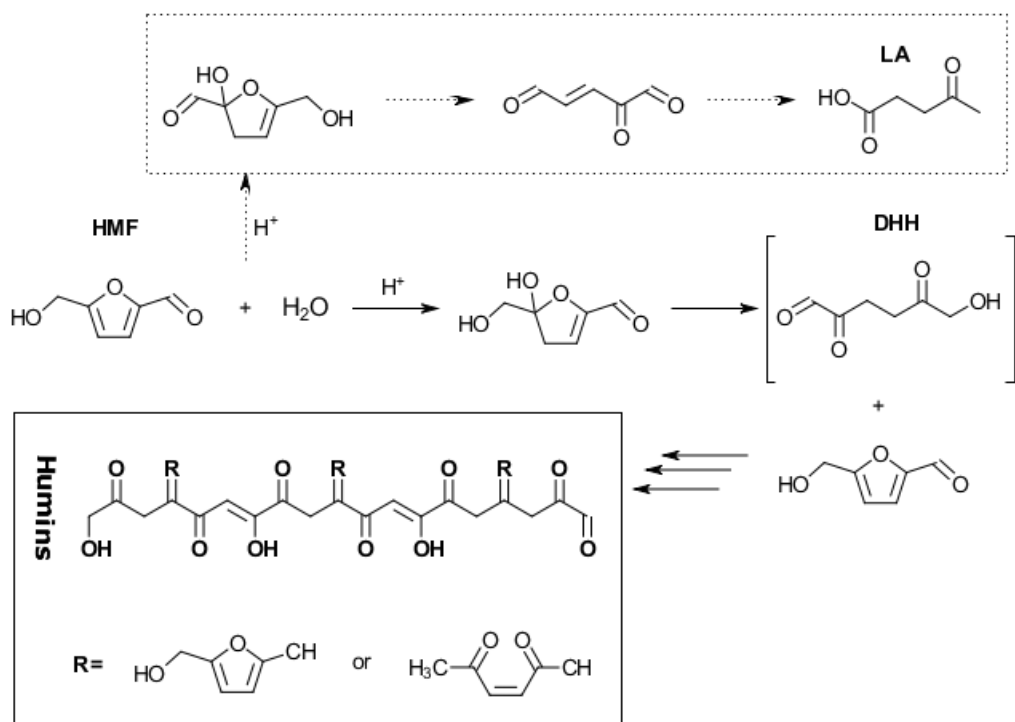
Scheme 4. Mechanism of humins formation proposed by Patil and Lund,[26,38] where DHH is in brackets ([]), in the dotted square the formation of levulinic acid (LA), and in the full square the proposed humins structure.
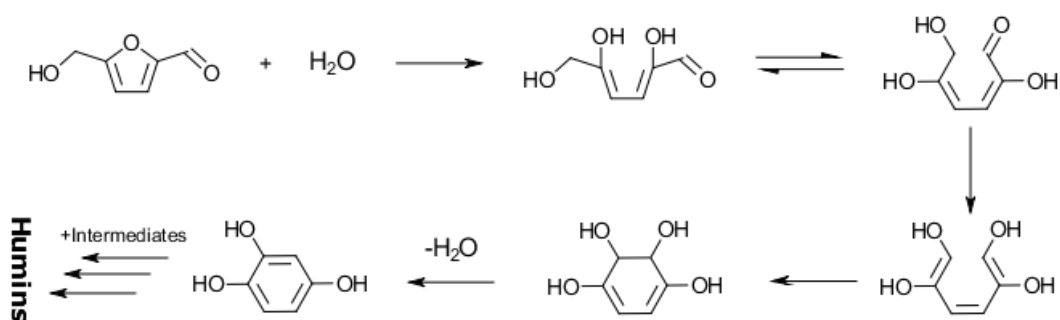
Scheme 5. Ring-opening hydrolysis of HMF towards highly-reactive intermediate 1,2,4-benzenetriol.[39-41]

It should be noted that the presence of both protons and water seems crucial in the formation of humins. Nonetheless, the presence of both is almost unavoidable in order to develop economically-feasible processes for biomass conversion which mainly employ mineral acids. For instance, the Biofine process dedicated to the production of furfural and levulinic acid relies on the use of dilute sulfuric acid, and the humins formation limits the overall process yields.[43] For this reason, further understanding of the governing mechanisms in humins formation may aid the development of cost-effective strategies for lignocellulosic biomass conversion. Also, structural characterization can give powerful insights into possible valorization opportunities for these by-products. However, at present only limited studies have been conducted for.[15,44-49]

Herein we propose structural and mechanistic identification of humin by-product formation by an approach different from the earlier proposed ones. Continuous flow hydrogenation and transfer hydrogenation (catalytic) decompositions in neutral conditions were employed in this study. The products were then qualitatively identified by GC-MS analysis which can give a better idea of the heterogeneous nature of these by-products, which include both starting materials and various (by-)products of the acid-catalyzed conversion of biomass. These findings will further stress the necessity of humins valorization for the economic feasibility of chemical biorefineries.

Results and Discussion

Relative combined severity of humins

A combined severity evaluation of production processes indicates the harshness of process operating conditions, by incorporating values of temperature, time, and pH in two formulas:[50]

$$Severity\ Factor\ (SF) = \log\left[t \times \exp\left(\frac{T-100}{14.75}\right)\right] \qquad \text{Eq. (1)}$$

$$Combined\ Severity\ Factor\ (CSF) = SF - pH \qquad \text{Eq. (2)}$$

Upon calculation of the CSFs of the industrial process, the values from literature humins and hydrothermal carbon were normalized giving an arbitral number of 1 to the humins employed in this study. In comparison, the process for these industrial humins is at a lower process severity of 1-2 orders compared to the literature processes (Table 1).

Table 1. Conditions and relative CSF (Combined Severity Factor) of the humins employed in this study, the humins synthesized in literature, and hydrothermal carbon.

	Humins (this study)	Humins (literature)	Hydrothermal Carbon
Feedstock	Biomass/sugars	Biomass/sugars	Biomass/sugars
Temperature (°C)	180-200	180-210	180-250
Environment	Acidic water/alcohol	Acidic water/alcohol	Water
Relative CSF	1	25-50	100-500

This particular result signals that lower extents of carbonization may have occurred to the humins, thus solubilization of said products and further decomposition into small organic molecules is easier. In fact, the humins employed in this study are viscous rather than solid (as traditional humins usually are), suggesting easier decomposition of the industrial humins into the comprising molecules.

Transfer hydrogenolysis of humin by-products

In the transfer hydrogenolysis of humins in isopropanol (1 wt%), a difference in catalytic effect between commercial 5% Pd/C and Raney Nickel (rNi) catalyst was observed. At room temperature the relative HMF and MMF concentrations were similar for both catalysts, whereas at higher temperatures (180 °C) the Pd catalyst yields higher concentrations of the two molecules (Figure 1). In fact, higher amounts of linear decomposition products were observed (*e.g.* 1,5-pentanediol) for the rNi catalytic system, which may signal the onset of hydrogenation or decomposition of the major products, HMF and MMF, yielding wider product distribution. This could be expected thanks to the higher catalytic transfer hydrogenation activity of rNi, as opposed to Pd catalysts,[51] where the latter favors the conservation of the molecular structures obtained from humins. Obtaining HMF and MMF from decomposition reactions would be preferred for the overall economics of a PEF process, thus the 5% Pd/C was chosen for the following catalytic studies.

In our reaction conditions, HMF and MMF represent >75% of the total mass balance in the decomposition products distribution. This is a first indication that indeed HMF, and its ether (MMF), are crucial in the formation of humins, being the main structural components, as already reported in literature.[25-30,34,38-41] MMF is

generally not included in the common compound libraries, thus GC-MS fragmentation pattern, ATR-IR and NMR spectra of MMF are given in Fig. S1-3 of the Supplementary Data (SD).
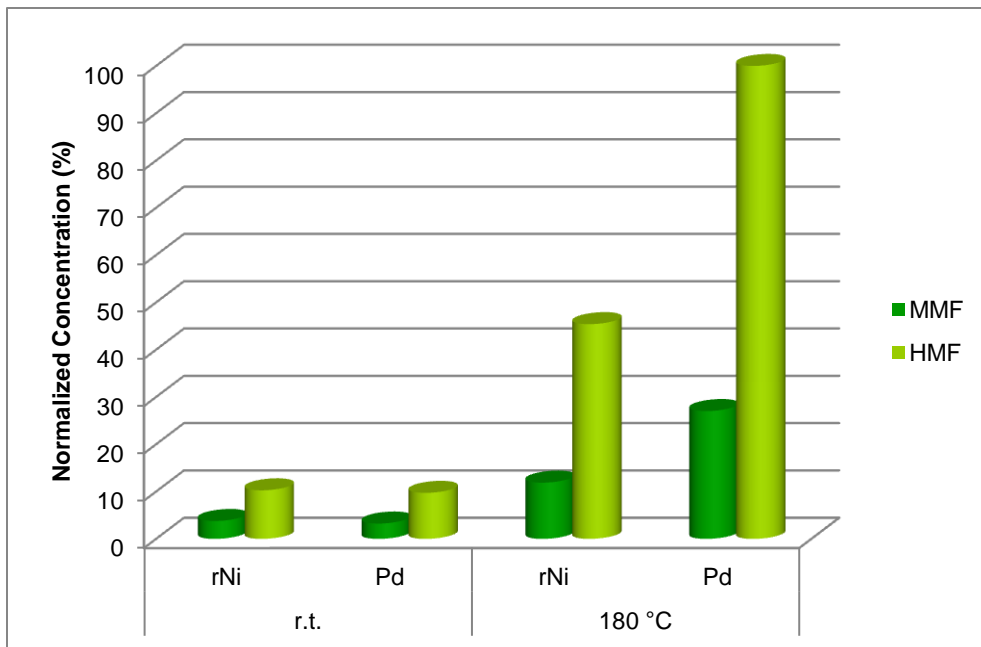
Figure 1. Catalyst effect on the relative intensities of HMF and MMF after transfer hydrogenolysis of humins in isopropanol (1 wt%) at room temperature (r.t.) and 180 °C, at 0.2 mL/min and 15 bar, after 20 minutes of reaction time.

The presence of HMF and MMF, however, could be also given by physisorption of these molecules on the humins surface, as seen elsewhere in literature.[52] In particular, research work on the same humins batches show the presence of up to 16 wt% of combined HMF and MMF (alkoxymethyl furaldehydes, RMF) for concentrated solutions.[44] GC-MS analyses of raw humins solutions used in this work (1 wt%) do indeed show residual HMF and MMF but with integrated areas of at least 3 orders of magnitude lower than the areas of the product mixtures obtained after thermal or hydrogen-assisted reactions. In fact, at room temperature reactions (Figure 1), 0.5% residual HMF is observed for the blank reaction, and *ca.* 33% if in the presence of an hydrogenation catalyst

(5% Pd/C). This phenomenon is not only a symptom of residual furanic monomers in the employed humins, but may also be a surprising catalytic activity at such low temperature. Furthermore, the relative HMF and MMF concentrations would increase thanks to heat treatment and presence of a catalytic system, as seen in Figure 2.

In particular, by considering the sum of the HMF and MMF GC-MS peak areas of the TIC chromatogram of the *i)* non-catalytic blank, *ii)* room temperature catalytic reaction, and *iii)* catalytic hydrogenolysis at 90 °C, a +765% increase of the peak areas sum is observed between *i)* and *ii)*, and a +460% increase between *ii)* and *iii)*, signaling that the monomers observed in the reaction mixtures are products of the humins decompositions. Nonetheless, the presence of physically embedded HMF is indeed observed as it elutes in the blank reaction (non-catalytic) and at lower temperature conditions. On the other hand, the increase of the HMF concentration under transfer hydrogenolysis conditions suggests the presence of easily cleaved monomers, thus presenting weak oxygenated bonds, such as esters. The systematic co-presence of MMF signifies the incorporation of said molecule, possibly through its aldehyde functionality *via* aldol condensations/additions.[30] The lower incorporation of MMF is due to the protection of the hydroxyl group by etherification with methanol, making it more stable towards the humins formation, thus less reactive towards condensation reactions.

A higher HMF and MMF concentration at 220 °C was expected as evidenced by TGA analysis.[44] In fact, a peak of decomposition at 210—220 °C was observed with a mass loss of *ca.* 40%, explaining the release of furanic molecules in oligomeric fractions. A slight

decrease in relative intensity of the molecules at higher temperatures could be attributed to onset decomposition of the actual products at higher temperatures.[53]
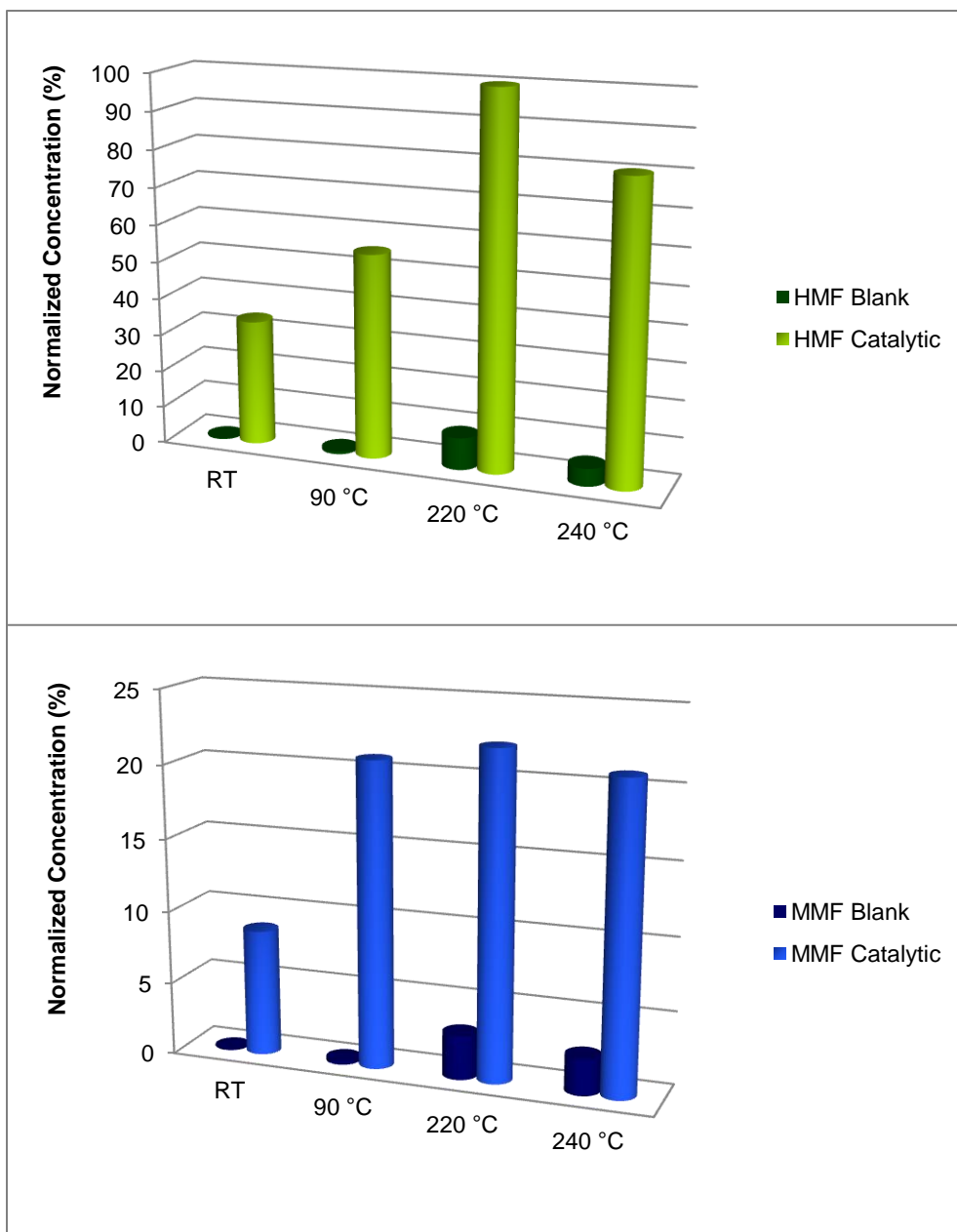
Figure 2. Temperature and catalytic effect in the decomposition of humins. The normalized concentrations were obtained over 5% Pd/C, 0.2 mL/min, in transfer hydrogenolysis (1 wt% humins in isopropanol) after 20 minutes of time-on-stream.

On the other hand, re-polymerization of the RMF monomers to humins in the same kinetic study is considered a parallel and co-existent mechanism. This phenomenon could explain why catalytic reactions in continuous flow would have extremely low catalyst lifetime (<60 minutes), causing fouling and blockage of the continuous flow system, particularly at higher temperatures. Hence, an increase of the reactor pressure and consequent full blockage after <40 minutes of time-on-stream was observed in most transfer hydrogenolysis reactions, signaling strong reactor fouling. In general, the main challenge of humins processing is the presence of heterogeneous molecules in solution, and thus coke formation. Although extreme dilutions of the feed may help reduce catalyst fouling (this work, 1 wt% solutions), fixed bed continuous flow reactors may not be feasible in the current form, requiring new engineering solutions for carbonaceous deposit removal.

Catalyst deactivation and solvent effect

To further assess the catalyst deactivation and solvent effect, the chosen catalytic system (5 % Pd/C) was investigated under hydrogenation conditions at mild reaction conditions (90 °C). By analyzing the relative HMF and MMF concentration over 60 minutes of reaction time (Figure 3), an increase of the concentration is observed after 20 minutes of time on-stream, which is then drastically reduced after 60 minutes. Although a wider product distribution is also obtained after 60 minutes, by considering the sum of the areas of the TIC as opposed to 20 minutes, a reduction of the total relative concentration is observed. Furthermore, the full blockage of the system's flow was a clear sign of reactor fouling.

In the mild temperature hydrogenation reactions (90 °C, 50 bar, 0.3 mL/min), a solvent effect was also observed for the

decomposition of humins in ethyl acetate solutions. Addition of 10 vol% of acetic acid increased the relative HMF and MMF concentrations (Figure 4).
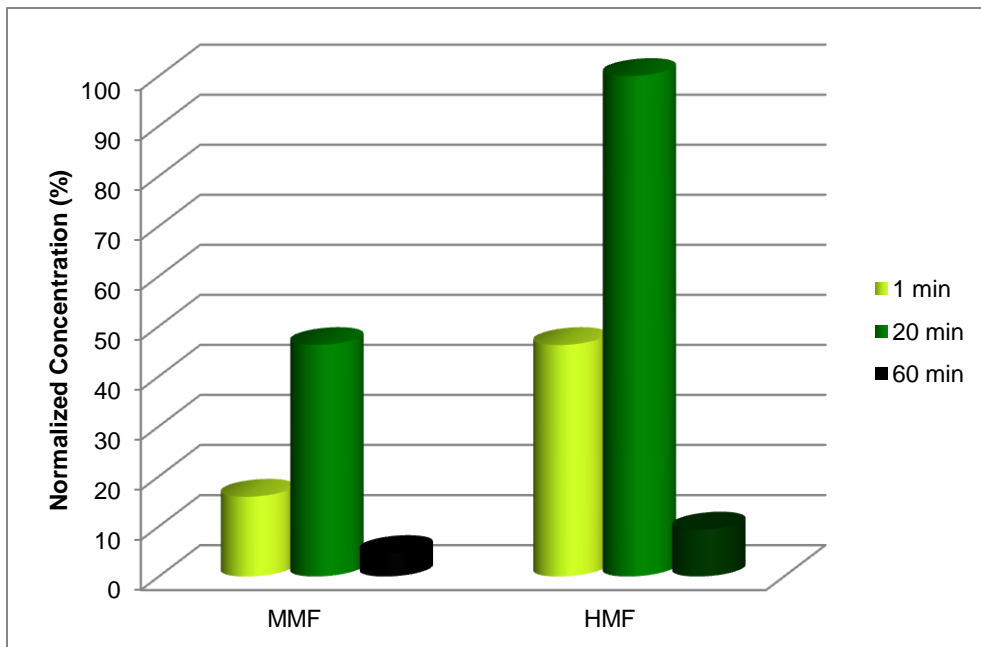
Figure 3. Effect of reaction time on normalized concentrations of HMF and MMF over a 5% Pd/C catalyst under hydrogenation conditions in continuous flow (1wt% humins solution in ethyl acetate, 90 °C, 50 bar, 0.3 mL/min).

Acetic acid may act as an acid-catalyst in the hydrolysis of humins, but also as a promoter for the carbonyl group hydrogenation by partial protonation of the oxygenated function, as seen in literature for other hydrogenation reactions.[54,55] In fact, apart from higher concentrations of HMF and MMF, wider product distribution was observed when acetic acid was added. In particular, a third intense peak was observed after 60 minutes of reaction time and was identified as 5-acetoxymethyl-2-furaldehyde, the acetylated product of HMF, signaling the influence of acetic acid on the product mixture and solvolysis. The existence of this side-reaction decreases the selectivity of the

conversion to a sole product, but may stabilize HMF against further decomposition reactions.
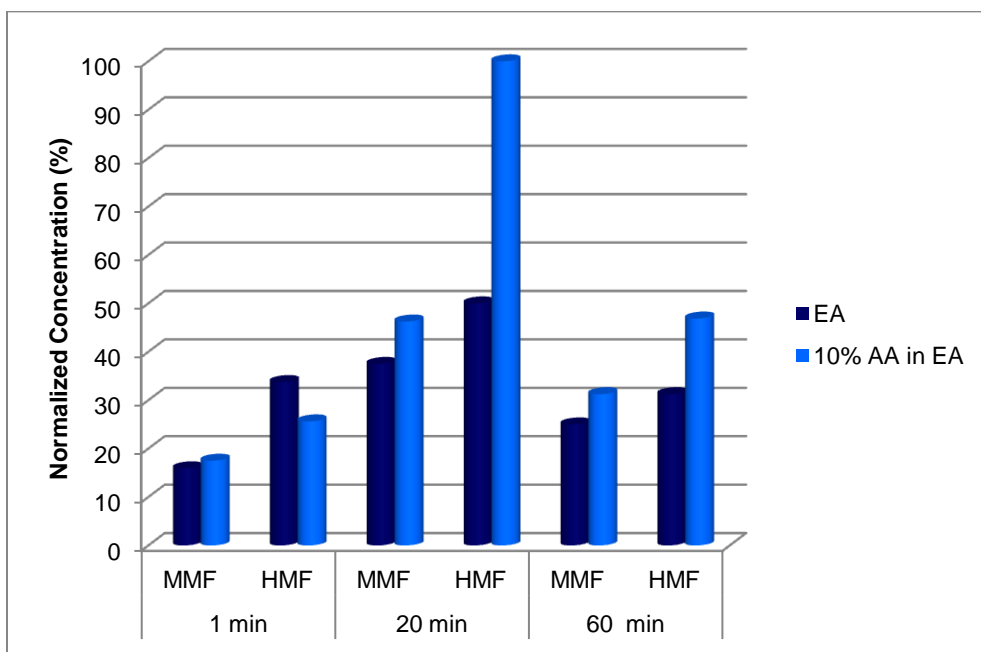
Figure 4. Solvent effect on the hydrogenation of humins in ethyl acetate (EA) or 10% acetic acid (AA) in EA at 90 °C, 50 bar, 0.3 mL/min over a 5% Pd/C catalyst at different reaction times (1-60 min).

On the other hand, it could be expected that the presence of acetic acid also catalyzes further condensation reactions to form humins and/or coke, leading to faster catalyst deactivation. In fact, a reaction of humins in glacial acetic acid (not analyzed) caused system fouling within 10 minutes of time-on-stream, which could be attributed to acid-catalyzed cross-linking.

Methanol and acetonitrile solutions caused rapid catalyst fouling, resulting in reactor plugging, and consecutive build-up and loss of system pressure. In fact, in these solvent systems reactions were possible for only <20 minutes. The solubility of humins had been addressed in several solvents,[31] and reported as water<acetonitrile<methanol/diethyl ether/methyl levulinate, among

others. In our solvent conditions (1 wt% humins solutions) we are probably dealing with a dispersion (even upon sonication and filtration), which further causes blockages in the plug flow reactors.
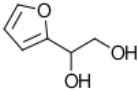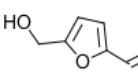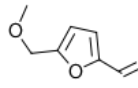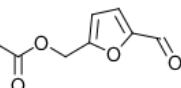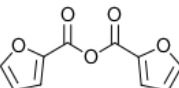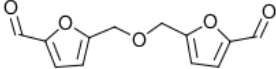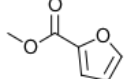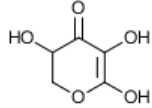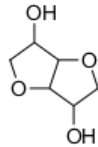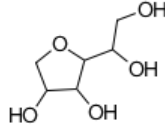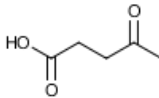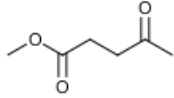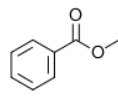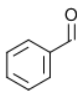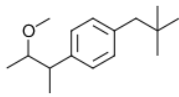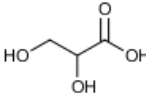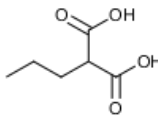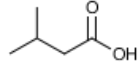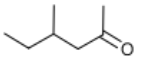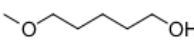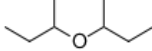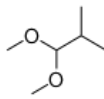
Qualitative analysis of overall decomposition products

Overall, the GC-MS analyses may give a small degree of uncertainty of the actual molecules observed. For this reason, in this study only molecules with a reversed match factor >700 are considered, and rather than looking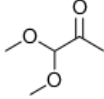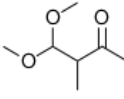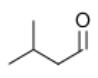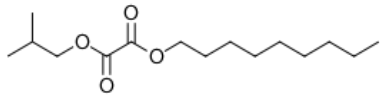 at the molecules as such, an analysis of the functional groups and plausible reactivity with other known moieties were taken into consideration. Aside from small differences, such as the 5-acetoxymethyl-2-furaldehyde only appearing upon addition of acetic acid, or 5-methoxypentanol and similar open-ring compounds appearing at high hydrogenation conditions (>180 °C), consistent and coherent molecules were identified from the humins decompositions in both blank, transfer hydrogenolysis, and hydrogenation conditions with different concentrations (Table 2).

A total of five classes of compounds were identified from the (hydrogen-assisted) decomposition reactions, namely: *i)* furanics, *ii)* sugar-derived molecules, *iii)* levulinates, *iv)* aromatics, and *v)* small organic acids and other oxygenated molecules, including organic acids, alcohols, esters, aldehydes/ketones, and acetals. Furthermore, the formation of a number of compounds is expected but these could not be collected due to their volatility. For instance, molecules such as CO, CO_2, furan, formaldehyde, methanol, are expected. The latter in particular may explain the presence of methyl esters in the decomposition mixtures.

Table 2. Identified molecules in the (catalytic) decompositions.

Furanics	
Sugar-derived molecules	
Levulinates	
Aromatics	
Small organic acids and other oxygenated molecules	

Furanics

The presence of HMF as the highest peak in our reaction mixtures confirms the crucial role of said molecule in the formation of humins, as already stated in literature,[24,25,27,28] present as loose and/or loosely bound. The ether counterpart, MMF, was also ubiquitously present in all decomposition samples. This suggests that although more stable towards humins formation thanks to the hydroxyl protection by etherification,[39] the aldehyde functionality of MMF is prone towards aldol additions/condensation reactions, thus leading to humins. Also, humins release water upon pyrolysis (*ca.* 20 wt%) as observed by Argawal *et al.*,[56] thus partial hydrogenolysis of the ether MMF to HMF can be expected. All the remaining furanics (<15% of product distribution) identified exhibit at least one oxygen functionality with only C_1—C_2 side linkages. This appearance stresses further the incorporation of furanics in the structure which would present only short bridging groups between furan groups. Ester, aldehyde, and hydroxyl side groups are predominant. The observation of cirsiumaldehyde, a dimer of HMF *via* an ether bridging bond, may support the mechanism proposed by Sumerskii *et al.* involving the formation of hemiacetal/acetal of HMF and may be produced by hydrogenolysis of the acetal functionality.[34] The aldehyde side-groups may undergo further condensation reactions, leading to the oligomeric molecules. Also the presence of a diol functional group in 1-(2-furyl)-1,2-ethanediol sustains the mechanism aforementioned by signaling the presence of an acetal bond.[34] Pd is known to cleave an acetal-carbonyl bond in favor of a diol under hydrogenation conditions.[57] However, the 1,2 positioning of the diol (instead of 1,1) would rather hint towards the formation of a cyclic acetal, following its reaction with a carbonyl functionality, which could explain the dismissal of the acetal presence, although

observed, in NMR analysis.[25] Considering the (acidic) environment of humins formation and the nature of the involved molecules (*i.e.* sugar chemistry), the formation of cyclic acetal can be expected (also seen elsewhere),[58] and incorporated to a very small extent. The other furanic molecules instead simply imply the multifaceted nature of humin by-products, involving different oxygen functionalities of the furanic molecules, with a facile incorporation in the structure *via* short linkages.

Sugar-derived molecules

Sugars and sugar-derived molecules were expected based on the literature data.[26,39] These molecules have been detected already from decomposition/hydrogenation at room temperature, suggesting that it is merely a weak incorporation in the humins structure (terminal/easily cleaved). Nonetheless, the molecules were also observed at higher temperatures with increasing relative concentration, thus small quantities become part of the humins backbone. In particular, sugar dehydration products (*e.g.* 3,5,6-trihydroxy-2,3-dihydropyran-4-one,[39] isosorbide) have been identified as decomposition products. Since the decompositions were run under neutral conditions (apart from in the presence of 10% acetic acid), these molecules are believed to be fragments of the humins structure. On the other hand, sugars are known to be derivatized for their analysis in GC-MS (poor volatility),[59] and it could be argued that they might be present and not detected. However, UPLC analyses did not show the presence of residual carbohydrates.

Levulinates

Similar to the sugar-derived molecules, levulinates are known to come from the acid-catalyzed decomposition of HMF (or similar),

alongside the formation of formic acid. The detection of levulinic acid and the corresponding methyl ester suggest that also these molecules take part of the humins structure, as it was proposed but not asserted in literature.[34,42] The incorporation of other acid-catalyzed biomass side-products further stresses the random and complex nature of humins, which are favored under common chemical conversions of lignocelluloses and similar.

Aromatics

Considering the low relative CSF of the humins employed in this study, the presence of aromatics may be surprising, although not completely unexpected. In fact, oxygen-containing aromatic functionalities were proposed in alkaline-treated humins,[33] and, in particular, 1,2,4-benzenetriol (*see* Scheme 5) was proposed as a minor reactive intermediate in the formation of humin by-products.[39-41] In our decomposition mixtures, multiple oxygen-containing molecules were observed at both room and higher temperatures. The presence of tri- and tetra-substituted aromatics (*i.e.* 2,4,6-trihydroxybenzaldehyde and 3,4-dimethoxycarbonylbenzoic acid) may be a suggestion of the involvement of the ring-opening hydrolysis of HMF and dehydration to the trisubstituted benzene. In particular, this latter molecule would provide ortho-directing reactivity for further addition/condensation reactions, explaining the tetrasubstituted molecule. The presence of monosubstituted benzenes (*e.g.* benzaldehyde, methyl benzoate) at room temperature (and higher) decompositions instead suggest possible Diels-Alder reactivity of biomass compounds as seen for other bio-based molecules,[60-63] as well as the hydrothermal carbons mentioned above.[36] For instance, methyl benzoate is known to be formed by the reaction between

furan (highly volatile molecule) and methyl acrylate, possibly derived from other decomposition products, *i.e.* methyl acetate and formaldehyde.[63]

This phenomenon can be observed in studies involving thermal treatment of humins, where FT-IR analyses showed that *i)* mild thermal treatment gave reduction of the typical OH stretching and increase of C=C intensity peak,[64] and *ii)* more intensive thermal treatment would yield polyaromatic structures, given by the disappearance of the FT-IR peak attributed to alkene out of plane bending.[44] These findings of aromatic structures not only give insight into the humins mechanism of formation, but also of the further reactivity of these plant-based by-products, suggesting the possibility of tuning the superficial oxygen functionalities upon heating.

Small organic acids and other oxygenated molecules

All of the molecules in this class sustain the high oxygenated character of humin by-products. The molecules indicated with an asterisk (*) were observed only at high temperature transfer hydrogenolysis over the rNi catalyst, attributed to further decomposition reactions of the obtained molecules (*e.g.* HMF) and not humins. Among the remaining molecules, the incorporation of products of sugar dehydrations (*e.g.* oxalic/malonic fragments) can again be seen. Furthermore, the presence of acetals again suggests the existence of the mechanism proposed by Sumerskii *et al.* for humins formation. The ketone functionalities may be also attributed to acetal-type functional groups.[34] The 1,1-dimethoxy-2-propanone could be obtained *via* acid-catalyzed retro-aldolization of C_6-sugars into dihydroxyacetone (DHA), followed by dehydration into pyruvic aldehyde (PY-A), and addition of methanol,[65,66] with the observance

of glyceric acid supporting the proposed pathway as parallel equilibrium reaction of DHA into glyceraldehydes (GLYA, Scheme 6).
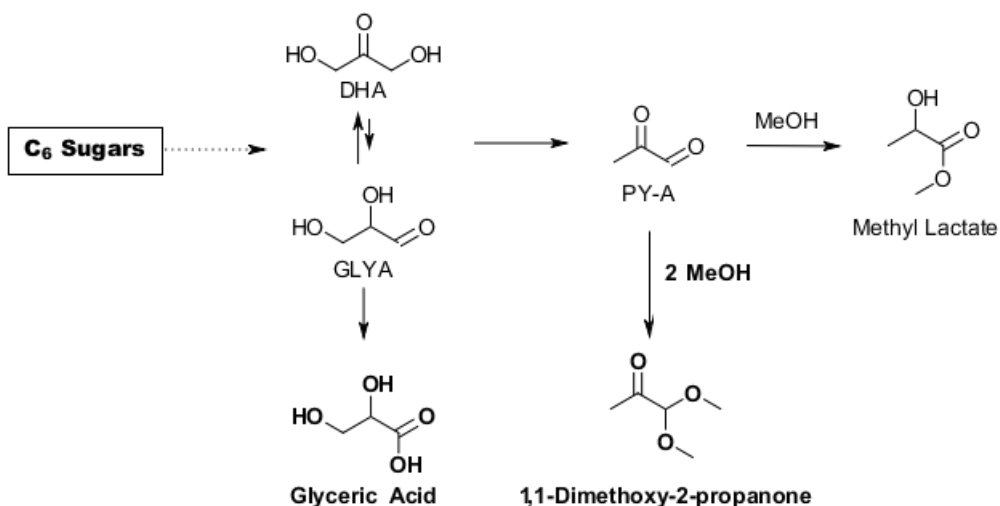
Scheme 6. Reaction pathway of the retro-aldolization of C6 sugars into pyruvic aldehyde. The molecules detected in this study are presented in **bold.**

Pyruvic aldehyde, in particular, could partially resemble the DHH molecule proposed by Horvat,[37] however requiring the cleavage of a carbon-carbon bond, which is not sustained by the mild combined severity of the process or the reaction conditions used in this study.

Small quantities (<3% of mass balance) of hydrocarbon-like molecules were also observed, in particular under high temperature treatment (> 180 °C, transfer hydrogenolysis) and in the presence of a catalyst (5% Pd/C). This could be similar to the observation of short aliphatic chains observed by van Zandvoort,[25,28] which represent the recalcitrant and fouling moieties of humins.

None of the observed molecules confirm the mechanism proposed by Patil and Lund involving DHH, although it cannot be disproven due to the high reactivity of said intermediate.[26,38] However, the decomposition products agree with the mechanisms involving acetal formation proposed by Sumerskii *et al.*,[34] and those

involving the 1,2,4-benzenetriol intermediate.[39-41] Based on the decomposition products distribution, a very variegated humins structure can be deduced, involving starting molecules, main identified products, and other side-products of the acid-catalyzed hydrolysis of biomass.

Proposed humins structure

Incorporating all decomposition studies and the behavioral/literary knowledge of humin by-products, a structure of such molecules is proposed herein (Scheme 7). The structure is representative of the possible functionalities and moieties that can appear in a particular batch, showing a higher heterogeneity of the humins structure as opposed to the furanic-based structure proposed in literature, becoming more similar to that of hydrothermal carbons.[36] In particular, furanics with (cyclic) acetal bonds are included in the structure, but also aromatics, sugar-derived molecules, and levulinates presenting ester and ether linkages. In particular, this structure represents the molecules that are easily cleaved by thermal and hydrogen-assisted decompositions. These observations are also in line with the FT-IR spectra of raw and thermally treated humins, where furanics are the major component.[44,64] The presence of furanic moieties linked by short aliphatic chains proposed by van Zandvoort *et al.* is not incorporated in the final humins structure, as evidence for their presence could not be found.[25,28] However, the observation of fouling and reactor plugging may hint at the existence of hydrocarburic linkages which are more prone to coking due to their recalcitrant nature. Overall, ring-opening hydrolysis of furanics appears to be crucial in humins formation, giving a structure closer to hydrothermal carbons from carbohydrates (Scheme 2). Furthermore, the presence of hydroxyl

and carbonyl groups favors condensation reactions to form humins, self-propagated by the presence of water. Hence, the presence of water seems crucial to humin by-product formation, as well as all reagents and products of biomass conversion *via* chemical transformations.
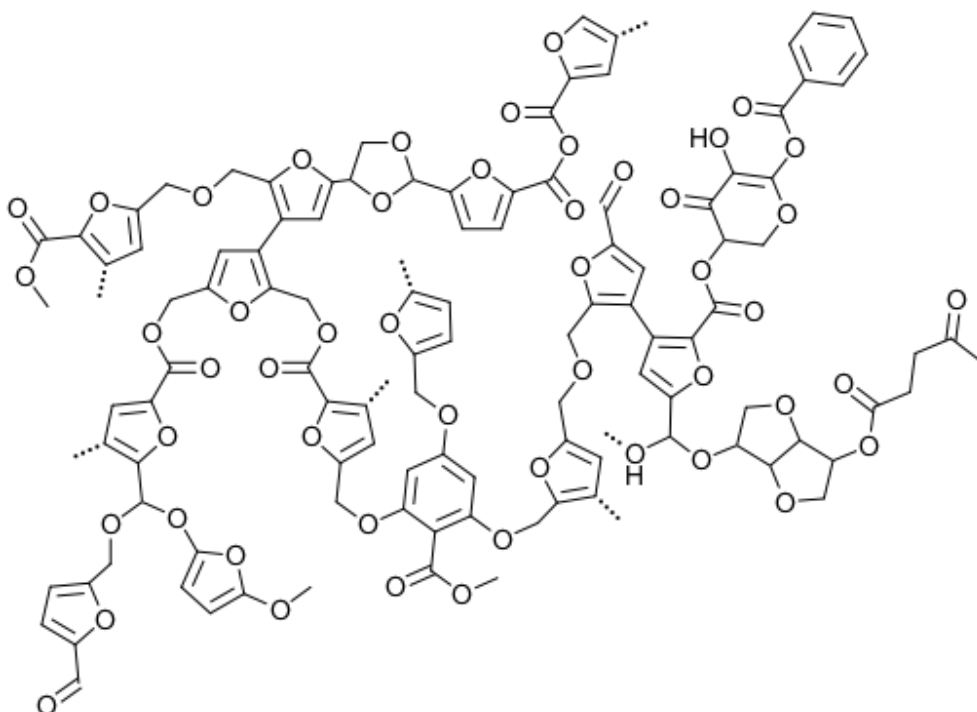
Scheme 7. Proposed humins structure based on the results of the (catalytic) decompositions and the structures given in literature.

Conclusions

The decomposition of humin by-products was achieved *via* thermal and hydrogen-assisted reactions in continuous flow under neutral pH, yielding easily cleaved molecules representative of the key intermediates in the formation of humins. A *down-up* approach in general structural identification can be applied to oligomers and macromolecules with mild and harsher thermal and hydrogen-assisted decomposition, and *pseudo*-reconstruction of the overall structure is possible from the product mixture. In this work, it was

found that humin by-products are heterogeneous molecules comprising a plethora of starting molecules and (by-)products of acid-catalyzed biomass conversion, as well as having multiple parallel mechanisms for their formation. The identification of key linkages such as acetal and ester suggest the presence of oxygen functionalities that could have potential as anchoring groups for catalytic systems,[45] production of oxygen-containing materials/composites,[46] or the removal of oxygen-containing groups upon carbonization.[44] Furthermore, humins and thermally-treated humins foams present fire behavior comparable to wood, thus have storage potential.[67] New applications for construction and automotive materials have also been investigated by combining humins with flax fibres.[68] As humins production can be minimized to a certain extent, upgrading the applications of these by-products is crucial to the development of a true circular economy, where waste is cipher, and value is added to any product.

Experimental Section

Materials

Humins were provided by Avantium Chemicals B. V. (Amsterdam, The Netherlands) and employed without further purification. In particular, the humins were produced by the conversion of fructose in methanol. Ethyl acetate (99.9%), acetonitrile (99.9%) and methanol (99.9%) were purchased from Panreac AppliChem; 2-propanol (99.9%) was bought from Fisher Scientific; glacial acetic acid from Panreac Quimica SA. All of the solvents were used as received.

Humins solutions

Different solutions of humins were made to achieve a concentration of 1 wt%. In particular, ethyl acetate, 10% acetic acid in ethyl acetate, acetonitrile, methanol, and isopropanol were chosen as solvent systems for the decomposition reactions. The solutions were sonicated for 15 minutes and filtrated over a 0.45 µm syringe filter in order to avoid the presence of heterogeneous molecules before their use in the continuous flow systems.

Decompositions

Thermal decompositions (blank) and transfer hydrogenolysis (humins in isopropanol) were carried out in a ThalesNano® Phoenix Flow Reactor™ (maximum operating temperature of 250 °C) at temperatures between 25-240 °C, and a flow of 0.2 mL min^{-1} (65.7 s of contact time). The system pressures were calculated applying the Clausius-Clayperon equation in order to ensure a liquid feed or sub/supercritical conditions. All hydrogenation reactions were run in a ThalesNano® H-Cube Mini Plus™ (maximum operating temperature of 100 °C) at temperatures 25-90 °C, with or without 50 bar of system pressure, a flow of 0.3 mL min^{-1} (43.8 s contact time) in the presence of hydrogen produced in by an electrocatalytic cell. The difference of contact time for the transfer hydrogenolysis and hydrogenation reactions were necessary to obtain significant conversions and stability of the reaction flow. *i)* Inert (TiO$_2$), *ii)* 5% Pd/C, and *iii)* RANEY®Ni CatCarts® provided by ThalesNano® were employed *i)* for thermal decompositions, and *ii)* and *iii)* for hydrogenation reactions.

Analytical methods

GC-MS analyses were employed for qualitative and semi-quantitative interpretations of decomposition products. In

particular, a BR-5MS (5%phenyl 95%dimethyl arylene siloxane) 30m x 0.25 mm x 0.25 µm column was employed. A PTV injector was used at 265 °C, split ratio of 50, and column flow of 1 mL min^{-1}. The oven was set at 80 °C, followed by 3 °C min^{-1} to 200 °C, 10 °C min^{-1} to 250 °C, and 30 °C min^{-1} to 280 °C (50 min). Ion source temperature was set to 275 °C (transfer line 280 °C), and ionization energy 70 eV.

Only molecules with a reverse match factor (RMF) higher than 700 were considered for a qualitative analysis of the humins decomposition products (**SD, S4-29**). Semi-quantitative analyses were carried out by the ratio of the compound's total ion chromatogram (TIC) peak area divided by the sum of the areas of all products. As it contains sensitive information for intellectual property of the Avantium YXY/Synvina technology, the relative concentrations were normalized to the highest relative concentration. This way trends are further evidenced, rather than quantitative concentrations. Not reported quantitative analyses of the decomposition products were carried out in GC and UPLC analyses in methods developed by the Analytical Team of the Renewable Chemistry department of Avantium. In particular, 1,4-dioxane (3 mg/mL) and saccharine (8 mg/mL) were used as external standard solutions, in a similar procedure previously reported from a project co-worker.[44] These values were used to further confirm the speculations reported herein.

References

[1] World population projected to reach 9.8 billion in 2050, and 11.2 billion in 2100, Department of economic and social affairs, United Nations. https://www.un.org/development/desa/en/news/population/world-population-prospects-2017.html (accessed Jan 08, 2019).

[2] Gao, Y.; Gao, X.; Zhang, X. The 2 °C global temperature target and the evolution of the long-term goal of addressing climate change – From the United Nations framework convention on climate change to the Paris agreement. *Eng.* **2017**, *3*(2), 272-278.

[3] Filiciotto, L; Luque, R. Biomass promises: A bumby road to a renewable economy. *Curr. Green Chem.* **2018**, *5*(1), 47-59.

[4] Wu, L.; Moteki, T.; Gokhale, A. A.; Flaherty, D. W.; Toste, F. D. Production of fuels and chemicals from biomass: Condensation reactions and beyond. *Chem.* **2016**, *1*(1), 32-58.

[5] Climent, M. J.; Corma, A.; Iborra, S. Conversion of biomass platform molecules into fuel additives and liquid hydrocarbon fuels. *Green Chem.* **2014**, *16*, 516-547.

[6] De, S.; Balu, A. M.; van der Waal, J. C.; Luque, R. Biomass-derived porous carbon materials: Synthesis and catalytic applications. *ChemCatChem* **2015**, *7*(11), 1608-1629.

[7] Pileidis, F.D.; Titirici, M.-M. Levulinic acid biorefineris: New challenges for efficient utilization of biomass. *ChemSusChem* **2016**, *9*(6), 562-582.

[8] Li, M.-F.; Yang, S.; Sun, R.-C. Recent advances in alcohol and organic acid fractionation of lignocellulosic biomass. *Bioresour. Technol.* **2016**, *200*, 971-980.

[9] Filiciotto, L.; Balu, A. M.; van der Waal, J. C.; Luque, R. Catalytic insights into the production of biomass-derived side products methyl levulinate, furfural and humins. *Catal. Today* **2018**, *302*, 2-15.

[10] Spierling, S.; Knüpffer, E.; Behnsen, H.; Mudersbach, M.; Krieg, H.; Springer, S.; Albrecht, S.; Hermann, C.; Endres, H.-J. Bio-based plastics–A review of environmental, social and economic impact assessments. *J. Clean. Prod.* **2018**, *185*, 479-491.

[11] YXY technology, Avantium. https://www.avantium.com/yxy/ (accessed Jan 08, 2019)

[12] Synvina. https://www.synvina.com/ (accessed Jan 08, 2019)

[13] Kang, S.; Fu, J.; Zhang, G. From lignocellulosic biomass to levulinic acid: A review on acid-catalyzed hydrolysis. *Renew. Sustain. Energ. Rev.* **2018**, *94*, 340-362.

[14] Rice, F. A. H. Effect of aqueous sulfuric acid on reducing sugars. V. Infrared structure on the humins formed by the action of aqueous sulfuric acid on the aldopentoses and on the aldehydes derived from them. *J. Org. Chem.* **1958**, *23*(3), 465-468.

[15] Hoang, T. M. C.; van Eck, E. R. H.; Bula, W. P.; Gardeniers, J. G. E.; Lefferts, L.; Seshan K. Humin based by-products from biomass processing as a potential carbonaceous source for synthesis gas production. *Green Chem.* **2015**, *17*(2), 959-972.

[16] Wang, S.; Lin, H.; Chen, J.; Zhao, Y.; Ru, B.; Qiu, K.; Zhou, J. Conversion of carbohydrates into 5-hydroxymethylfurfural in an advanced single-phase reaction system consisting of water and 1,2-dimethoxyethane. *RSC Adv.* **2015**, *5*(102), 84014-84021.

[17] Tang, X.; Sun, Y.; Zeng, X.; Hao, W.; Lin, L.; Liu, S. Novel process for the extraction of ethyl levulinate by toluene with less humins from the ethanolysis products of carbohydrates. *Energy Fuels* **2014**, *28*(7), 4251-4255.

[18] von Hebel, K. L.; Lange, J.-P. Process for liquefying a cellulosic material. US Patent 20110277378A1, November 17, 2011.

[19] Eminov, S.; Brandt, A.; Wilton-Ely, J. D. E. T.; Hallett, J. P. The highly selective and near-quantitative conversion of glucose to 5-hydroxymethylfurfural using ionic liquids. *PLoS ONE* **2016**, *11*(10), e0163835.

[20] Heltzel, J.; Patil, S. K. R.; Lund, C.R.F. Humin Formation Pathways. In *Reaction Pathways and Mechanisms in Thermocatalytic Biomass Conversion II;* Schlaf, M., Zhang, Z., Eds.; Springer Science+Business Media: Singapore, 2016; Chapter 5, pp 105-118.

[21] Herzfeld, J.; Rand, D.; Matsuki, Y.; Daviso, E.; Makjurkauskas, M.; Mamajanov, I. Molecular structure of humin and melanoidin via solid state NMR .*J. Phys. Chem. B* **2011**, *115*(19), 5741-5745.

[22] Kang, S.; Li, X.; Fan, J.; Chang, J. A direct synthesis of adsorbable hydrochar by hydrothermal conversion of lignin. *Energy Sourc. A, Recovery Util. Environ. Effects* **2016**, *38*(9), 1255-1261.

[23] Sevilla, M.; Fuertes, A. B. Chemical and structural properties of carbonaceous products obtained by hydrothermal carbonization of saccharides. *Aust. J. Soil Res.* **2010**, *15*(16), 4195-4203.

[24] Sevilla, M.; Fuertes, A. B. The production of carbon materials by hydrothermal carbonization of cellulose. *Carbon* **2009**, *47*(9), 2281-2289.

[25] van Zandvoort, I.; Koers, E. J.; Weingarth, M.; Bruijnincx, P. C. A.; Baldus, M.; Weckhuysen, B. M. Structural characterization of ^{13}C-enriched humins and alkali-treated ^{13}C humins by 2D solid-state NMR. *Green Chem.* **2015**, *17*(8), 4383-4392.

[26] Patil, S. K. R.; Heltzel, J.; Lund, C. R. F. Comparison of structural features of humins formed catalytically from glucose, fructose, and 5-hydroxymethylfurfuraldehyde. *Energy Fuels* **2012**, *26*(8), 5281-5293.

[27] Aida, T. M.; Sato, Y.; Watanabe, M.; Tajima, K.; Nonaka, T.; Hattori, H.; Arai, K. Dehydration of D-glucose in high temperature water at pressures up to 80 MPa. *J. Supercrit. Fluids* **2007**, *40*(3), 381–388.

[28] van Zandvoort, I.; Wang, Y.; Rasrendra, C. B.; van Eck, E. R. H.; Bruijnincx, P. C. A.; Heeres, H. J.; Weckhuysen, B. M. Formation, molecular structure, and morphology of humins in biomass conversion: Influence of feedstock and processing conditions. *ChemSusChem* **2013**, *6*(9), 1745–1758.

[29] Reiche, S.; Kowalew, N.; Schlögl, R. Influence of synthesis pH and oxidative strength of the catalyzing acid on the morphology and chemical structure of hydrothermal carbon. *ChemPhysChem* **2015**, *16*(3), 579–587.

[30] Tsilomelekis, G.; Orella, M. J.; Lin, Z.; Cheng, Z.; Zheng, W.; Nikolakis, V.; Vlachos, D. G. Molecular structure, morphology and growth mechanisms and rates of 5-hydroxymethyl furfural (HMF) derived humins. *Green Chem.* **2016**, *18*(7), 1983–1993.

[31] Mija, A.; van der Waal, J.C.; Pin, J.-M.; Guigo, N.; de Jong, E. Humins as promising material for producing sustainable polysaccharide-derived building materials. *Constr. Build. Mater.* **2017**, *139*, 549-601.

[32] van Zandvoort, I.; van Eck, E. R. H.; de Peinder, P.; Heeres, H. J.; Bruijnincx, P. C. A.; Weckhuysen, B. M. Full, reactive solubilization of humin by-products by alkaline treatment and characterization of the alkali-treated humins formed. *ACS. Sustainable Chem. Eng.* **2015**, *3*(3), 533-543.

[33] Constant, S.; Lancefield, C. S.; Weckhuysen, B. M.; Bruijnincx, P. C. A. Quantification and classification of carbonyls in industrial humins and lignins by ^{19}F NMR. *ACS Sustainable Chem. Eng.* **2016**, *5*(1), 965-972.

[34] Sumerskii, I. V.; Krutov, S. M.; Zarubin, M. Y. Humin-like substances formed under conditions of industrial hydrolysis of wood. *Russ. J. Appl. Chem.* **2010**, *83*(2), 320-327.

[35] Filiciotto, L.; de Miguel, G.; Balu, A. M.; Romero, A. A.; van der Waal, J. C.; Luque, R. Towards the photophysical studies of humin by-products. *Chem. Commun.* **2017**, *53*, 7015-7017.

[36] Titirici, M.-M.; White, R. J.; Falco, C.; Sevilla, M. Black perspectives for a green future: hydrothermal carbons for environment protection and energy storage. *Energy Environ. Sci.* **2012**, *5*, 6796-6822.

[37] Horvat, J.; Klaić, B.; Metelko, B.; Šunjić, V. Mechanism of levulinic acid formation. *Tetrahedron Lett.* **1985**, *26*(17), 2111-2114.

[38] Patil, S. K. R.; Lund, C. R. F. Formation and growth of humins via aldol addition and condensation during acid-catalyzed conversion of 5-hydroxymethylfurfural. *Energy Fuels* **2011**, *25*(10), 4745-4755.

[39] Hu, X.; Lievens, C.; Larcher, A.; Li, C. Z. Reaction pathways of glucose during esterification: effects of reaction parameters on the formation of humin type polymer. *Bioresour Technol.* **2011**, *102*(21), 10104-10113.

[40] Chuntanapum, A.; Matsumura, Y. Formation of tarry material from 5-HMF in subcritical and supercritical water. *Ind. Eng. Chem. Res.* **2009**, *48*(22), 9837-9846.

[41] Luijkx, G. C. A.; van Rantwijk, F.; van Bekkum, H. Hydrothermal formation of 1,2,4-benzenetriol from 5-hydroxymethyl-2-furaldehyde and D-fructose. *Carbohydr. Res.* **1993**, *242*, 131-139.

[42] Tarabanko, V. E.; Smirnova, M. A.; Chernyak, M. Y.; Kondrasenko, A. A.; Tarabanko N. V. The nature and mechanism of selectivity decrease of the acid-catalyzed fructose conversion with increasing the carbohydrate concentration. *J. Sib. Fed. Univ. Chem.* **2015**, *8*(1), 6-18.

[43] Hayes, D. J.; Ross, J.; Hayes, M. H. B.; Fitzpatrick, S. W. The Biofine process—Production of levulinic acid, furfural, and formic acid from lignocellulosic feedstocks. In *Biorefineries-Industrial Processes and Products: Status Quo and Future Directions*; Kamm, B., Gruber, P. R., Kamm, M., Eds.; Wiley-VCH Verlag GmbH & Co.: Weinheim, 2006; Chapter 7, pp 139-164.

[44] Tosi, P.; van Klink, G. P. M.; Celzard, A.; Fierro, V.; Vincent, L.; de Jong, E.; Mija, A. Auto-crosslinked rigid foams derived from biorefinery byproducts. *ChemSusChem* **2018**, *11*(16), 2797-2809.

[45] Filiciotto, L.; Balu, A. M.; Romero, A. A.; Rodríguez-Castellón, E.; van der Waal, J. C.; Luque, R. Benign-by-design preparation of humin-based iron oxide catalytic nanocomposites. *Green Chem.* **2017**, *19*(18), 4423-4434.

[46] Pin, J. M.; Guigo, N.; Mija, A.; Vincent, L.; Sbirrazzuoli, N.; van der Waal, J. C.; de Jong, E. Valorization of biorefinery side-stream products: combination of humins with polyfurfuryl alcohol for composite elaboration. *ACS Sustain. Chem. Eng.* **2014**, *2*(2), 2182-2190.

[47] Wang, Y.; Agarwal, S.; Kloekhorst, A.; Heeres, H. J. Catalytic hydrotreatment of humins in mixtures of formic acid/2-propanol with supported ruthenium catalysts. *ChemSusChem* **2016**, *9*(9), 951-961.

[48] Kang, S.; Zhang, G.; Yang, Q.; Tu, J.; Guo, X.; Qin, F. G. F.; Xu, Y. A new technology for utilization of biomass hydrolysis residual humins for acetic acid production. *Bioresources* **2016**, *11*(4), 9496-9505.

[49] de Jong, E.; van der Waal, J. C.; Boot, M. D. Fuel composition comprising humins. WO Patent, 2016130005A1, August 18, 2016.

[50] Carvalho, D. M.; Queiroz, J. H.; Colodette, J. L. Hydrothermal and acid pretreatments improve ethanol production from lignocellulosic biomasses. *Bioresour*ces **2017**, *12*(2), 3088-3107.

[51] Yang, Z.; Huang, Y.-B.; Guo, Q.-X.; Fu, Y. RANEY® Ni catalyzed transfer hydrogenation of levulinate esters to γ-valerolactone at room temperature. *Chem. Commun.* **2013**, *49*, 5328-5330.

[52] Baccile, N.; Laurent, G.; Babonneau, F.; Fayon, F.; Titirici, M.-M.; Antonietti, M. Structural characterization of hydrothermal carbon spheres by advanced solid-state MAS ^{13}C NMR investigations. *J. Phys. Chem.* **2009**, *113*(22), 9644-9654.

[53] Girisuta, B.; Janssen, L. P. B. M.; Heeres, H. J. A kinetic study on the decomposition of 5-hydroxymethylfurfural into levulinic acid. *Green Chem.* **2006**, *8*(8), 701-709.

[54] McManus, I.; Daly, H.; Thompson, J. M.; Connor, E.; Hardacre, C.; Wilkinson, S. K.; Sedaie Bonad, N.; ten Dam, J.; Simmons, M. J. H.; Stitt, E. H.; D'Agostino, C.; McGregor, J.; Gladden, L. F.; Delgado, J. J. Effect of

solvent on the hydrogenation of 4-phenyl-2-butanone over Pt based catalyst. *J. Catal.* **2015**, *330*, 344-353.

[55] von Arx, M.; Mallat, T.; Baiker, A. Unprecedented selectivity behavior in the hydrogenation of an α,β-unsaturated ketone: hydrogenation of ketoisophorone over alumina-supported Pt and Pd. *J. Mol. Catal. A* **1999**, *148*(1-2), 275-283.

[56] Agarwal, S.; van Es, D.; Heeres, H. J. Catalytic pyrolysis of recalcitrant, insoluble humin byproducts from C6 sugar biorefineries. *J. Anal. Appl. Pyrol.* **2017**, *123*, 134-143.

[57] Miljković, M. *Carbohydrates: Synthesis, mechanisms, and stereoelectronic effects*; Springer-Verlag: New York, 2009; Chapter 6, pp 143-167.

[58] Penczek, S.; Kubisa, P. Cationic ring-opening polymerization: Acetals. In *Comprehensive polymer science and supplements*; Allen, G., Bevington, J. C., Eds.; Elsevier Ltd.: New York, 1989; Volume 3, Chapter 49, pp 787-812.

[59] Ruiz-Matute, A. I.; Hernández- Hernández, O.; Rodríguez-Sánchez, S.; Sanz, I. Martínez-Castro, M. L. Derivatization of carbohydrates for GC and GC-MS analyses. *J. Chromatogr. B* **2011***, 879*(17-18), 1226-1240.

[60] Serun, E. M.; Selvakumar, S.; Zimmermann, N.; Sibi, M. P. Valorization of 2,5-furandicarboxylic acid. Diels-Alder reactions with benzyne. *Green Chem.* **2018**, *20*(7), 1448-1454.

[61] Cheng, Y.-T.; Huber, G. W. Production of targeted aromatics by using Diels-Alder classes of furans and olefins over ZSM-5. *Green Chem.* **2012**, *14*(11), 3114-3125.

[62] Ni, L.; Xin, J.; Jiang, K.; Chen, L.; Yan, D.; Lu, X.; Zhang, S. One-step conversion of biomass-derived furanics into aromatics by Brønsted acid ionic liquids at room temperature. *ACS Sustainable Chem. Eng.* **2018**, *6*(2), 2541–2551.

[63] Mahmoud, E.; Yu, J.; Gorte, R. J.; Lobo, R. F. Diels-Alder and dehydration reactions of biomass-derived furan and acrylic acid for the synthesis of benzoic acid. *ACS Catal.* **2015**, *5*(11), 6946–6955.

[64] Sangregorio, A.; Guigo, N.; van der Waal, J. C.; Sbirrazzuoli, N. Humins from biorefineries as thermoreactive macromolecular systems. *ChemSusChem* **2018**, *11*(24), 4246-4255.

[65] Dapsens, P. Y.; Kusema, B. T.; Mondelli, C.; Pérez-Ramírez, J. Gallium-modified zeolites for the selective conversion of bio-based dihydroxyacetone into C1-C4 alkyl lactates. *J. Mol. Catal. A* **2014**, *388-389*, 141-147.

[66] Asghari, F. S.; Yoshida, H. Acid-catalyzed production of 5-hydroxymethyl furfural from D-fructose in subcritical water. *Ind. Eng. Chem. Res.* **2006**, *45*(7), 2163-2173.

[67] Muralidhara, A.; Tosi, P.; Mija, A.; Sbirrazzuoli, N.; Len, C.; Engelen, V.; de Jong, D.; Marlair, G. Insights on the thermal and fire hazards of humins in support of their sustainable use in advanced biorefineries. *ACS Sustainable Chem. Eng.* **2018**, *6*(12), 16692-16701.

[68] Sangregorio, A.; Guigo, N.; van der Waal, J. C.; Sbirrazzuoli, N. All 'green' composites comprising flax fibres and humins' resins. *Compos. Sci. Technol.* **2019**, *171*, 70-77.

Supplementary Data (SD)
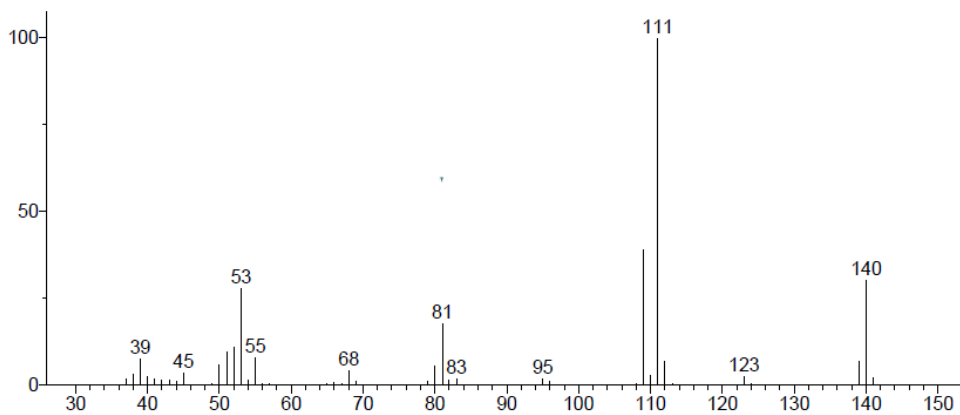
S1. Fragmentation pattern of MMF given by GC-MS analysis.
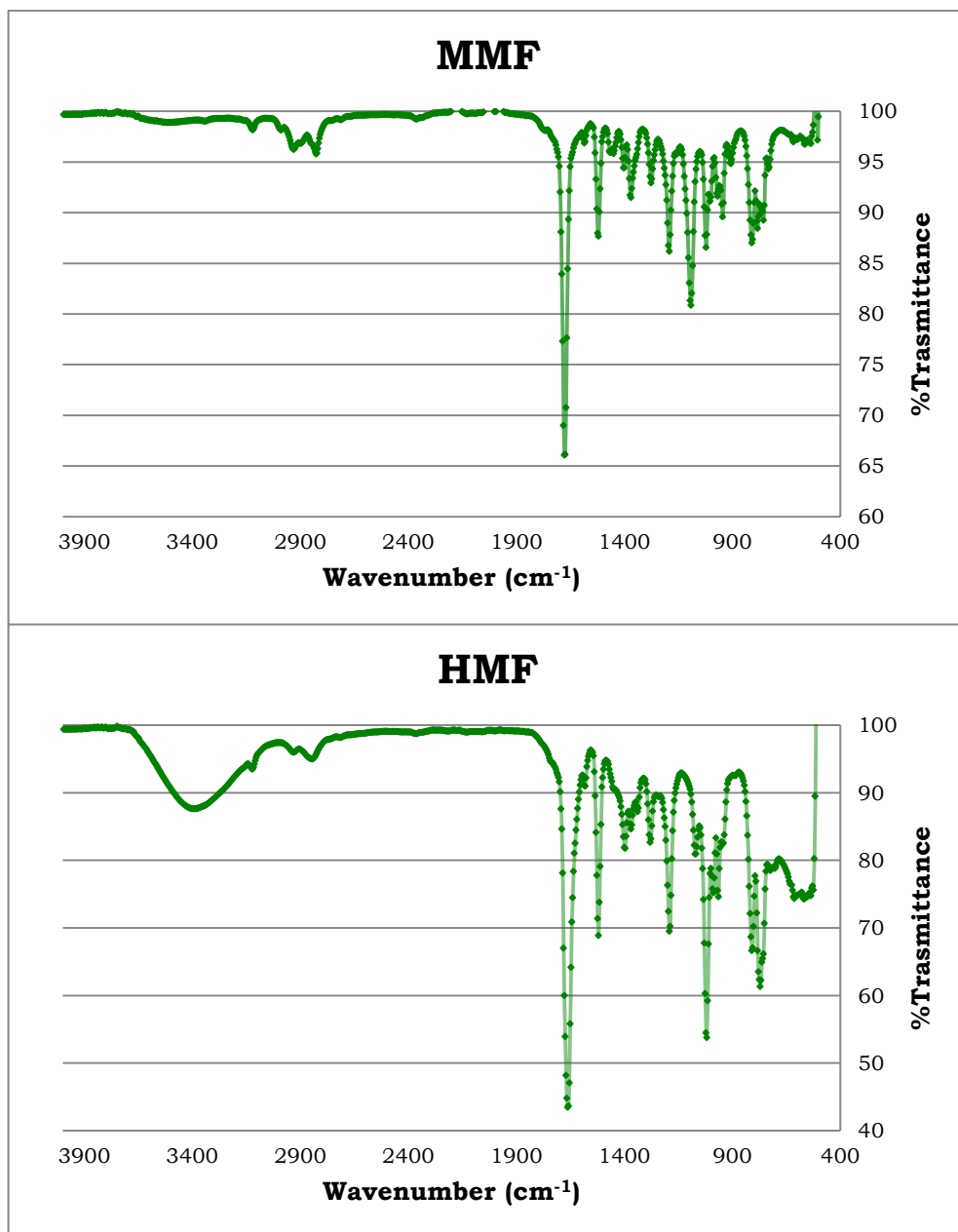
S2. ATR-IR analyses of MMF (top) and HMF (bottom).
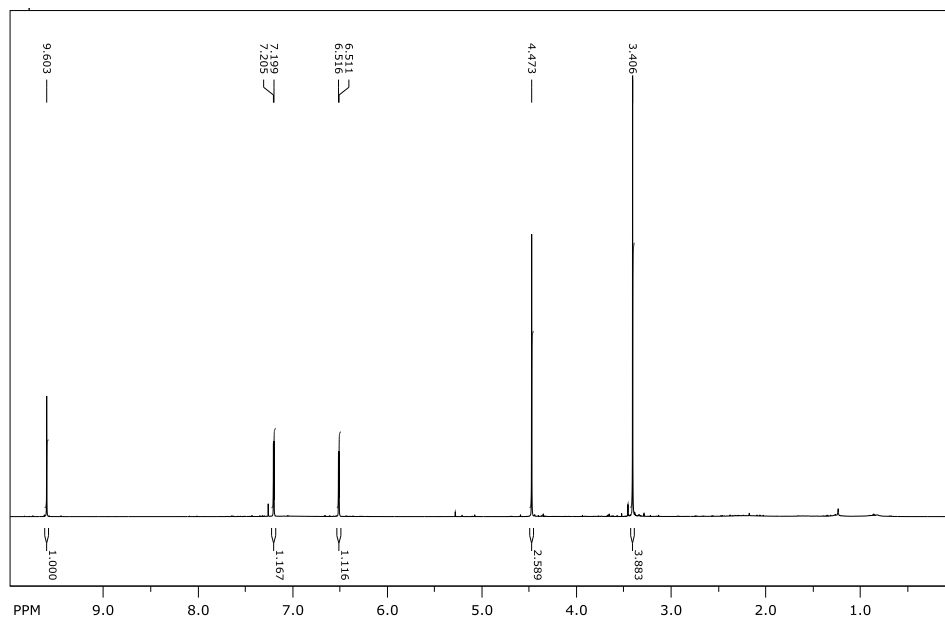
S3. ¹H NMR of MMF (CDCl₃). Singlets: 9.603, 4.473, 3.406;Doublets: 7.205-7.199, 6.515-6.511.
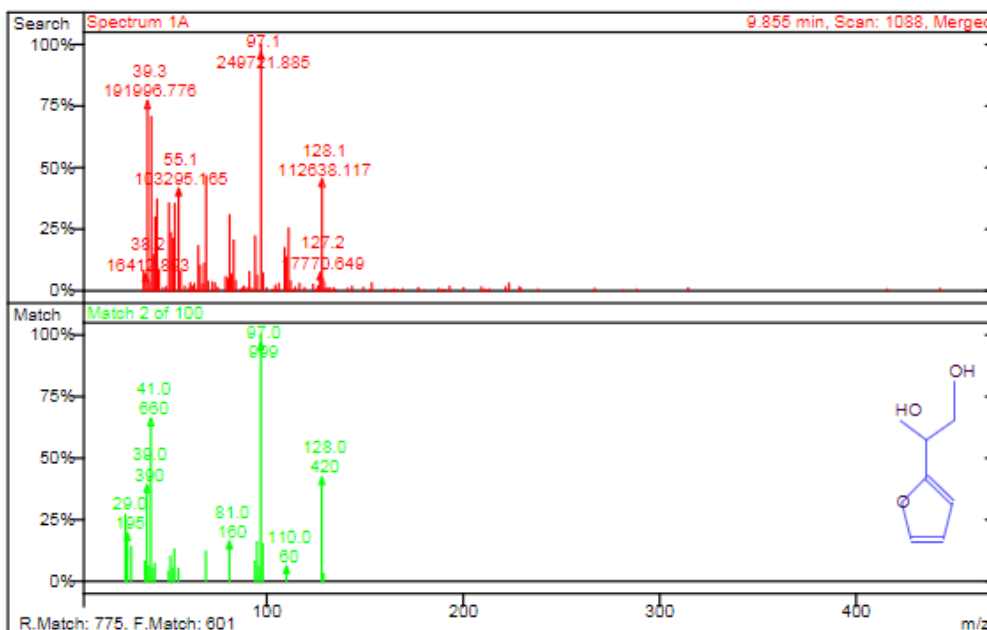
S4. Mass fragmentation spectra and comparison of 1-(2-Furyl)-1,2-ethanediol.
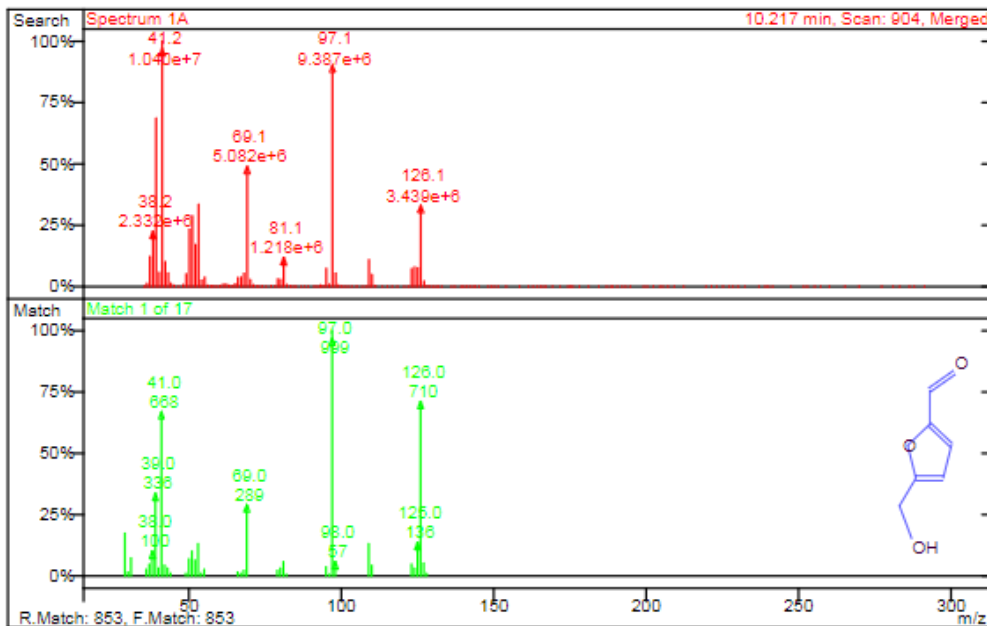
S5. Mass fragmentation spectra and comparison of HMF.
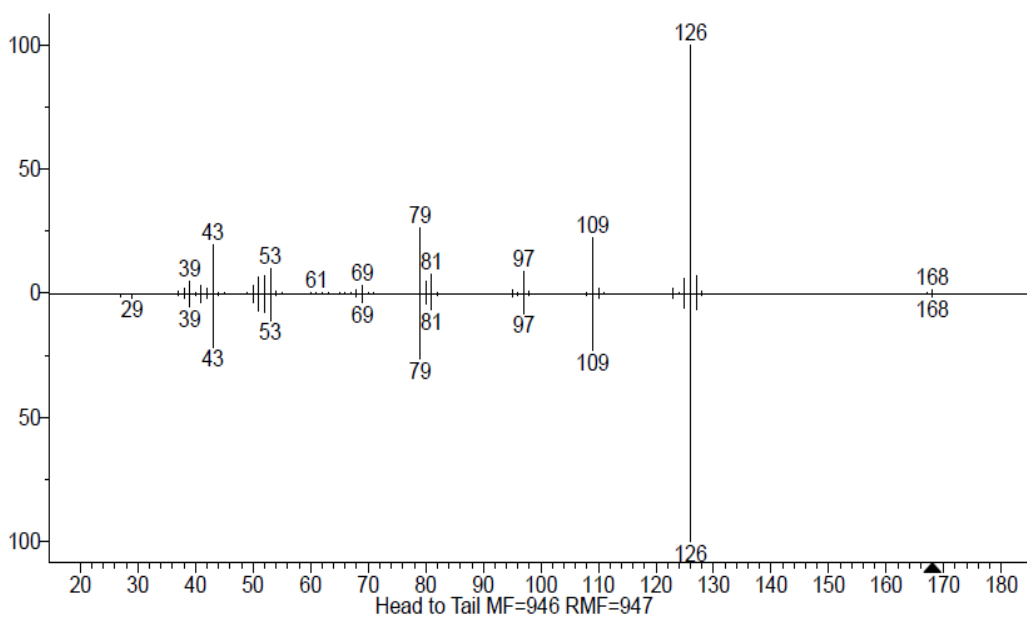
S6. Mass fragmentation spectra and comparison of 5-Acetoxymethyl-2-furaldehyde.

116
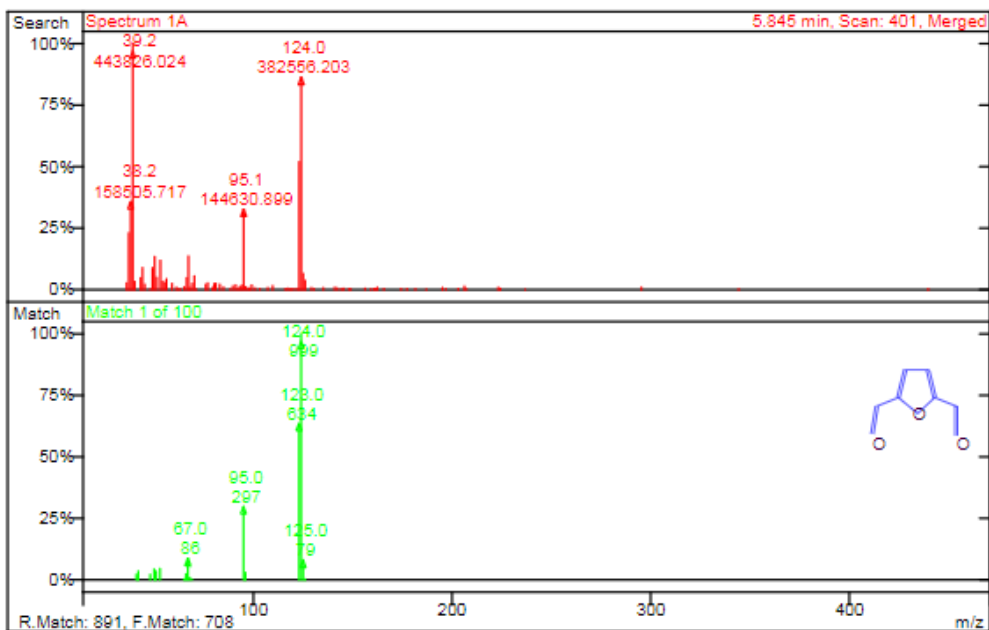
S7. Mass fragmentation spectra and comparison of 2,5-Diformylfuran.

S8. Mass fragmentation spectra and comparison of 2-Furyl anhydride.
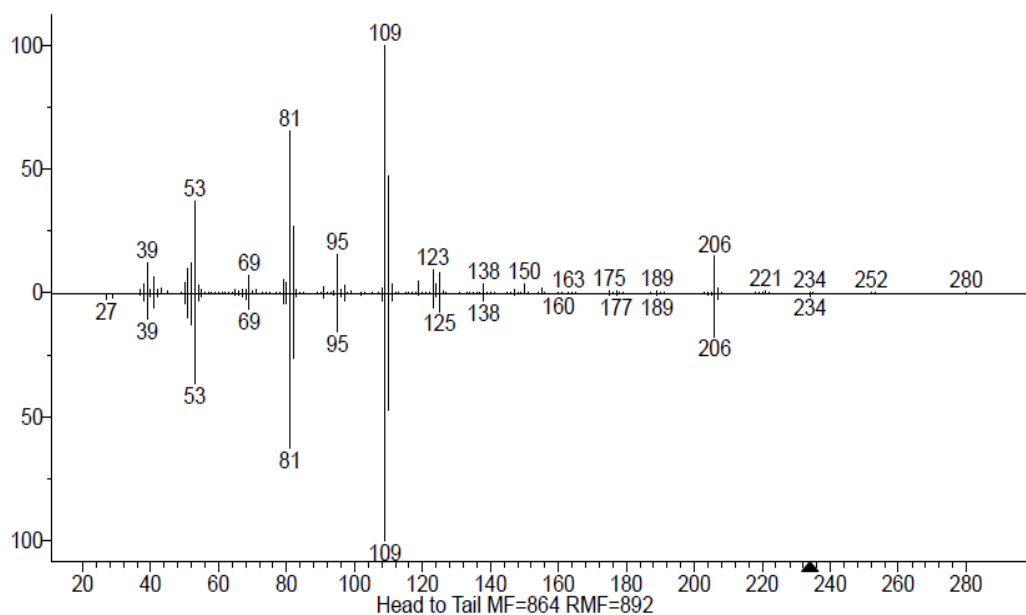
S9. Mass fragmentation spectra and comparison of Cirsiumaldehyde.
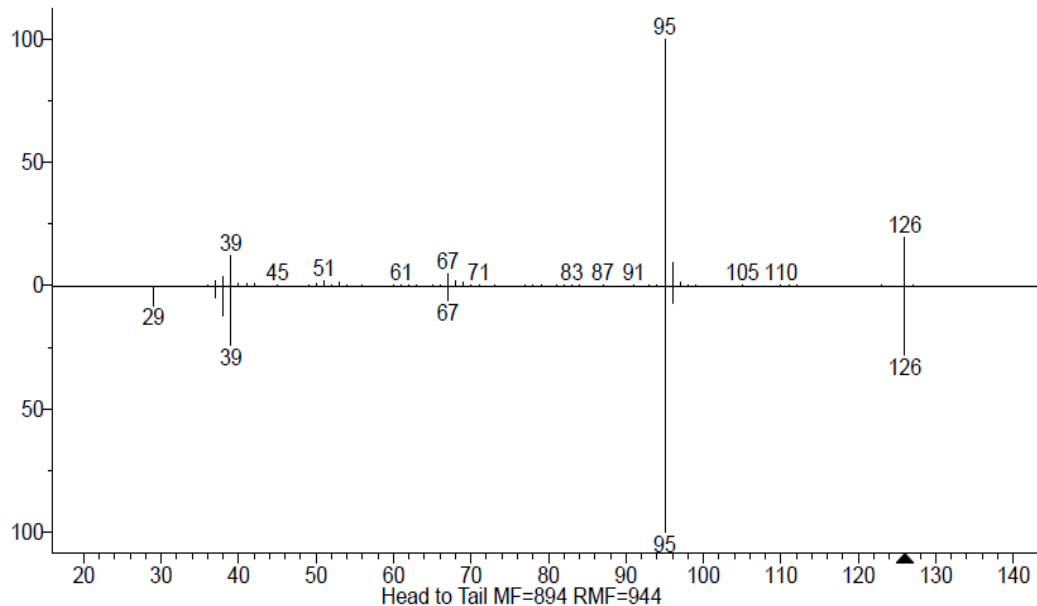
S10. Mass fragmentation spectra and comparison of Methyl 2-furoate.
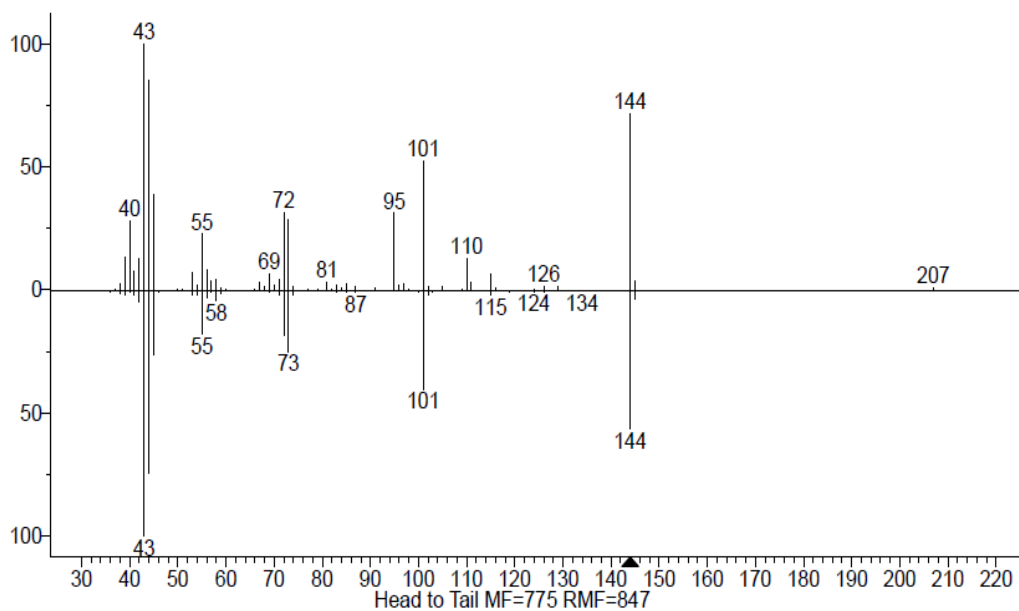
S11. Mass fragmentation spectra and comparison of
3,5,6-Trihydroxy-2,3-dihydropyran-4-one.
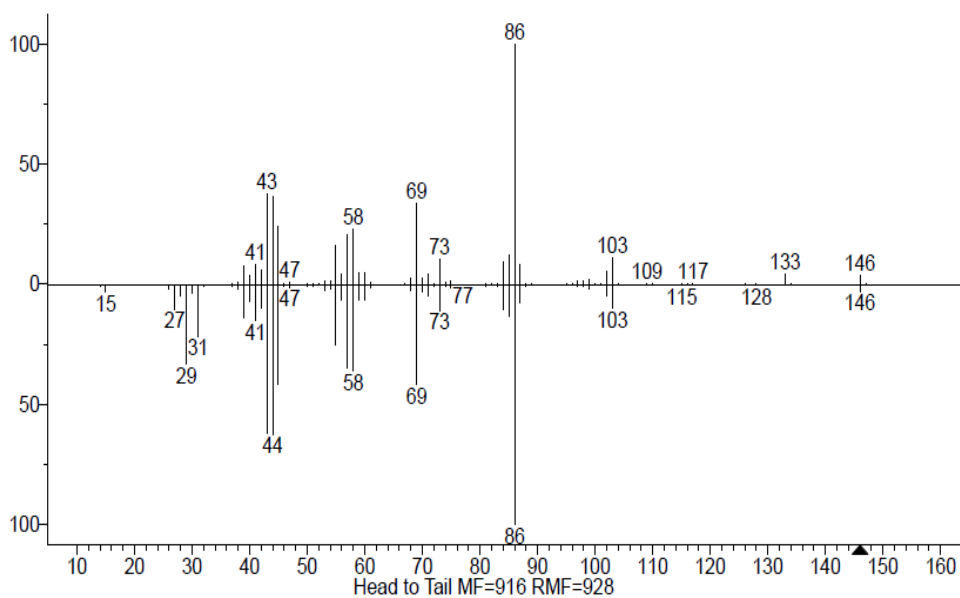
S12. Mass fragmentation spectra and comparison of Isosorbide.
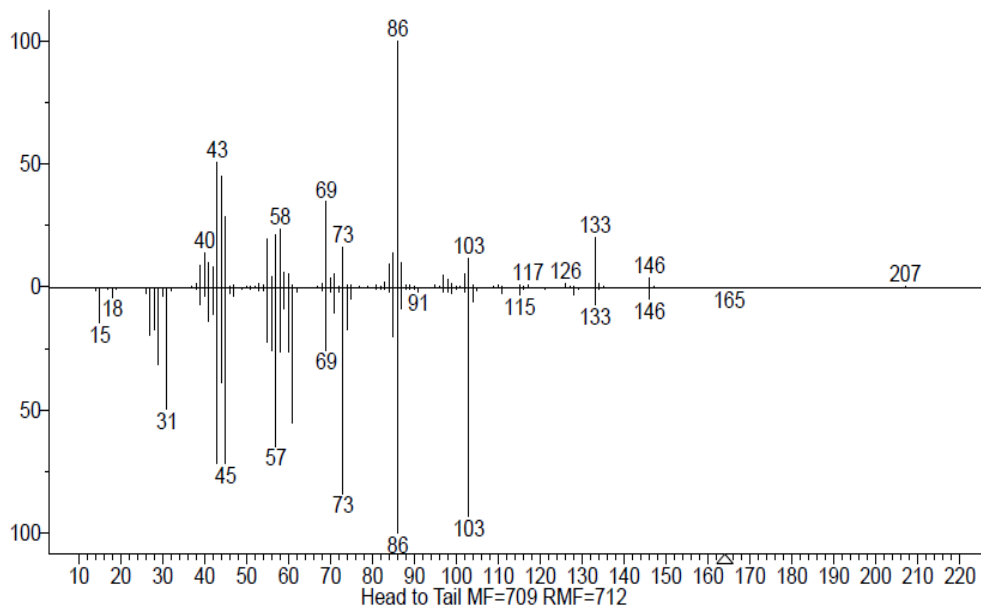
S13. Mass fragmentation spectra and comparison of
2-(1,2-Dihydroxyethyl)tetrahydrofuran-3,4-diol.
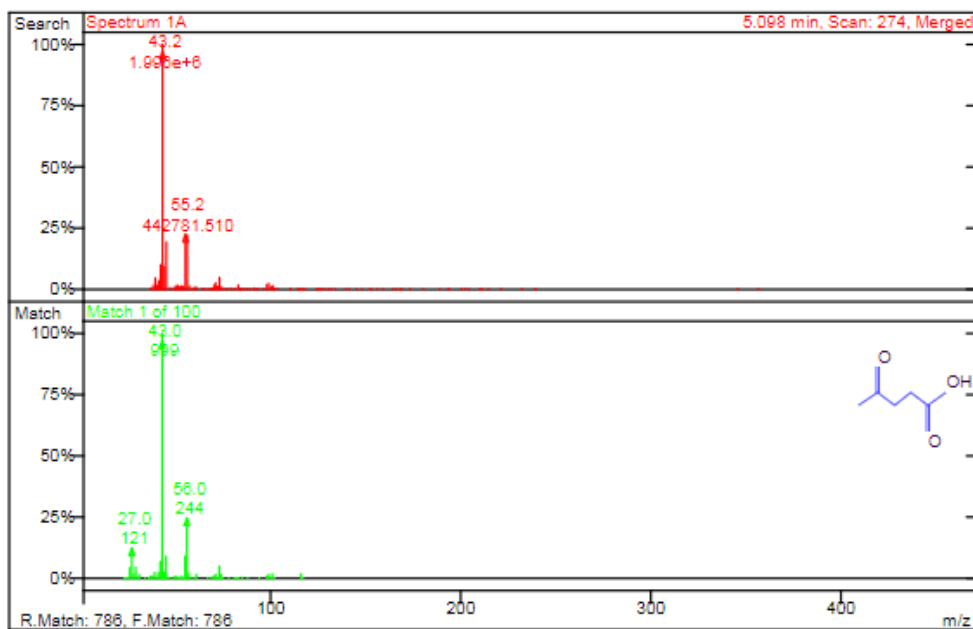
S14. Mass fragmentation spectra and comparison of Levulinic Acid.
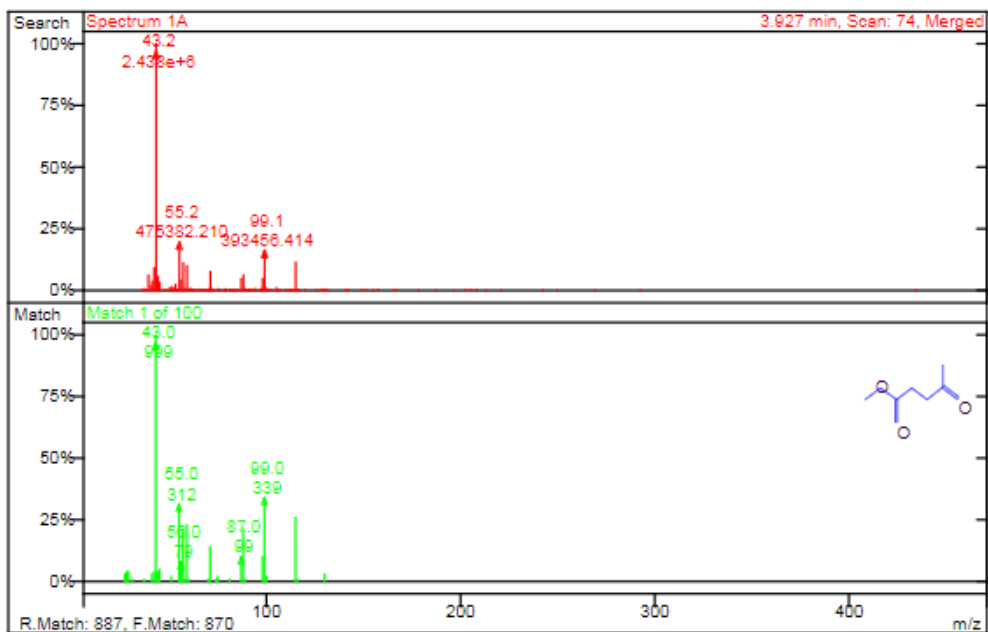
S15. Mass fragmentation spectra and comparison of Methyl Levulinate.
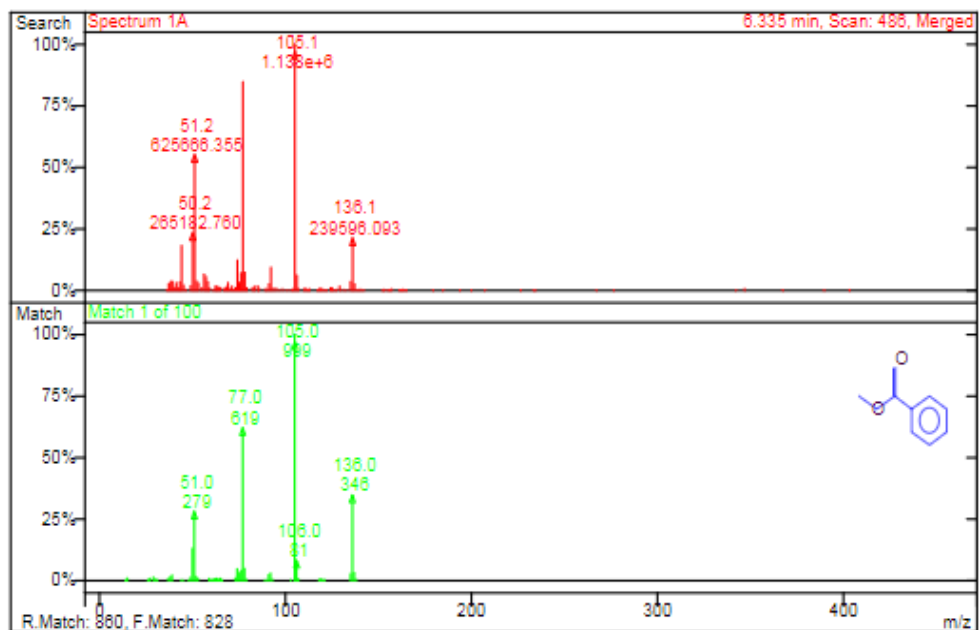
S16. Mass fragmentation spectra and comparison of Methyl Benzoate.
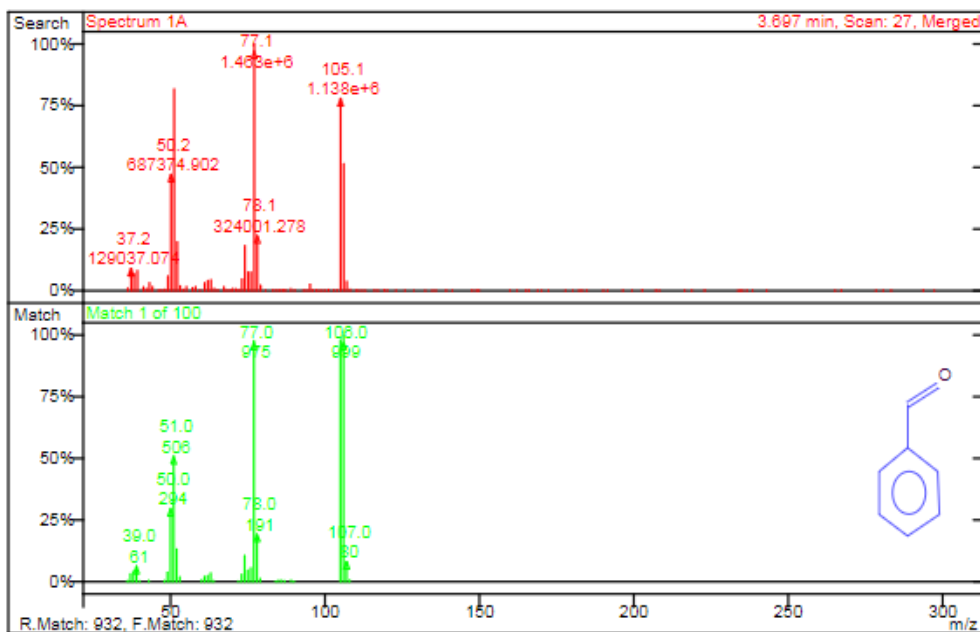
S17. Mass fragmentation spectra and comparison of Benzaldehyde.
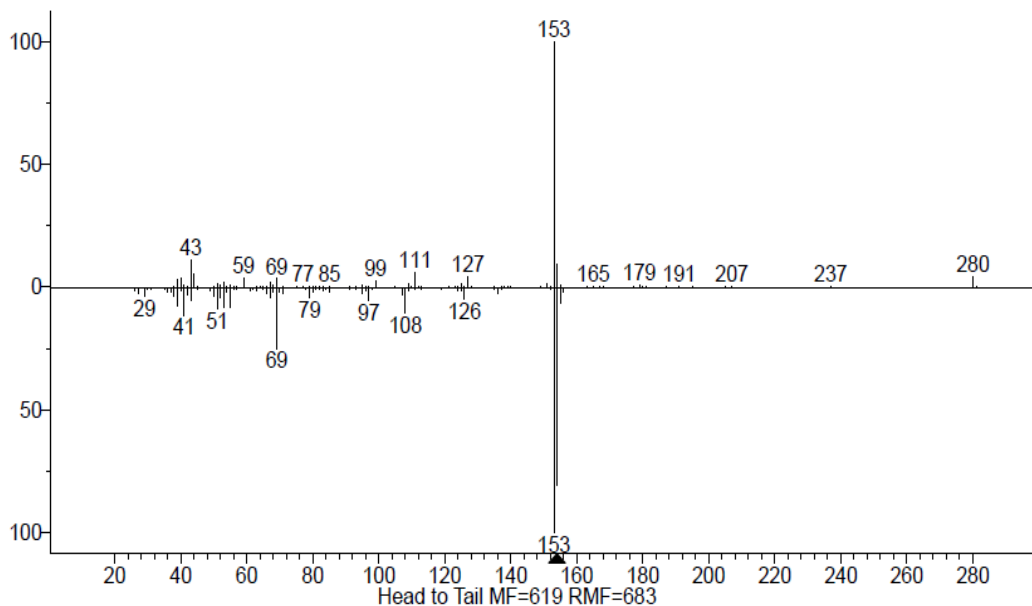
S18. Mass fragmentation spectra and comparison of 2,4,6-Trihydroxybenzaldehyde.
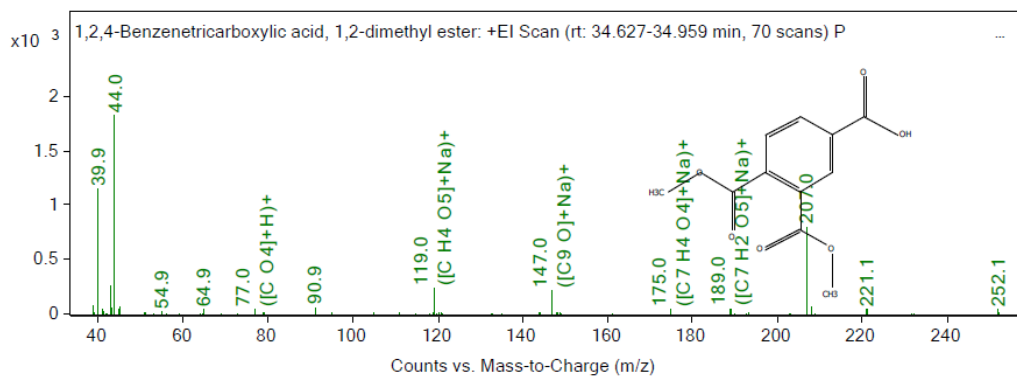
S19. Mass fragmentation spectra and comparison of
3,4-Dimethyoxycarbonylbenzoic acid.
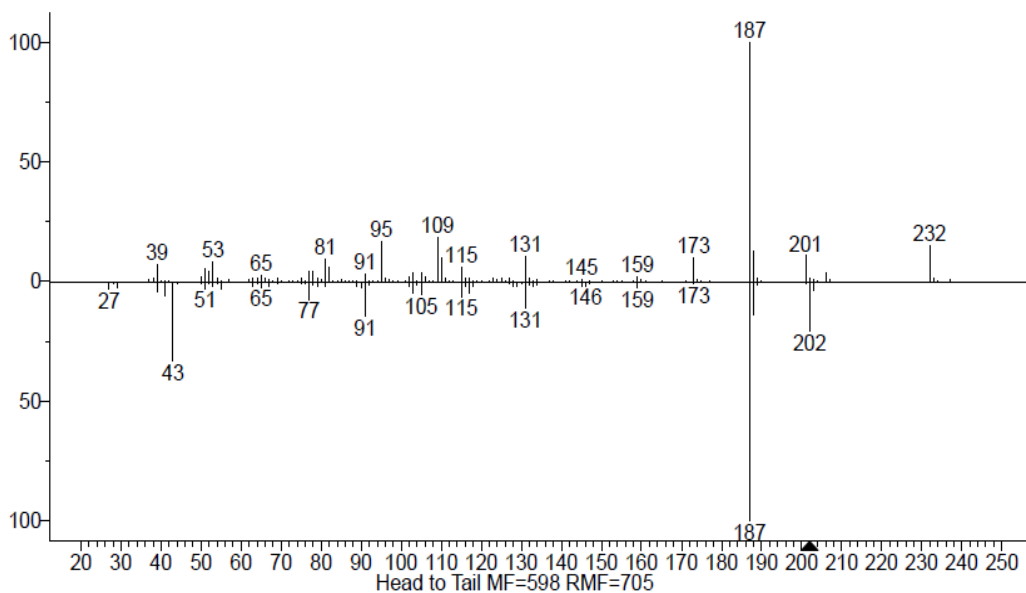
S20. Mass fragmentation spectra and comparison of
1-(4-cycloxehylphenyl)-ethanone.
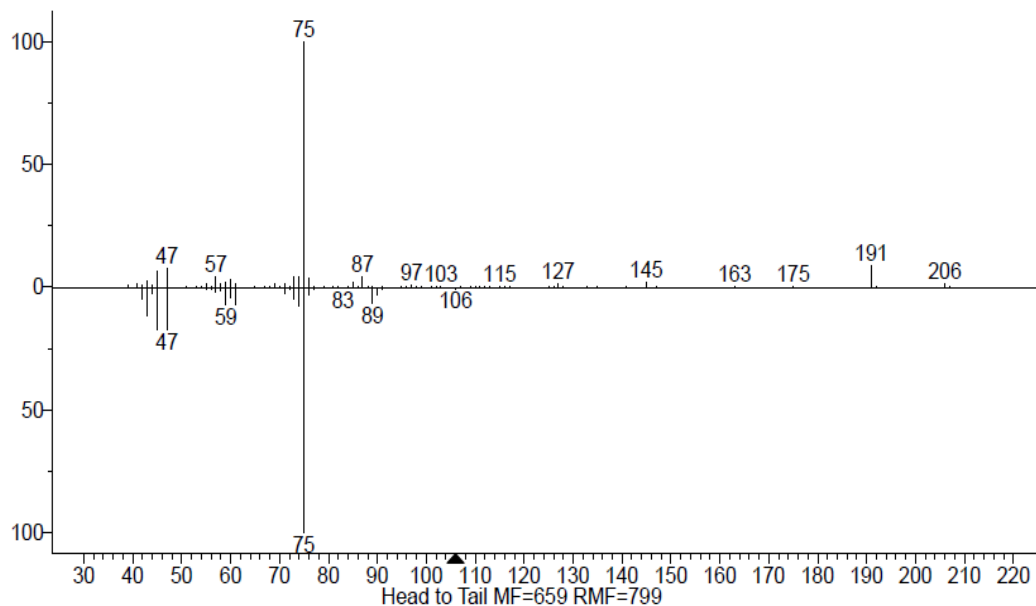
S21. Mass fragmentation spectra and comparison of Glyceric Acid.
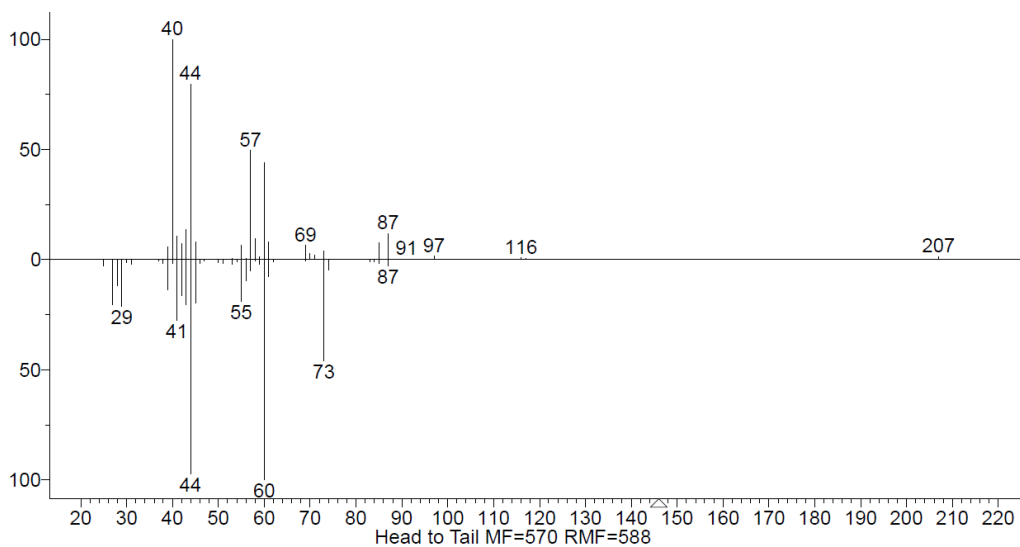
S22. Mass fragmentation spectra and comparison of Propylmalonic Acid.
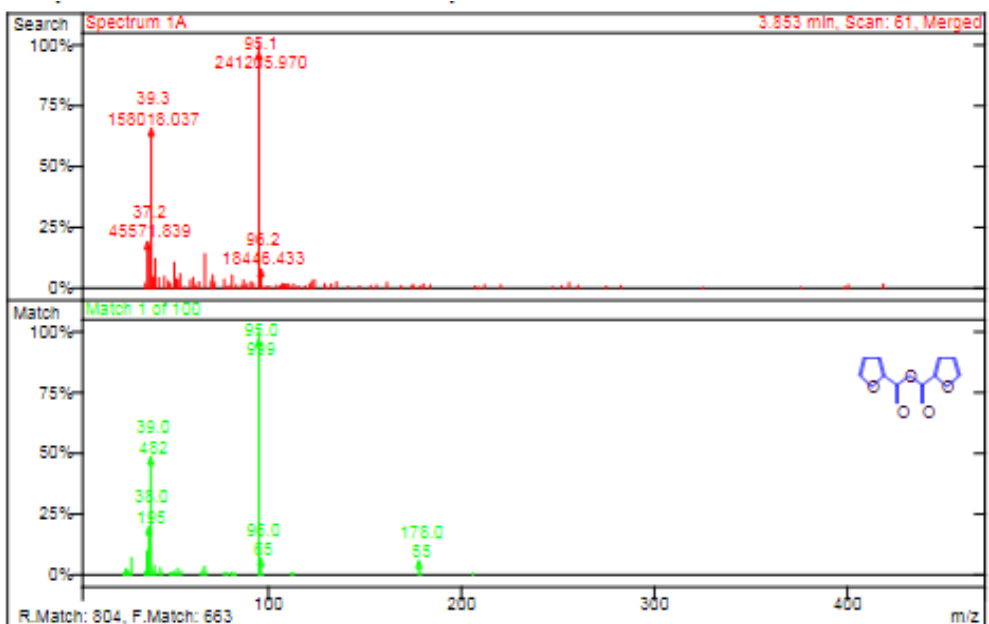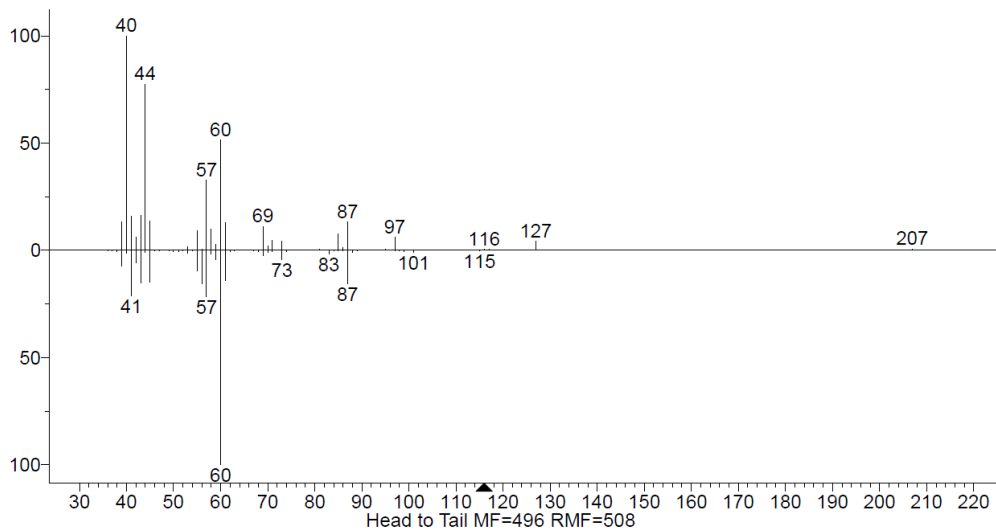
S23. Mass fragmentation spectra and comparison of Isovaleric Acid.
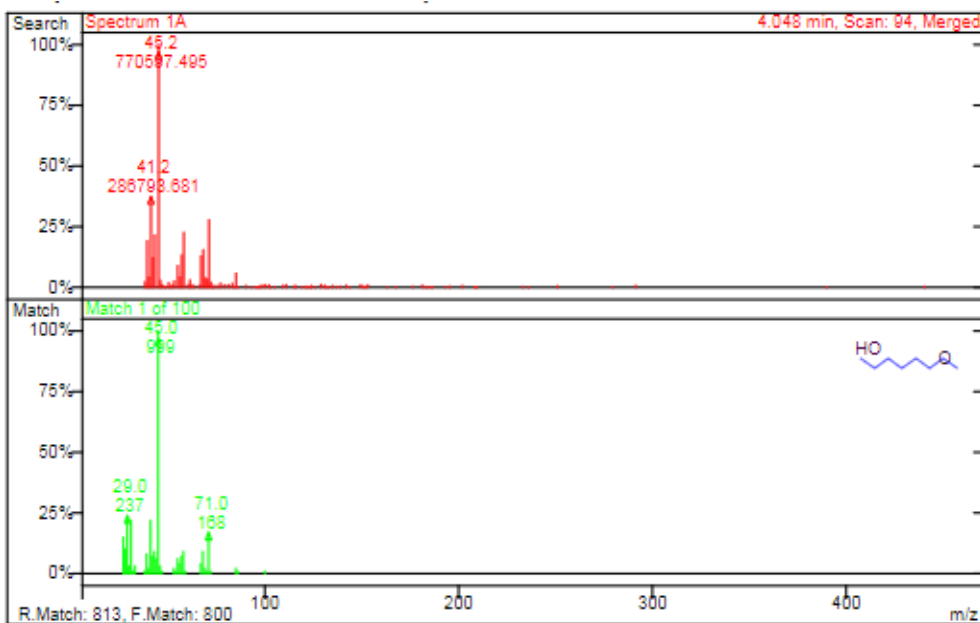
S24. Mass fragmentation spectra and comparison of 5-Methoxypentanol.
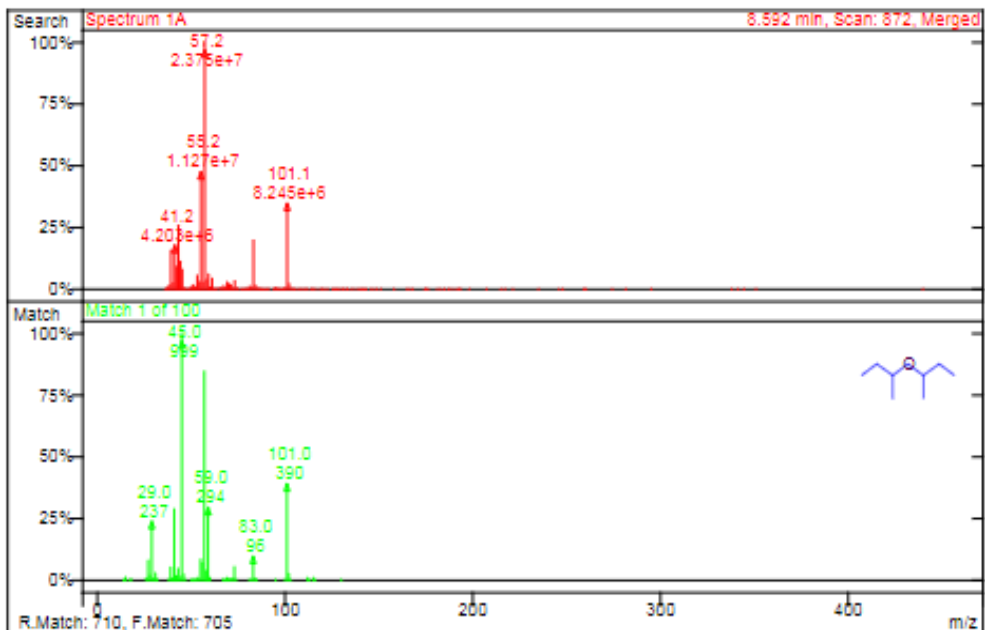
S25. Mass fragmentation spectra and comparison of 2-sec-Butoxybutane.
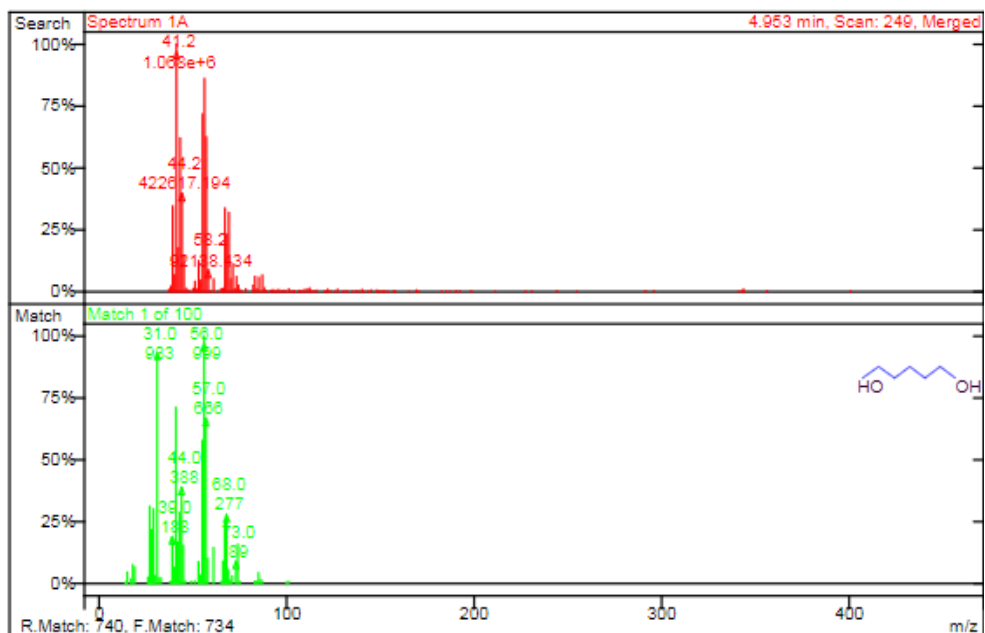
S26. Mass fragmentation spectra and comparison of 1,5-Pentanediol.
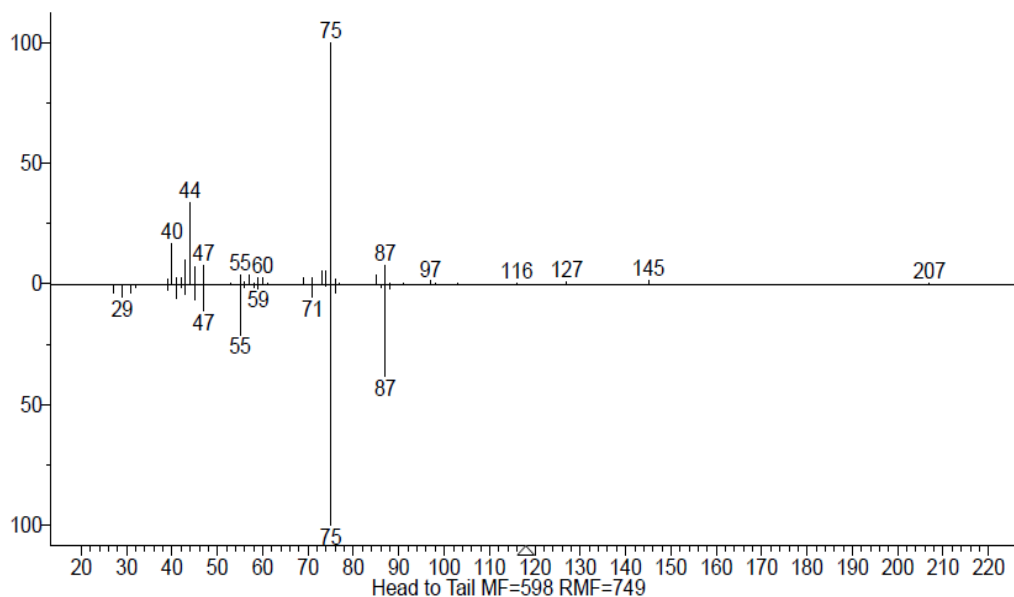
S27. Mass fragmentation spectra and comparison of 1,1-Dimethoxy-2-methylpropane.
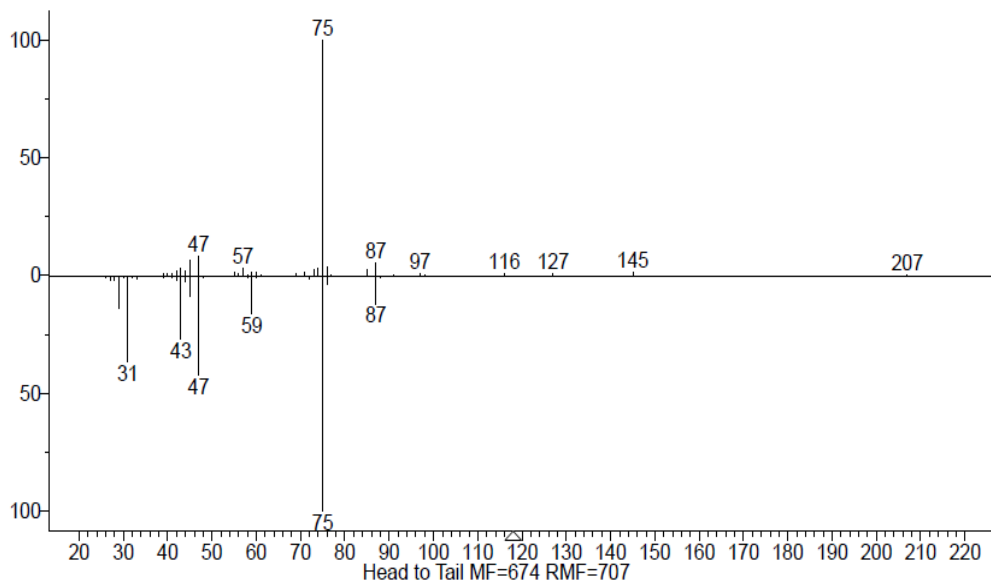
S28. Mass fragmentation spectra and comparison of 1,1-Dimethoxy-2-propanone.

(mainlib) Oxalic acid, isobutyl nonyl ester
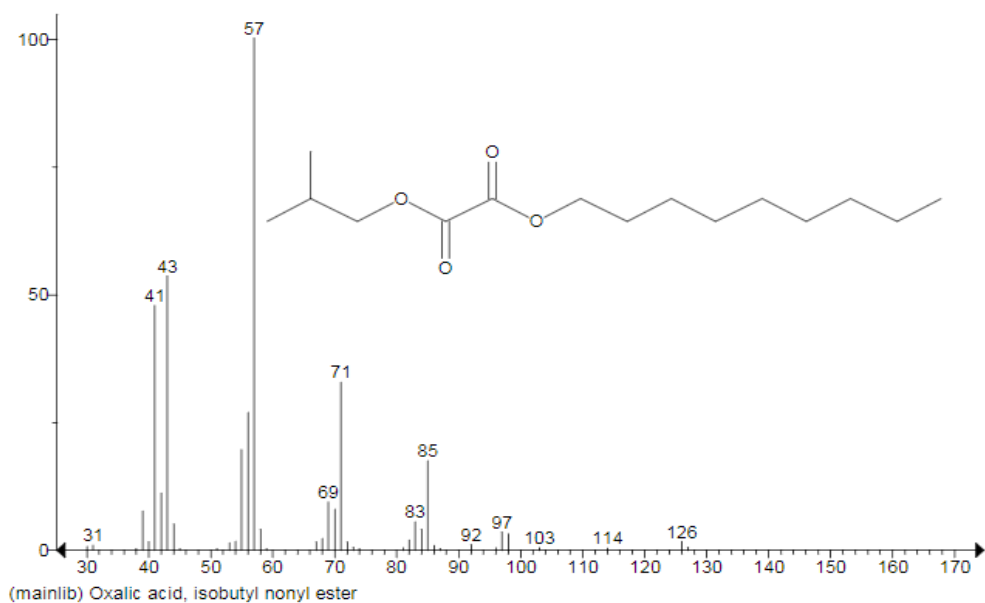
S29. Mass fragmentation spectra and comparison of Isobutoxycarbonyl decanoate.

Chapter 4

Humins as catalytic materials

This chapter is based on: Filiciotto, L.; Balu, A. M.; Romero, A. A.; Rodríguez Castellón, E.; van der Waal, J. C.; Luque, R. Benign-by-design preparation of humin based iron oxide catalytic nanocomposites. Green Chem., 2017, 19(18), 4423-4434.

Abstract

The current acid-catalyzed conversion of biomass feedstocks yields substantial quantities of undesired by-products called humins, for which applications are yet to be found. This work aims to provide a starting point for valorization of humins via preparation of humin-based iron oxide catalytic nanocomposites from humins and thermally treated humins (foams) *via* solvent-free methodologies including ball milling and thermal degradation. The prepared materials were found to be active in the microwave-assisted selective oxidation of isoeugenol (conversions >87%) to vanillin, proving the feasibility to use humin by-products as template/composite materials.

Introduction

Continuous scientific improvement, alongside the depletion of fossil feedstocks worldwide, calls for the investigatio of new sustainable processes using renewable sources. The synthesis of new active catalytic materials will play an important role in achieving this. Recent progress in biorefinery concepts leads the way in the production of platform chemicals from biomass as a widely available renewable resource.[1-6] As a matter of fact, Avantium's YXY technology has announced plans to build a 50 kta plant to convert biomass-derived sugars into platform chemicals (e.g. furanics and levulinics) for the synthesis of bio-plastics and fuels. In particular, the polymerization of a YXY furanic building block (furandicarboxylic acid, FDCA) with mono-ethylene glycol gives rise to PEF (polyethylene furanoate), a polyester with superior barrier and thermal properties compared to extensively used PET (polyethylene terephthalate).[7] However,the current conversion of plant-based stocks yields parallel substantial quantities of insoluble and intractable, black, sticky substances usually referred to as humins.[8-10] These humins are generally considered to comprise of a series of oligomers (270–650 g mol^{-1}) containing furanics, sugars, and aromatic moieties linked by mainly short aliphatic chains. Additionally, they include to a smaller extent acetal or ether bonds derived from the random condensation reactions of the main bio-derived molecules formed during the acid-catalyzed dehydration of sugars (*e.g.*, HMF, furfural, carbohydrates, and levulinates; Scheme 1).[11,12]
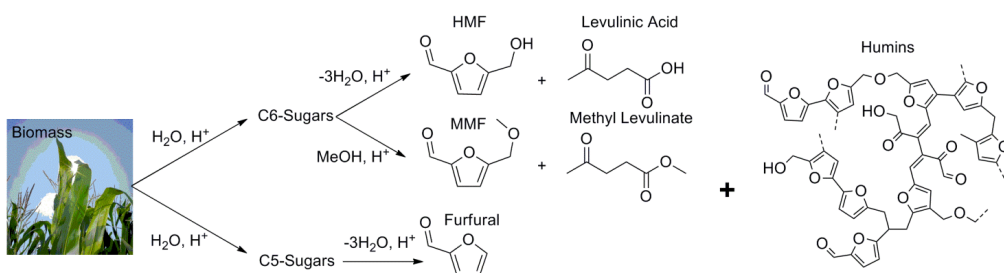
Scheme 1. Pathways for formation of humin by-products.

Functional groups including carboxylic, ketone, aldehyde and/or hydroxyl are shown by bulk analysis in the final structure of humin by-products, thus the presence of superficial oxygen functionalities is expected.[13] A typical elemental composition of humins is found to be in the order of *ca.* 65 wt% carbon, 5 wt% hydrogen, and 30 wt% oxygen.[14] Recently, Bruijnincx et *al.*[15] reported the quantification and classification of carbonyl groups for industrial humins and lignin, finding a higher content of both aliphatic and conjugated carbonyl groups in the humin sample (6.6 wt%) compared to Alcell (3.3 wt%) and Indulin Kraft (1.7 wt%) lignins. The significant presence of organic functional groups and the broad range of molecular weights suggest a wide applicability of humin by-products as stabilizers, templates and combustible agents, to name a few. It could be hypothesized that the residual oxygen functionalities could play an important role as catalytic active sites for redox and oxidation reactions, in a similar fashion to graphene oxide.[16]

Current research on humins is mainly focused on limiting the production of these compounds, so far considered waste.[17] Nonetheless, a few humin valorization studies have been carried out, *e.g.* gasification to syngas,[18] hydrocracking and hydrodeoxygenation to hydrocarburic molecules[9] or as a resin additive as shown by the improved mechanical properties of PFA (perfluoroalkoxy

alkanes)/humins composite.[19] The limited number of valorization studies so far, promted us to research the possibilities of employing humins as a material additive or a platform chemical. Alternatively, this study has been aimed to provide an alternative valorization of humins by-products as material composite/template in the synthesis of active catalytic materials.

Selective oxidative cleavage of hydrocarbons is one of the most relevant reactions in organic synthesis, finding applications in the conversion of both fossil and renewable feedstocks to industrial bulk and fine chemicals.[20-24] Traditional approaches often resort to toxic and/or environmentally harmful oxidants, *e.g.* ozone, permanganate, dichromate, or hypervalent iodine reagents,[26-31] which also often lead to extremely high *E*-factors (*i.e.* the ratio of mass of waste products over the mass of the desired compound).[25] Thanks to not only increasingly stringent environmental policies, but also an increased awareness of the scientific community in terms of sustainability and renewability, research focus has shifted towards the implementation of catalytic alternatives that allow the use of greener oxidants, such as molecular oxygen and hydrogen peroxide.[32] Homogeneous and heterogeneous catalytic systems have been both investigated in the selective oxidative cleavage of various olefins, where (i) homogeneous catalysts are often difficult to prepare and recover, and (ii) heterogeneous catalysts are often non-selective and prone to deactivation. Nonetheless, major improvements in both fields of catalysis have been reported in the literature, as well as metal-free conversions of alkenes, which are throughly discussed in a recent excellent review by Urgoitia *et al.*[33] Among the metal-based catalytic systems, iron catalysts show promising results in the oxidative cleavage of olefins.

In fact, as one of the most abundant, inexpensive and environmentally friendly metals on earth, iron has attracted the attention of researchers as a candidate in the synthesis of catalytic materials, finding applicability in a variety of emerging fields, ranging from energy storage to biomedicine.[34,35] Moreover, iron-based catalysis has shown potential in the green and selective oxidative cleavage of alkenyl aromatics (*e.g.* styrene), both in homogeneous and heterogeneous systems. Regarding homogeneous catalysis concerns, Pillai *et al.* have reported the innovative solventless oxidation of a variety of cyclic olefins employing hydrated iron(III) nitrate and 3.4 bar of molecular oxygen at 60-80 °C, obtaining high yields in the oxidation of styrene to benzaldehyde, while lower conversion to the corresponding carbonyls were obtained for the other alkenes present in the study.[36] A ligand bearing homogeneous Fe(III)-based catalyst was instead investigated more recently by Xiao and coworkers in the aerobic cleavage of a plethora of mono- and disubstituted styrenes, showing remarkable isolated yields of the corresponding aldehydes or ketones with only 1 bar of O_2 at 70-78 °C.[37]

Although homogeneous catalysis often results in exceptionally high conversions and selectivities, the reusability and separation from the reactor mixture of the catalyst still a cause of major concern in the scientific community. Thus, the development of catalytic systems with facile recoverability often resorts to heterogenization of the active material. Along these lines, the high stability and the magnetic properties of iron oxides nanoparticles make these materials attractive for use as catalytic materials.[38,39] Iron oxide is found as different polyforms including magnetite, *i.e.* Fe_4O_3 (iron(II,III) oxide); or α-Fe_2O_3 (hematite) and γ-Fe_2O_3 (maghemite), *i.e.* iron(III) oxide phases.[40] The magnetic properties of

magnetite and maghemite make their oxides highly attractive as a convenient approach for separation and reusability of these materials. Furthermore, iron oxide has proven to be an effective catalyst for various oxidation reactions, *e.g.* ref. 41-43. In the light of these properties, iron oxide-based catalytic systems have been investigated as well in the selective oxidation of vinyl aromatics. For instance, Rak *et al.* compared hollow, etched and solid ferrite nanoshells in the conversion of styrene to benzaldehyde under 4 bar of oxygen at 90 °C, obtaining satisfactory results.[44] Hong *et al.* reported the oxidation of styrene employing iron oxide coated platinum nanowires finding acetonitrile as the best solvent and, even though the highest benzaldehyde yield was obtained with the use of molecular oxygen (38.2% at 70 °C for 24 h under 1 atm of oxygen), the highest selectivity to the aldehyde was achieved by employing hydrogen peroxide as an oxidant.[45]

Since the only theoretical by-product produced is water, hydrogen peroxide has also attracted the attention of green researchers involved in the selective oxidation of alkenyl aromatics with remarkable results and Fe-based catalysts have been found able to activate such oxidant.[46-48] For iron oxide, Shi *et al.* investigated nano-γ-Fe_2O_3 in the oxidation of alcohols and olefins including styrene, obtaining higher yields using higher equivalents of hydrogen peroxide.[49] Exceptionally high isolated yields were reported by Rajabi *et al.* in the hydrogen peroxide-iron oxide nanoparticles oxidation of styrene derivatives in aqueous media under reflux conditions.[50] Thus, iron oxide nanoparticles coupled to hydrogen peroxide have proven to be active in the selective oxidation of alkenyl aromatics.

Vanillin is one of the most important flavoring employed in pharmaceuticals, food, beverages, and perfume industries;[51] however, natural extraction of vanillin from vanilla beans only yields to a mere fraction (*ca.* 50 tons) of the total annual vanillin demand (>15 000 tons), making synthetic vanillin a must.[52,53] The current production of synthetic vanillin is mainly based on the guacaiol-based route using depleting fossil feedstocks as a carbon source, thus raising an environmental and sustainability concern,[54] while bioconversion strategies of isoeugenol are often complex processes that lead to low vanillin yields.[55-57] Hence, more sustainable, efficient and green routes need to be developed, comprising the use of bio-derived substrates (*e.g.* isoeugenol) and green oxidants (*e.g.* H_2O_2).

Isoeugenol is an alkenyl aromatic present in certain essential oils, such as clove oil, tobacco, dill seed, gardenia, petunia, to name a few;[58-60] moreover, isoeugenol can also be derived from the extraction of sawdust and the controlled depolymerization of lignin, *i.e.* an important component of inedible biomass, whose conversion to high-end products still requires further research.[61] For this reason, isoeugenol has been generally viewed as a model compound, facilitating the identification of the best catalyst to be further upgraded for the conversion of lignin residues. As a consequence, the selective oxidative cleavage of the vinyl group of isoeugenol is a promising strategy towards a lignin-based production of synthetic vanillin, thanks to its possible derivation from inexpensive, natural, and inedible sources. Focusing on non-enzymatic isoeugenol conversion strategies, Herrmann *et al.* investigated the use of methyltrioxorhenium catalyst in the oxidative cleavage of isoeugenol and *trans*-ferulic acid to vanillin in the presence of anhydrous hydrogen peroxide which was postulated to run *via* subsequent epoxidation and diolization steps followed by a final oxidation to

vanillin.[62] Shul'pin *et al.* reported the oxidation of isoeugenol to vanillin by hydrogen peroxide with a combined *n*-Bu$_4$NVO$_3$/pyrazine-2-carboxylic acid (PCA) catalytic system under air proposing a radical mechanism.[63] The mechanistic differences given by a strict dependency between the oxidant/catalytic stystem further complicate the understanding and implementation of the oxidative cleavage of isoeugenol. Moreover, these homogeneous systems present the usual drawbacks of these types of catalysis (*vide supra*), thus incentivizing research towards the use of heterogeneous catalysts. Heterogenized co-porphyrin complexes intercalated into lithium taeniolite clay were studied by Adilina *et al.*, affording a vanillin yield of 72% when employing low isoeugenol concentrations (0.3 mmol) and high 100% O$_2$ pressure (3 bar) in acetonitrile.[64] The benefits of a low isoeugenol concentration were also observed by Bohre *et al.* in the aerobic oxidation of isoeugenol over reduced graphene oxide-supported copper oxide, but also a higher pressure and temperature (4 bar O$_2$ at 50 °C) were found to suppress by-products formation and improve overall vanillin yields. Moreover, the authors suggest a synergistic effect of the electron-rich graphene oxide in stabilizing the copper species, which could be expected from the humin by-products as well.[16] Both of the aforementioned heterogeneous isoeugenol conversion studies imply the formation of a dioxygenated intermediate between the isoeugenol radical and the activated metal centre prior the selective cleavage to vanillin, discarding the epoxidation route proposed by Herrmann *et al.* (*vide supra*). A radical-free mechanism is more likely to favor the selectivity towards one particular product (*e.g.* aldehyde, epoxide), and suppress the formation of high molecular weight co-products. Thus, although an unequivocal mechanism for the selective oxidation of the vinyl group of isoeugenol is yet to be established, the

consistency in the mechanistic speculations further support the investigation of heterogeneous catalytic systems. To the best of our knowledge, iron-based heterogeneous catalysts have yet to be reported in the oxidative cleavage of isoeugenol to vanillin, in particular, if combined to a carbon-based side-product such as humins.

One of the 12 principles of Green Chemistry developed by Anastas and Warner[65] states the importance of minimizing the use of solvents whenever possible. Keeping this principle in mind, this work aimed to prove the possibility of synthesizing catalytic active materials from humins and iron precursors without the aid of any solvent. In particular, mechanochemical synthesis holds a promising route for the preparation of catalytic materials in solvent-free conditions. It was speculated that the combination of the accumulated potential energy, shear and friction forces in the milling process create a highly defective surface, which could lead to an improved reactivity of the material.[66] Thus, ball milling (BM) and alternative thermal degradation (TD) techniques in the absence of any solvent were investigated for the preparation of magnetic catalytic materials, employing thermally treated (humins foams)[67] and fructose-derived humins provided by Avantium B.V. (Netherlands), respectively. The catalytic activity of these materials was subsequently investigated in the microwave-assisted selective oxidation of isoeugenol to the high added value product, vanillin.

Experimental

Materials

Humins and humins foams[67] were provided by Avantium B.V. (Netherlands) and used as received. The catalysts precursors,

ferrous chloride tetrahydrate (99%, FeCl$_2$·4H$_2$O) and ferric nitrate nonahydrate (≥98%, FeNO$_3$·9H$_2$O) were purchased from Sigma Aldrich, as well as Fe$_2$O$_3$ and Fe$_3$O$_4$ nanopowders (nano-Fe$_2$O$_3$ and nano-Fe$_3$O$_4$, respectively) which were used as a comparison to the synthesized nanocomposites in the catalytic testing. Concerning the materials for the reaction mixture, hydrogen peroxide (50 wt%) and isoeugenol (98%) were purchased from Sigma Aldrich, whereas acetonitrile (99.9%) was purchased from PanReac. All of the materials were used without further purification.

Catalyst preparation

Ferrous chloride tetrahydrate (FeCl$_2$·4H$_2$O) and ferric nitrate nonahydrate (FeNO$_3$·9H$_2$O) were used for the synthesis of iron oxide composites. F-BM-CL and F-BM-NO catalysts were both prepared from humins foams (**F**) in a planetary ball mill (**BM**) Retsch, model PM 100. In particular, 2 g of ferrous chloride (**CL**) were employed for F-BM-CL, and the same amount in weight of ferric nitrate (**NO**) for F-BM-NO; the iron precursors were respectively milled at 350 rpm for 45 minutes (2 minutes intervals) with 4 g of humins foams, in order to assure the complete grinding of the carbonaceous material. Samples were subsequently dried overnight at 100 °C and calcined at 400 °C for 4 hours (β=5 °C min^{-1}).

H-catalyst series were instead synthesized by alternative thermal degradation (**TD**) of humins (**H**) and FeNO$_3$·9H$_2$O. The intrinsic stickiness of humins (caramel-like, *i.e.* highly viscous black liquid) makes these compounds difficult to handle, therefore an uncertainty of ±0.3 g in the quantities of humins used should be taken into consideration. H-TD-C and H-TD-W were synthesized by liquefying the humins in an oven at 100 °C over the iron precursor. In particular, H-TD-C was prepared by close contact (**C**) melting of

humins (4 g) over a layer of ferric nitrate (4 g) in a crucible for ten minutes at 100 °C; for H-TD-W, instead, the humins (5 g) were liquefied at 100°C from a higher altitude compared to the layer of the iron precursor (2.5 g) by employing a watchglass (**W**) over the crucible.
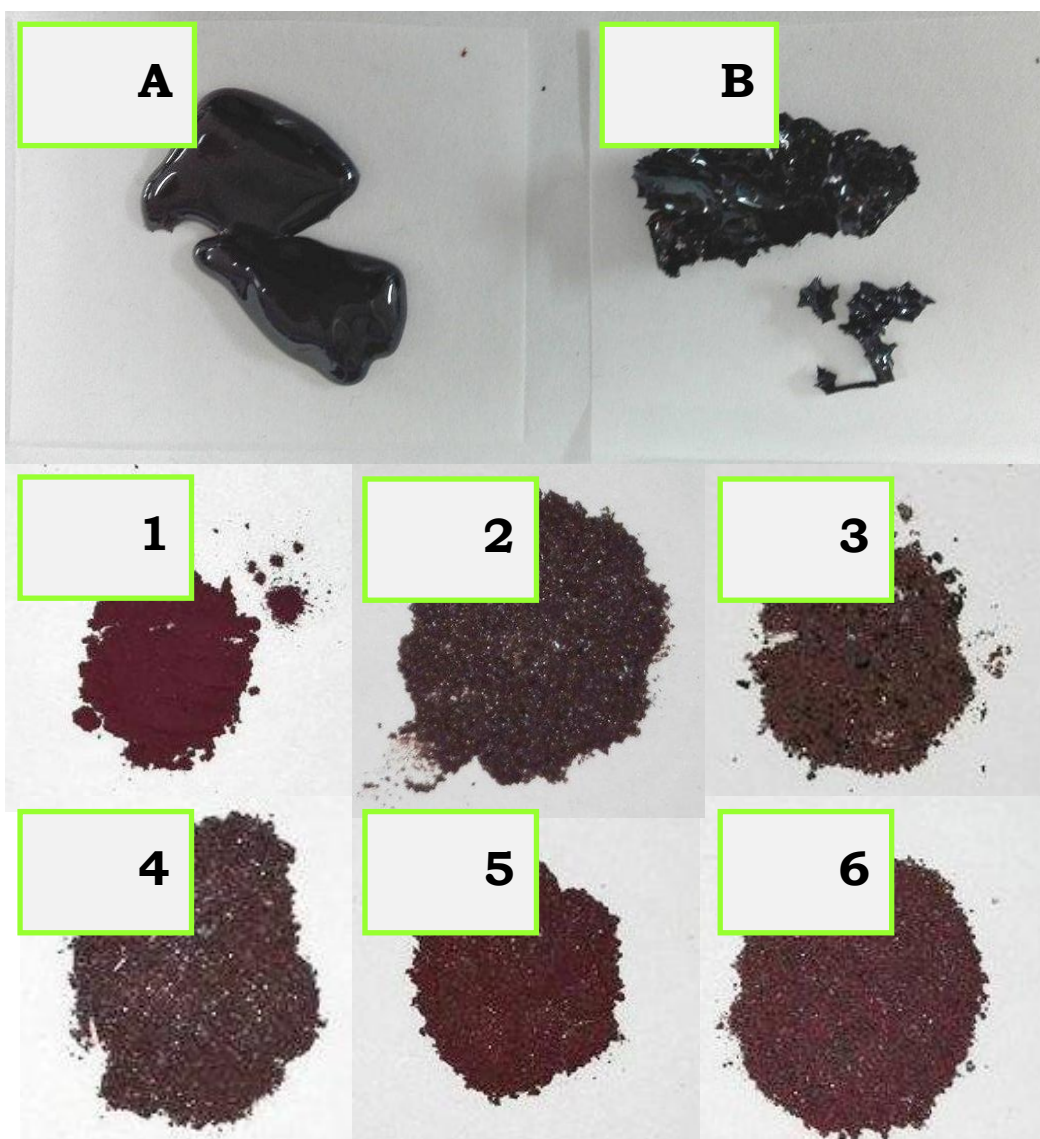
Figure 1. Images of the starting materials (A-humins, B-humins foams), and synthesized nanocomposites (1-F-BM-CL, 2-F-BM-NO, 3-H-TD-E, 4-H-TD-L, 5-H-TD-W, 6-H-TD-C).

For both samples, an increase of the volume of the solid solution has been observed, seemingly due to an incorporation of gases in the mix. A plausible explanation would be that upon decomposition of the iron(III) precursor, the humins undergo partial mineralization to CO_2, causing a visible increase of volume. Both of the samples were then manually ground, and calcined with the same conditions of the iron-foams materials (*vide supra*). For the H-TD-L and H-TD-E catalysts, discs of humins were prepared by melting the caramel-like carbon material at 100 °C over a non-sticky surface and subsequently solidified in a fridge. In particular, a layer (**L**) of 3 g of humins was covered with 0.66 g of iron precursor (maximum quantity that the surface of the layer could take up) and calcined in a folded position, yielding to H-TD-L; H-TD-E was synthesized by rolling a 2 g humins disc around 1 g of $FeNO_3 \cdot 9H_2O$, in a way that all the iron(III) nitrate would be embraced (**E**) by the carbon material. Both samples were then directly calcined at 400 °C, as all the other samples.

Catalyst Characterization

Nitrogen physisorption measurements were performed at 77 K by using an ASAP 2000 volumetric adsorption analyzer from Micrometrics. Samples were degassed for 24 h at 130 °C under constant vacuum (p < 10^{-2} Pa) before performing the measurements. Surface areas were calculated according to the BET equation, whereas average pore diameter and pore volume were obtained from the N_2 desorption branch.

X-ray Powder Diffraction (XRD) experiments were recorder on a Bruker D8 Discover diffractometer (40 kV, 40 mA), equipped with a goniometer Bragg Brentano θ/θ of high precision, using $Cu_{K\alpha}$ (λ=0.15406 nm) radiation. Scans were performed over a 2θ range

from 10 to 80, at step size of 0.05° with a counting time per step of 143.3 s.

The chemical composition of the surface and the chemical state of the elements constituent of solids were studied by XPS. A Physical Electronics spectrometer (PHI Versa Probe II Scanning XPS Microprobe) was used with scanning monochromatic X-ray Al Kα radiation (100 µm, 100 W, 20 kV, 1,486.6 eV) as the excitation source and a dual beam charge neutralizer. High-resolution spectra were recorded at a given take-off angle of 45° by a concentric hemispherical analyzer operating in the constant pass energy mode at 23.5 eV, using a 1400 µm line (with a 100 µm diameter of the x-ray highly focused beam) analysis area. The spectrometer energy scale was calibrated using Cu $2p_{3/2}$, Ag $3d_{5/2}$, and Au $4f_{7/2}$ photoelectron lines at 932.7, 368.2 and 84.0 eV, respectively. Under a constant pass energy mode at 23.5 eV condition, the Au $4f_{7/2}$ line was recorded with 0.73 eV FWHM at a binding energy (BE) of 84.0 eV. The PHI Smart Soft-VP 2.6.3.4 software package was used for acquisition and data analysis. A Shirley-type background was subtracted from the signals. Recorded spectra were always fitted using Gauss–Lorentz curves. Atomic concentration percentages of the characteristic elements of the surfaces were determined taking into account the corresponding area sensitivity factor for the different measured spectral regions.

Scanning electron micrographs (SEM) and elemental composition of materials were recorder using both the JEOL JSM 6300 and the JEOL JSM 7800F microscopes, the latter employed for energy-dispersive X-ray microanalysis (EDX) X-max 250 (detector SiLi, ATW2), at 20 kV.

Transmission electron micrographs (TEM) were recorded on a JEOL JEM 1400 instrument at 120 kv with a lattice resolution of *ca.* 0.4 nm. Samples were suspended in ethanol and deposited straight away on a copper grid prior to analysis.

Magnetic susceptibility was measured at room temperature with the Bartington MS-2 instrument at low frequency (470 Hz).

Catalytic testing

The microwave-assisted oxidation of isoeugenol to vanillin was performed in a CEM-Discover microwave reactor equipped with a PC-controlled interface. In particular, the Discover method in a sealed vessel was employed, which allows the system to build up pressure with the formation of gaseous products during the reaction. The observed pressure increase could however not be ascribed to mineralization of isoeugenol to CO_2, or decomposition of H_2O_2 to O_2, based on ideal gas law calculations. In all experiments, 2.5 mg of catalyst, 0.2 mL of isoeugenol, 0.3 mL of H_2O_2 (50wt%), and 1 mL of acetonitrile were employed, under 300 W of irradiation. Different reaction times were identified for these experiments, due to the runaway character of the oxidation (rapid increase of pressure). Therefore, 3 minutes reactions with a maximum reachable temperature of 140 °C under variable irradiation (0-300 W) were performed in order to have a better understanding of the catalytic activities. In particular, blank reactions were also carried out under these conditions: (i) a reaction with solely the reagent mixture, (ii) a reaction with the reagent mixture in the presence of the humins foams (2.5 mg), (iii) a reaction in the presence of (commercial) nano-Fe_2O_3 and (iv) a reaction in the presence of presence of (commercial) nano-Fe_3O_4 (2.5 mg). Recyclability tests were run for all the magnetic nanocomposites up to the first reuse with 2.5 mg of

catalyst. Reusability was investigated for the most stable nanocomposites with 50 mg of catalyst, under the same reaction conditions stated before. Results were analyzed by GC using an Agilent 7890A fitted with a Supelco column (100 m x 0.25 nm x 0.5µm) and a flame ionization detector (FID). Quantification of the products was obtained from the ratio of the corresponding peak areas, as justified by a close agreement of some representative product/reagent mixtures compared against a multicomponent calibration curve previously done by our research group. Furthermore, no solid residues or increase in viscosity was observed at the end of the reactions, thus indicating no unwanted polymerization of isoeugenol. This further was substantiated by consistent total peak areas in the GC analysis (*vide supra*). The reaction products were confirmed by HPLC and GC-MS analysis, carried out by the staff of the Central Service for Research Support (SCAI) of the University of Córdoba, Spain.

Results and Discussion

The catalysts presented in this study have been synthesized via ball milling of humins foams with two different iron precursors (F-BM-CL, iron(II) chloride; and F-BM-NO, iron(III) nitrate) or by alternative thermal degradation of humins combined to Fe(III) nitrate in alternative ways, resulting into the H-catalyst series (H-TD-E, H-TD-L, H-TD-C, H-TD-W). In particular, H-TD-E and H-TD-L were synthesized by employing humins discs either embracing (H-TD-E) or being covered (H-TD-L) by the iron precursor; H-TD-C and H-TD-W were instead prepared by the melting of humins either in close contact with the iron precursor (H-TD-C) or from a higher altitude (H-TD-W) with the aid of a watchglass over the crucible.

The resulting textural properties determined by the BET-N$_2$ physisorption method of the composites are summarized in Table 1. The physical nature of humins implies no porosity, whereas the BET analysis of humins foams (entry 2) shows generally low values of surface area and pore volume. Interestingly, all of the composites, present systematically higher surface areas and pore volumes, with pore diameters in the mesopore range (2-50 nm). Prominently, the use of the ferrous chloride precursor (F-BM-CL, entry 3) led to a very low surface area solid (*ca.* 8 m^2 g^{-1}), found to be consistently higher when ferric nitrate was employed (S.A.$_{F-BM-NO}$=34 m^2 g^{-1}). For the H-series, H-TD-L possessed the highest surface area with a smaller average pore diameter, given probably by the layer disposition of the iron(III) precursor on the humins disc; the encapsulation of iron(III) nitrate into a humins disc (H-TD-E, entry 5) led, as expected, to a lower surface area and pore volume.

Table 1. Textural properties of humins and foams composites.

		Surface area/m^2 g^{-1}	Pore volume/cm^3 g^{-1}	Average pore diameter/Nm
1	Humins[a]	-	-	-
2	Foams[b]	<5	0.06	11.8
3	F-BM-CL	<10	0.11	43.2
4	F-BM-NO	34	0.15	12.5
5	H-TD-E	20	0.11	16.4
6	H-TD-L	58	0.19	9.6
7	H-TD-W	45	0.20	12.9
8	H-TD-C	43	0.17	12.1

[a]Physical nature of humins (black liquid phase) does not allow BET analysis
[b]Starting material of F-catalyst series

Nonetheless, the average pore diameter of the H-TD-E composite is larger than other H-series materials, indicating the formation of shorter and wider pores, probably due to the spatial constriction given by the humins embrace during preparation.

X-ray Powder Diffraction (XRD) analysis results of the materials are presented in Fig. 2. The high intensity of the peaks shows a high degree of cristallinity for all the samples.
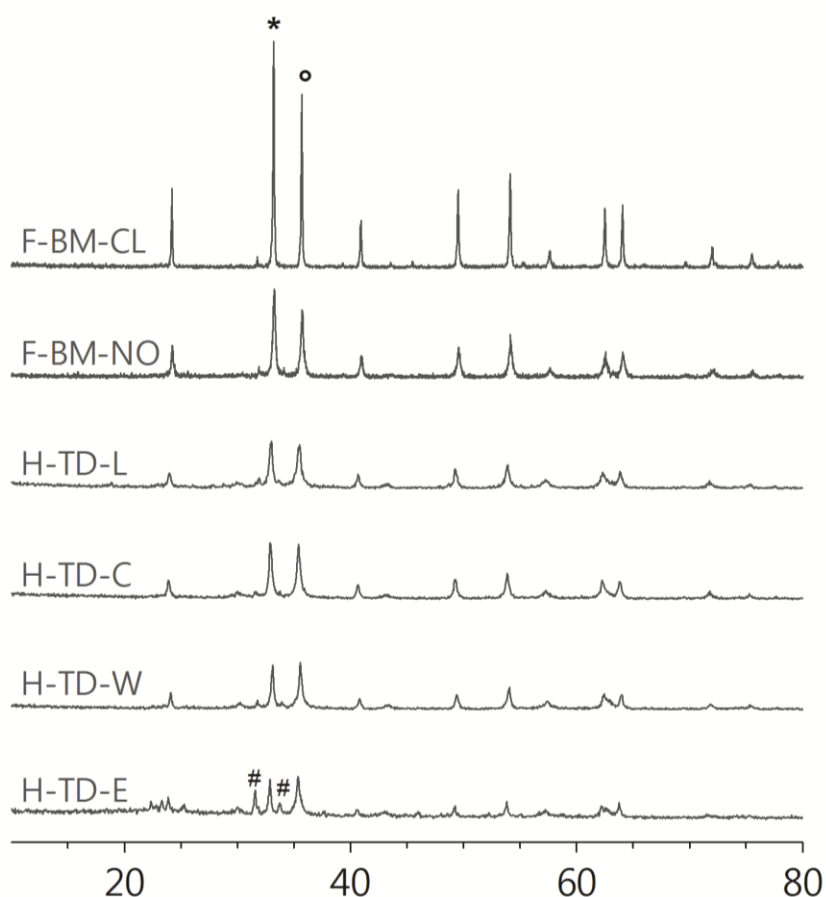
Figure 2. XRD patterns of the F- and H-series composites. (*,hematite; °, either maghemite, magnetite, or hematite; #, sodium sulfate or similar, *see text*).

In particular, F-BM-CL presents an almost pure hematite phase, indicating the previously reported oxidation of Fe(II) precursor to Fe(III) during the preparation under ambient atmosphere.[48,68] Mixtures of iron oxide phases were observed, with a lower degree of cristallinity, when Fe(III) precursors were employed probably due to impurities. In fact, the peak at 33.1° (**, Fig. 2) is typical of hematite, whereas the $2\theta = 35.5$ (°, Fig. 2) can be adscribed to either maghemite, magnetite, or hematite, indistinguishable by XRD. As a first analysis, F-BM-NO and H-TD-L exhibited a higher hematite content (H-TD-C has an almost 50:50 ratio of the iron oxides phases), while H-TD-W and H-TD-E exhibited a lower hematite content. XRD analysis of H-TD-E also shows the presence at 31.6° and 33.7° (**#**, Fig. 2), probably due to the presence of impurities including sodium sulfate or similar most probably coming from the humins matrix.

In fact, X-ray Photoelectron Spectroscopy (XPS) analysis showed for all the samples the presence of Fe, C and O (Table 2), but also Cl (0.3-1.1 wt%), S (1.1-7.6 wt%, as sulfate) and Na (3.5-13.3 wt%), was in good agreement with XRD results and supporting its origin from intrinsic impurities in humins and foams. In particular, H-TD-E showed the highest sodium and sulfur contents of respectively 13.3 wt% and 7.6 wt%, which justifies the presence of the unidentified XRD peaks (*vide supra*). Importantly, only Fe(III) species were found for all the samples (Fig. 3), concluding that the composites are mixtures of hematite and maghemite phases, except for F-BM-CL which is purely hematite (see XRD patterns).
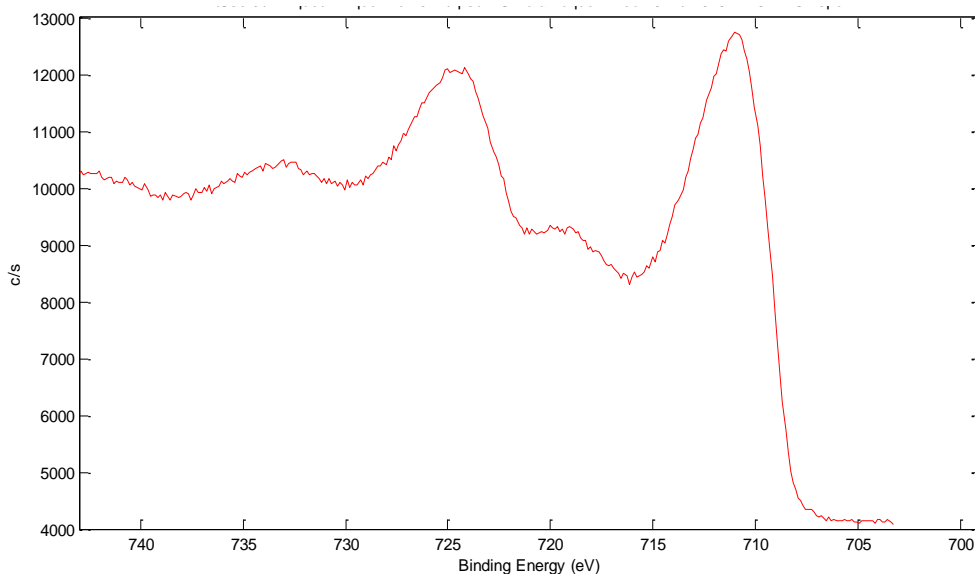
Figure 3. XPS spectra of the Fe 2p regions of F-BM-NO, representative of all the nanocomposites.

A detailed analysis of the C 1s spectra (Fig. 3) showed the presence of C—C (48.7-70.2%), C—O (19.3-34%), C=O (3.8-12.4%), and –COO⁻ (4.8-8.6%) species. These contributions can be adscribed to residual humins which are expected to have a higher degree of aromatization upon heating as previously found by Hoang[9] and van Zandvoort,[14] which might lead to rapid electron trasmission, thus higher catalytic activity.

Table 2 summarizes the mass concentrations of Fe, C, and O obtained from XPS, alongside the magnetic susceptibility of the composites. The use of Fe(II) chloride precursor led to a non-magnetic material (F-BM-CL, entry 1), whereas the use of Fe(III) nitrate resulted in the formation of promising magnetic nanocomposites.

For the H-series catalysts, it is possible to correlate a higher iron concentration with a greater magnetic susceptibility, thus a lower hematite content, in line with the first interpretation by XRD

148

analysis. Nonetheless, the extremely high superficial oxygen content (>50 at%, XPS) suggests a potential use of these composites as oxidation catalysts. The order of iron content determined by XPS decreased in the order: H-TD-W≈H-TD-C>F-BM-NO>H-TD-L>F-BM-CL>H-TD-E.

Morphological studies and SEM-EDX of the foams and humins composites show a highly defective and non-homogeneous surface for most of the samples. Tendentiously, the composites form curious agglomerates from which independent nanoparticles can be clearly visualized at higher magnifications.

Table 2. Mass concentrations of iron, carbon and oxygen deducted by XPS analysis, and magnetic susceptibility.

		Mass Concentrations (%)			Magnetic susceptibility/ 10^{-6} m^3 kg^{-1}
		Fe 2p	C 1s	O 1s	
1	F-BM-CL	46.28	11.07	34.99	_a
2	F-BM-NO	53.85	9.27	33.63	51.8
3	H-TD-E	39.64	15.07	36.25	118.9
4	H-TD-L	48.72	9.08	35.12	176.8
5	H-TD-W	57.12	6.28	32.14	202.3
6	H-TD-C	57.06	8.11	31.9	178.4

[a]Non-magnetic material

SEM micrographs of F-BM-CL (Fig. 4-A) shows the most regularity in shape, being hexagonal particles of various sizes (100-500 nm), in good agreement with the crystal lattice shape of iron oxide nanoparticles from TEM analysis (Fig. 5-A).
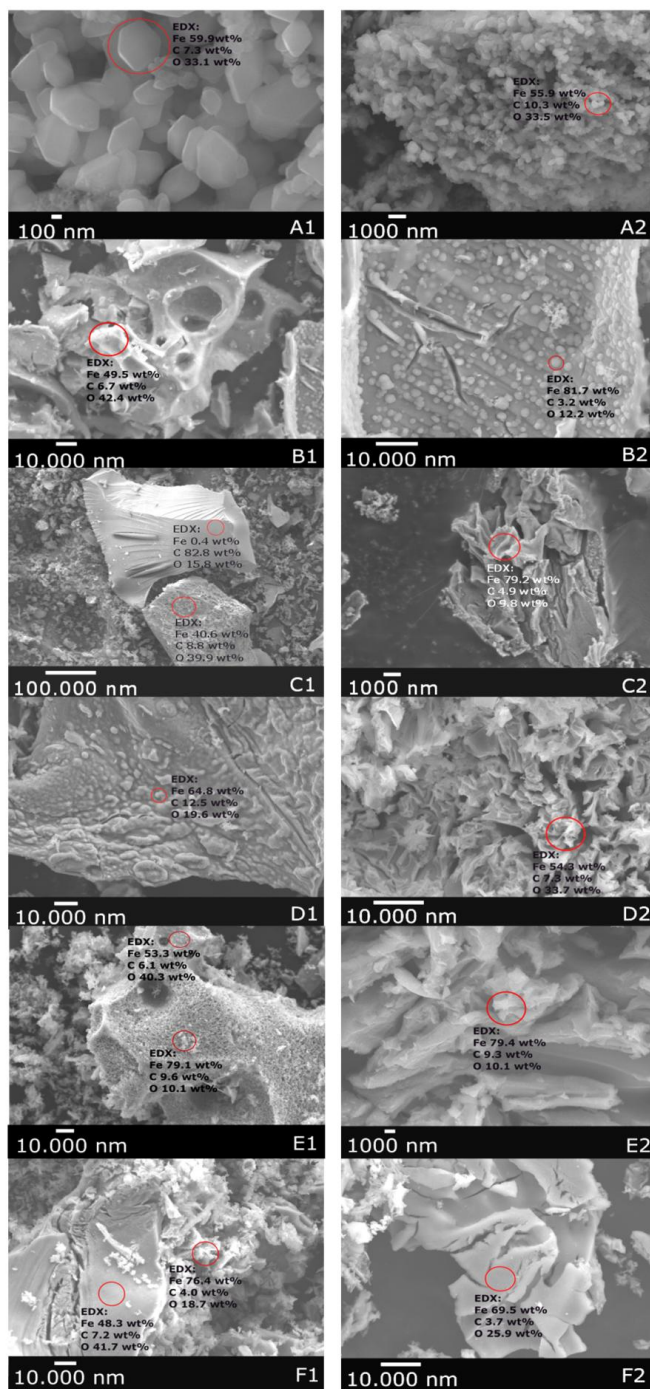
Figure 4. SEM micrographs of the iron oxide/humins composites. A1-A2: F-BM-CL; B1-B2: F-BM-NO; C1-C2: H-TD-E; D1-D2: H-TD-L; E1-E2: H-TD-W; F1-F2: H-TD-C.

The hexagonal particles of F-BM-CL were found to contain *ca.* 56 wt% Fe, 10 wt% C and 33 wt% O, and the remaining 1 wt% as impurities (*i.e.* Na, S, and Cl) *via* SEM-EDX analysis independent from the area of sampling, showing a fairly homogeneous sample. Similar values of weight percentages of the elements found with XPS analysis (*vide supra*) suggests the presence of iron oxide both in the bulk and the surface of the particles.

The strucuture of F-BM-NO (Fig. 4-B1), instead, reminds the macroscopic structure of untreated humins foams (Figure 1-B), however presenting embedded spherical iron-rich particles (SEM-EDX: Fe 82 wt%, C 3 wt%, O 12 wt%) of the order of 1-2 µm (Fig. 4-B2). This could be due to the reduction by carbon of the iron(III) species towards metallic iron, creating an iron-rich core. TEM analysis of F-BM-NO (Fig. 5-B) depicts irregular nanoparticles of 20 nm on average (extremes identified as between 6 and 32 nm) arranged to create a porous material, suggesting that the ball milling of foams and iron(III) nitrate gave a simil-template synthesis.

The H-series of materials are even less homogeneous, even at higher magnification. SEM micrographs show a more flake-like structure of iron oxide agglomerates in all samples, however differing from the preparation method (Fig. 4-C–F). For instance, H-TD-L, where the iron precursor was layered on a humins disc, shows areas where the iron oxide has directly deposited onto the disc (Fig. 4-D1, SEM-EDX: Fe 65 wt%, C 13 wt%, O 20 wt%), with the flake-like structures having an elemental composition of similar order (Fig. 4-D2, SEM-EDX: Fe 54 wt%, C 7 wt%, O 34 wt%). On the other hand, for the carbon-embraced iron precursor preparation, which resulted in H-TD-E, SEM-EDX analysis shows blocks of high carbon content materials (Fig. 4-C1, SEM-EDX: Fe 0.4 wt%, C 83 wt%,

O 16 wt%), probably derived from the outside shell of the humins disc not in contact with the iron precursor, and at the same time flake-like structures of high iron content (Fig. 4-C2, SEM-EDX: Fe 79 wt%, C 5 wt%, O 10 wt%). Fig. 3-E and -F show instead the SEM pictograms of the samples prepared by either close contact or higher altitude melting of humins, thus H-TD-C and H-TD-W, respectively. SEM-EDX of both samples showed high iron content of the flake-like structures in a similar fashion as H-TD-E, finding 76 wt% of iron for H-TD-C (Fig. 4-F1) and 79 wt% for H-TD-W (Fig. 4-E2). As for F-BM-NO (*vide supra*), the presence of humins could reduce the iron species towards a zero-valent state. Fig. 4-F2, instead, shows a highly defective iron oxide block in H-TD-C (SEM-EDX: Fe 69 wt%, C 4 wt%, O 26 wt%) which resembles a carbonaceous agglomerate, suggesting again a template-like synthesis.

TEM images (Fig. 4-C-F) of the H-series show, where possible to determine, nanoparticles of up to 300 nm, with the majority in the 4-30 nm range. In general, an amorphous carbon can be identified in the samples, often making it difficult to determine the single nanoparticles. Figures 5-C1, -D1, -F1, and -F2 are representative of the challenging determination of the nanoparticles in the various samples, almost resembling high resolution pictograms of solid solutions. Fig. 5-C2, in particular, shows what resembles a carbon block decorated with nanoparticles in the range of 12-14 nm. This could be ascribed to the chosen synthesis of this sample (*i.e.* H-TD-E), since the encapsulation of the iron precursor by the humins layer might have dispersed the nanoparticles in the carbon matrix.

Figure 5. TEM micrographs of the iron oxide/humins composites. A: F-BM-CL; B: F-BM-NO; C1-C2: H-TD-E; D1-D2: H-TD-L; E1-E2: H-TD-W; F1-F2: H-TD-C.
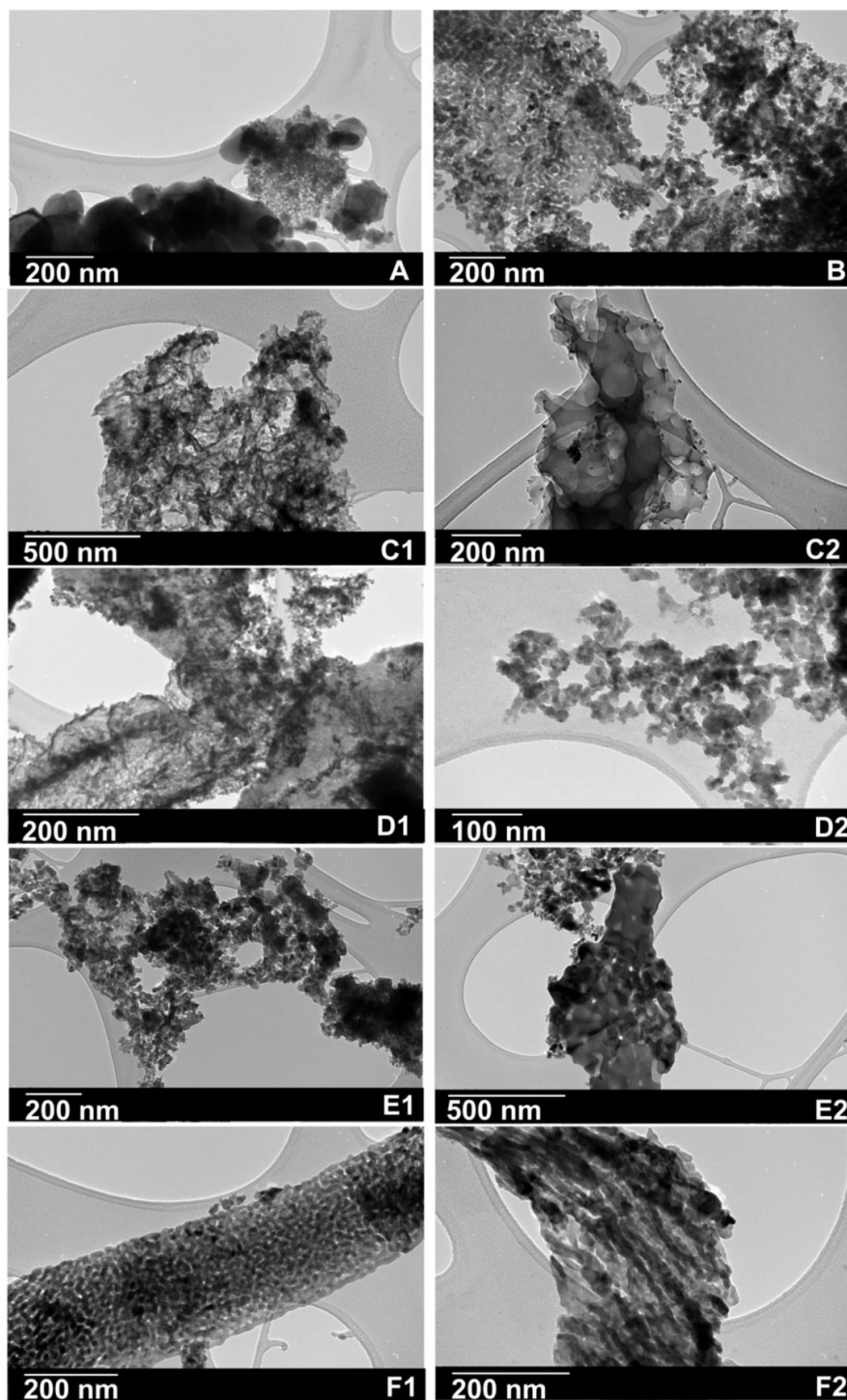
The catalytic activity of all synthesized nanocomposites was subsequently investigated in the microwave-assisted selective oxidation of isoeugenol to vanillin (Scheme 2) at a fixed microwave power (300 W) with a remarkably low catalyst loading of 2.5 mg. Results of conversion and selectivity for the different catalytic systems have been summarized in Table 3, obtaining the optimum results for F-BM-CL with selectivity over 60% to vanillin at *ca.* 90% conversion after 2 minutes reaction. In general, high conversions could be achieved (>87%), with selectivities to vanillin ranging between 42 and 64%, although with each system requiring different reaction times and reaching different temperatures, though of similar order.

Table 3. Catalytic activities of the humins/foams composites in the microwave-assisted oxidation of isoeugenol to vanillin.

	Catalyst	Time (min)	T (°C)	P (PSI)	Conversion (%)	Selectivity (%)
1	F-BM-CL	2.2	169	241	89	64
2	F-BM-NO	4.8	152	246	88	54
3	H-TD-C	4.2	152	246	89	63
4	H-TD-W	3.5	155	244	91	63
5	H-TD-E	5.5	156	247	>99	50
6	H-TD-L	4.7	149	248	>99	42

Reaction conditions: 2.5 mg of catalyst, 0.2 mL isoeugenol, 0.3 mL H_2O_2 (50 wt%), 1 mL acetonitrile, irradiation of 300 W until runaway reaction.

The conversion of isoeugenol with hydrogen peroxide by the humin-iron oxide nanocomposites leads to vanillin as the main reaction product, alongside a plethora of by-products (Scheme 2), comprising vanillin methyl ketone (**1**), isoeugenol diol (**2**), eugenol (**3**), and dihydrodiisoeugenol (**4**), with **1** and **2** being the most

prominent co-products, in order. Similar molecules were reported in the past reports of said reactions.[16,62-64] In particular, the literature on the conversion of isoeugenol to vanillin claimed maximum: (a) 50% yield at 80 °C and 0.4 M of H_2O_2 after 2 hours;[63] (b) 53% yield at 50 °C and 4 bar of O_2 after 24 hours;[16] and (c) 72% yield at 50 °C and 3 bar of O_2 after 24 hours;[64] the nanocomposites reported herein, instead, afford vanillin yields between 42-57% in less than 5 minutes of reactions, although at higher operating temperatures (*i.e.* 149-169 °C). Nonetheless, further optimization of the reaction conditions is needed, as well as a better understanding of the mechanism of reaction.
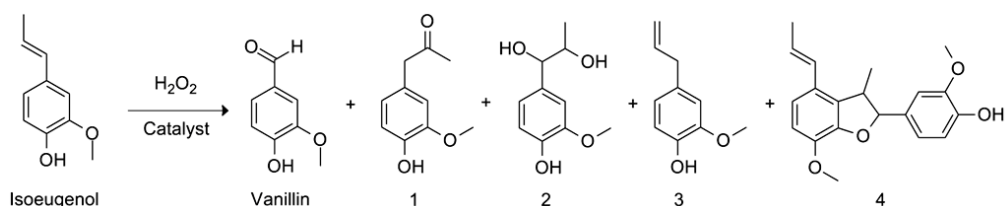
Scheme 2. Reaction scheme of isoeugeneol conversion to vanillin and co-products: vanillin methyl ketone (**1**), isoeugenol diol (**2**), eugenol (**3**), and dihydrodiisoeugenol (**4**), presented in order of magnitude.

By analyzing the reaction products, a mechanistic evaluation might be drafted. Notably, the absence of vanillic acid as co-product with our strong oxidizing conditions (isoeugenol/H_2O_2 ratio: 1:5) and high temperature is rather surprising. Nonetheless, this particular compound was only reported within biotransformations of isoeugenol to vanillin,[55,69] suggesting that both homogeneous and heterogeneous catalytic systems do not promote further oxidation of vanillin to its carboxylic acid form. In fact, kinetic studies on vanadium complexes carried out by Shul'pin research group[63] suggested a faster consumption of isoeugenol compared to vanillin under oxidizing conditions, therefore limiting the formation of vanillic acid. Thus, short reaction times, such as the ones reported

herein, would minimize the formation of higher oxidized products, although a higher temperature is required in order to activate the catalytic material in such small time frame. Moreover, isoeugenol epoxide was not detected among the reaction products, in contrast to the aforementioned reports; this difference with literature can be simply ascribed to the water-rich environment given by the H_2O_2 aqueous solution employed which favors the hydrolysis to the observed corresponding diol (**2**), whereas the previous findings in literature operated in anhydrous environments (O_2 or anhydrous H_2O_2). Furthermore, the production of **4** suggests the formation of radical intermediates of isoeugenol which undergo radical coupling, as supported by previous reports (*e.g.* see ref. 16). However, first row transition metal-catalyzed oxidations with hydrogen peroxide are believed to follow the non-radical oxometal pathway,[32] where H_2O_2 oxidizes the metal centers that eventually coordinate the reagent. Furthermore, the contribution from residual humins must be taken into consideration. In fact, disordered and electron-rich carbon materials have been found to be highly active in the decomposition of hydrogen peroxide into radicals.[70] The synergy between the metal and carbon active sites further complicates the understanding of the overall mechanism governing the reaction; however, the absence of higher condensation or polymerization products may suggest the prevalence of a non-radical mechanism, which can be justified by the higher concentration of iron species on the surface (see XPS spectra). Nonetheless, further kinetic studies are indeed required to further ascertain the mechanism of iron-carbon nanocomposites. As the scope of this work is to prove the employability of humins as carbon source for catalytic purposes, particular focus is given to the selectivity to vanillin throughout this study.

Due to the fixed microwave power employed, resulting in different reaction temperatures and time, the catalytic activity of the nanocomposites cannot be unequivocally ascribed. As an attempt to better compare the catalytic activities, all reactions were performed for 3 minutes with a maximum reachable temperature of 140 °C, with the same catalyst loading, and results are reported in Table 4. A blank test of the reaction (no catalyst) was carried out under these conditions (Table 4, entry 0), also in the solely presence of the humins foams (*i.e.* the support for the F-BM-CL and F-BM-NO nanocomposites) (Table 4, entry 1), and commercial Fe_2O_3 and Fe_3O_4 nanopowders (Table 4, entry 2 and 3, respectively).

Table 4. Catalytic activities of the humins/foams composites in the oxidation of isoeugenol to vanillin under microwave irradiation (300 W), with a maximum temperature of 140 °C.

	Catalyst	Time (min)	T (°C)	P (PSI)	Conversion (%)	Selectivity (%)
0	Blank	3	120*	67	36	<20
1	Foams	3	140	120	91	<20
2	nano-Fe_2O_3	3	140	N/A	25	<20
3	nano-Fe_3O_4	3	140	N/A	28	<20
4	F-BM-CL	3	140	96	76	48
5	F-BM-NO	3	140	103	66	26
6	H-TD-E	3	140	112	66	32
7	H-TD-L	3	140	120	75	47
8	H-TD-W	3	140	107	53	35
9	H-TD-C	3	140	95	60	28

*Temperature results lower due to the absence of a catalytic material.

In general, the results evidenced a moderate to high activity of all nanocomposites under the investigated conditions, improved as compared to the blank reactions. Notably, the humins foams resulted into an incredibly remarkable conversion of >90%, although with low selectivity to vanillin. This is a clear signal that humins, similar to that reported for graphene oxide,[16] possess exceptional oxidation properties thanks to the high presence of electron-rich functionalities. The low selectivity to vanillin might be ascribed to higher H_2O_2 decomposition rates in unselective radical species.

However, an extreme loss of the support at the end of the reaction was observed, suggesting that the humins themselves might undergo oxidation by OH$^\bullet$ species. When the commercial nanopowders were employed (entries 2 and 3), low conversion were obtained (<30%), even lower as compared to the blank reaction in the absence of any catalytic material (36%, entry 0). This could be ascribed to differences in the governing mechanisms, where (i) the solely presence of hydrogen peroxide under microwave irradiation leads to the formation of OH$^\bullet$ species and, thus, fair conversion although unselective; whereas (ii) the commercial nanopowders promote the non-radical oxometal pathway, although resulting ineffective activity under the same reaction conditions. This strongly suggests that a positive synergistic effect must exist between the iron oxide and carbon residues, given by the systematically higher conversions and selectivities of the nanocomposites (Table 4, entry 4-9). Surprisingly, vanillic acid was detected only when nano-Fe_3O_4 (*i.e.* Fe(II) and Fe(III) mixed oxide, *alias* magnetite) was employed. A reason for the over oxidation of vanillin to its carboxylic acid could be given by a possible higher oxidation activity of the Fe(II) species present in the magnetite nanopowder, which further limit the selectivity to vanillin. This speculation is in line with the

proposed mechanism of styrene oxidation by iron(III) nitrate species.[36]

As for the nanocomposites synthesized for this study, F-BM-CL (entry 4) yielded the highest conversion and selectivity to vanillin. This result can be ascribed to the larger presence of highly crystalline hematite in the catalyst, which has been found to be the active iron oxide phase.[71] Comparably, the order of reactivity (in terms of conversion) for the maghemite-hematite mixed phase catalysts was found to be as follows: H-TD-L > H-TD-E > F-BM-NO > H-TD-C > H-TD-W.

According to the findings of Gurol and Lin,[72] hydrogen peroxide activation should be directly proportional to the iron oxide concentration. However, by analyzing the conversion efficiency of the H-series catalysts (Table 4, entries 6-9), the superficial iron concentration (see XPS spectra), and the relative hematite/maghemite concentration (see XRD patterns), a similar trend is evidenced if considering solely the hematite concentration. This suggests that hematite is thus the catalytically active morph of iron oxide. Along these lines, the higher activity of H-TD-L could thus be attributed to the higher hematite content. From a synthetic point of view, the use of a layer (disc) of humins in the synthesis of H-TD-L and H-TD-E has led to better performing catalytic materials, as compared to the use of native humins (namely in the preparation of H-TD-C and H-TD-W). The process of melting and subsequent cooling the humins into a thin layer might induce the polymeric chains to re-orientate in a more crystalline conformation, playing an overall positive effect in the electron transfer ability of the by-products.

Recyclability tests were subsequently conducted for all catalysts, with those presenting magnetic properties included in Fig. 6. A substantial loss of activity (-15% *ca.*) is noted for the H-TD-L and H-TD-C composites, whereas only a very small activity loss (<5%) could be observed for reused H-TD-E material. Comparably, F-BM-NO and H-TD-W fully preserved their initial activity after the first (Fig. 6), illustrating their potential—particularly F-BM-NO and F-BM-CL as highly stable and reusable humin-based oxidation catalysts.
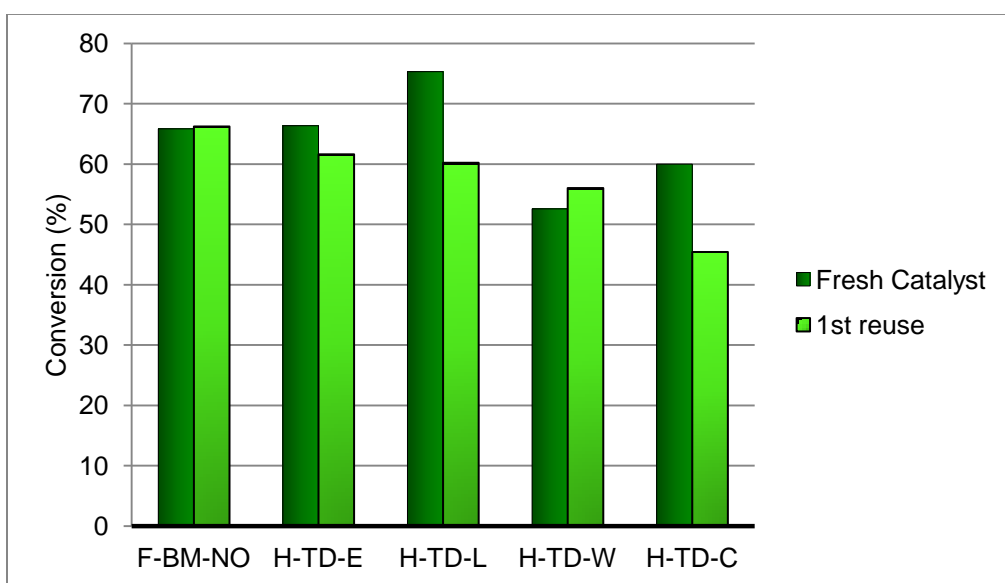
Figure 6. Recyclability tests for the magnetic humins/foams composites.

We believe the stability of F-BM-CL and F-BM-NO systems relates to its mechanochemical synthesis and thus inherent chemical modification of the surface in the final material, in good agreement with previous studies of the group.[48] Additionally, no color change was observed in the final solution/filtrate after recovery of the catalyst, which may indicate a negligible Fe leaching. In contrast, the high stability of H-TD-W may be related to the observed phase transition from maghemite to hematite after reuses (results

not shown). The final solution after reaction was also yellowish, in good agremeent with similar results observed for F-BM-NO. H-TD-W and F-BM-NO were therefore investigated further up to four reuses, with a higher catalyst loading of 50 mg in the same reaction conditions.

Fig. 7 shows conversion and selectivity of the two nanocomposites, F-BM-NO and H-TD-W. To be noted, a higher catalyst loading (20 times higher) did improve the conversion of isoeugenol, but at the expense of the selectivity, in particular for the sample H-TD-W. This could be ascribed to a higher hydrogen peroxide decomposition rate which decreases the selectivity to the aldehyde, while favoring the formation of the co-products, in particular the vanillin methyl ketone (Scheme 2, **1**).
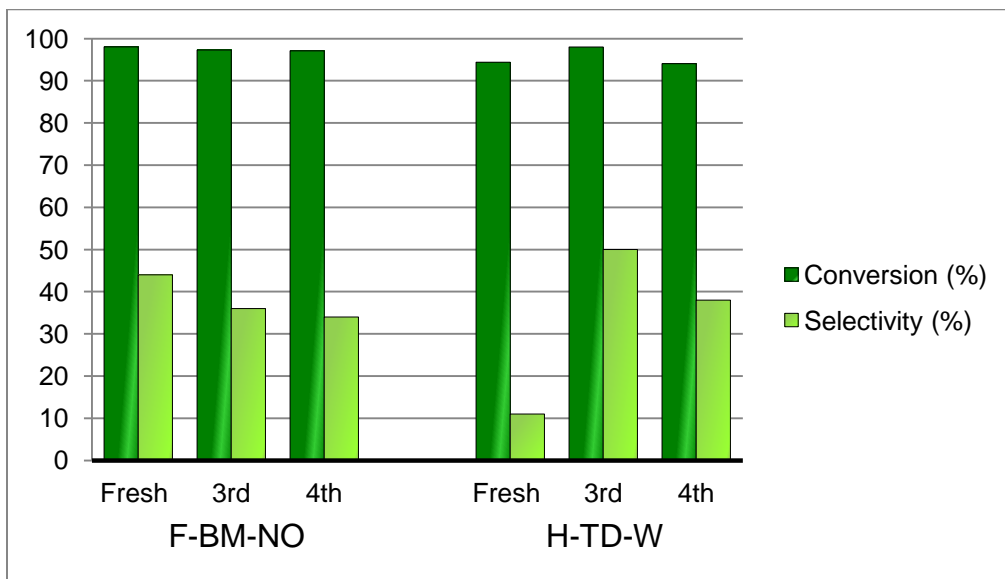
Figure 7. Recyclability runs for F-BM-NO and H-TD-W up to the fourth reuse with increased catalyst loading (50 mg).

At a first glance, an incredible stability can be seen for both of the catalysts; however, a curious behavior has been noted for the H-TD-W composite. In fact, the results of the 4th reuse of H-TD-W

are referred to a spontaneous room temperature reaction (see the video in the ESI†) that occurred when the catalyst entered in contact with the reaction medium. Fe content after reaction (filtrate/reused catalyst) measured by ICP/MS showed negligible leaching (<2 ppm Fe into solution, cumulative after five use) after subsequent reuses, with investigated catalysts (*i.e.* F-BM-NO and H-TD-W) exhibiting an almost Fe content in the 4th reused catalyst as compared to the fresh one (<5% Fe loss after 5 uses).

Overall, not only a satisfactory vanillin yield is obtained, but also the nanocomposites seem to improve its activity with its use. This could be ascribed to a phase rearrangement of the nanocomposites iron oxide phase towards a more active species, *i.e.* hematite, arising from the oxide/peroxide functionalities of the humin residue. Nonetheless, this behavior could represent a breakthrough in both the carbon-based materials (*e.g.* humins) and the catalysis fields.

In any case, further investigations are already ongoing to fully understand and improve the chemical structure, surface and stability of the synthesized humin/iron nanocomposites, alongside the optimization of the reaction conditions for the production of vanillin from lignocellulosic derivatives.

Conclusions

Humins have been generally regarded as undesired by-products in the acid-catalyzed conversion of biomass. This work shows the possibility of employing humins in the preparation of catalytic nanocomposites. All of the composites were prepared *via* solvent-free direct methodologies, in particular: F-BM-CL and F-BM-NO were mechanochemically synthesized via inexpensive ball milling, whereas H-TD-E, H-TD-L, H-TD-W, and H-TD-C *via*

alternative thermal degradation. The use of iron(III) nitrate precursor yielded magnetic composites with mixed iron oxide phases. All of the composites were found to be highly active in the microwave-assisted oxidation of isoeugenol to vanillin, with a particularly high stability after reuses of mechanochemically synthesized nanomaterials. The proposed approach proves the feasibility of producing catalytically active composites from biorefinery waste and may pave the way of a more intensive utilization of biomass-derived waste feedstocks towards their valorization to high added value products.

References

[1] Filiciotto, L.; Balu, A.M.; van der Waal, J. C.; Luque, R. Catalytic insights into the production of biomass-derived side products methyl levulinate, furfural and humins. *Catal. Today* **2018**, *302*, 2-15.

[2] Wu, L.; Moteki, T.; Gokhale, A.A.; Flaherty, D. W.; Toste, F. D. Production of fuels and chemicals from biomass: Condensation reactions and beyond. *Chem* **2016**, *1*(1), 32-58.

[3] Climent, M. J.; Corma, A.; Iborra, S. Conversion of biomass platform molecules into fuel additives and liquid hydrocarbon fuels. *Green Chem.* **2014**, *16*, 516-547.

[4] De, S.; Balu, A. M.; van der Waal, J. C.; Luque, R. Biomass-derived porous carbon materials: Synthesis and catalytic applications. *ChemCatChem* **2015**, *7*(11), 1608-1629.

[5] Pileidis, F. D.; Titirici, M.-M. Levulinic acid biorefineris: New challenges for efficient utilization of biomass. *ChemSusChem* **2016**, *9*(6), 562-582.

[6] Li, M.-F.; Yang, S.; Sun, R.-C. Recent advances in alcohol and organic acid fractionation of lignocellulosic biomass. *Bioresour. Technol.* **2016**, *200*, 971-980.

[7] Avantium. http://www.avantium.com (accessed Feb 15, 2017).

[8] Rice, F. A. H. Effect of aqueous sulfuric acid on reducing sugars. V. Infrared studies on the humins formed by the action of aqueous sulfuric acid on the aldopentoses and on the aldehydes derived from them. *J. Org. Chem.* **1958**, *23*(3), 465-468.

[9] Hoang, T. M. C.; Lefferts, L.; Seshan, K. Valorization of humin-based byproducts from biomass processing—a route to sustainable hydrogen. *ChemSusChem* **2013**, *6*(9), 1651-1658.

[10] Sumerskii, I. V.; Krutov, S. M.; Zarubin, M. Y. Humin-like substances formed under conditions of industrial hydrolysis of wood. *Russ. J. Appl. Chem.* **2010**, *83*(2), 320-327.

[11] van Zandvoort, I.; Wang, Y.; Rasrendra, C. B.; van Eck, E. R. H.; Bruijnincx, P. C. A.; Heeres, H. J.; Weckhuysen, B. M. Formation, molecular structure, and morphology of humins in biomass conversion: Influence of feedstock and processing conditions. *ChemSusChem* **2013**, *6*(9), 1745–1758.

[12] van Zandvoort, I.; Koers, E. J.; Weingarth, M.; Bruijnincx, P.C.A.; Baldus, M.; Weckhuysen, B.M. Structural characterization of ^{13}C-enriched

humins and alkali-treated ^{13}C humins by 2D solid-state NMR. *Green Chem.* **2015**, *17*(8), 4383-4392.

[13] Mija, A.; van der Waal, J. C.; Pin, J.-M.; Guigo, N.; de Jong, E. Humins as promising material for producing sustainable polysaccharide-derived building materials. *Constr. Build. Mater.* **2017**, *139*, 549-601.

[14] van Zandvoort, I.; van Eck, E. R. H.; de Peinder, P.; Heeres, H. J.; Bruijnincx, P. C. A.; Weckhuysen, B. M. Full, reactive solubilization of humin by-products by alkaline treatment and characterization of the alkali-treated humins formed. *ACS Sustainable Chem. Eng.* **2015**, *3*(3), 533-543.

[15] Constant, S.; Lancefield, C.S.; Weckhuysen, B.M.; Bruijnincx, P.C.A. Quantification and classification of carbonyls in industrial humins and lignins by ^{19}F NMR. *ACS Sustainable Chem. Eng.* **2016**, *5*(1), 965-972.

[16] Bohre, A.; Gupta, D.; Alam, M. I.; Sharma, R. K.; Saha, B. Aerobic oxidation of isoeugenol to vanillin with copper oxide dope reduced graphene oxide. *ChemistrySelect* **2017**, *2*(10), 3129-3136.

[17] Tang, X.; Sun, Y.; Zeng, X.; Hao, W.; Lin, L.; Liu, S. Novel process for the extraction of ethyl levulinate by toluene with less humins from the ethanolysis products of carbohydrates. *Energy Fuels* **2014**, *28*(7), 4251-4255.

[18] Lange, J.-P. Renewable feedstocks: The problem of catalyst deactivation and its mitigation. *Angew. Chemie Int. Ed.* **2015**, *54*(45), 13186-13197.

[19] Wang, Y.; Agarwal, S.; Kloekhorst, A.; Heeres, H. J. Catalytic hydrotreatment of humins in mixtures of formic acid/2-propanol with supported Ruthenium catalysts. *ChemSusChem* **2016**, *9*(9), 951-961.

[20] Sheldon, R. A.; Kochi, J. K. *Metal-catalyzed oxidations of organic compounds*; Academic Press: New York, 1981; pp 1-397.

[21] Bäckvall, J.-E. *Modern oxidation Methods*; Wiley-VCH Verlag GmbH & Co.: Weinheim, 2004; pp 1-326.

[22] Roberts, S. M.; Poignant, G. *Catalysts for fine chemical synthesis: Hydrolysis, oxidation and reduction*; John Wiley & Sons: Chichester, 2007; Volume I, pp 1-217.

[23] Tabushi, I.; Yazaki, A. P-450-type dioxygen activation using hydrogen/colloidal platinum as an effective electron donor. *J. Am. Chem. Soc.* **1981**, *103*(24), 7371-7373.

[24] Joergensen, K. A. Transition-metal-catalyzed epoxidations. *Chem. Rev.* **1989**, *89*(3), 431-458.

[25] Sheldon, R. A. The *E* factor 25 years on: the rise of green chemistry and sustainability. *Green Chem.* **2017**, *19*(1), 18-43.

[26] Whitehead, D. C.; Travis, B. R.; Borhan, B. The OsO_4-mediated oxidative cleavage of olefins catalyzed by alternative osmium sources. *Tetrahedron Lett.* **2006**, *47*(22), 3797-3800.

[27] Ranu, B. C.; Bhadra, S.; Adak, L. Indium (III) chloride-catalyzed oxidative cleavage of carbon-carbon multiple bonds by tert-butyl hydroperoxide in water—a safer alternative to ozonolysis. *Tetrahedron Lett.* **2008**, *49*(16), 2588-2591.

[28] Kumar, V. A.; Reddy, P.; Sridhar, R.; Srinivas, B.; Rao, K. R. An improved protocol for the oxidative cleavage of alkynes, alkenes, and diols with recyclable Ru/C. *Synlett* **2009**, *5*, 739-742.

[29] Shaikh, T. M.; Hong, F.-E. Iron-catalyzed oxidative cleavage of olefins and alkynes to carboxylic acids with aqueous *tert*-butyl hydroperoxide. *Adv. Synth. Catal.* **2011**, *353*(9), 1491-1496.

[30] Ghosh, K.; Kumar, P.; Goyal, I. Synthesis and characterization of chromium(III) complexes derived from tridentate ligands: Generation of phenoxyl radical and catalytic oxidation of olefins. *Inorg. Chem. Commun.* **2012**, *24*, 81-86.

[31] Maurya, M. R.; Kumar, N. Chloromethylated polystyrene cross-linked with divinylbenzane and grafted with vanadium(IV) and vanadium(V) complexes having ONO donor ligand for the catalytic activity. *J. Mol. Catal. A.* **2014**, *383-384*, 172-181.

[32] Wójtowicz-Młochowska, H. Synthetic utility of metal catalyzed hydrogen peroxide oxidation of C—H, C—C and C=C bonds in alkanes, arenes and alkenes: Recent advances. *Arkivoc* **2016**, *2017*(2), 12-58.

[33] Urgoitia, G.; SanMartin, R.; Herrero, M. T.; Domínguez, E. Aerobic cleavage of alkenes and alkynes into carbonyl and carboxyl compounds. *ACS Catal.* **2017**, *7*(4), 3050-3060.

[34] Liu, H. L.; Sonn, C. H.; Wu, J. H.; Lee, K.-M.; Kim, Y. K. Synthesis of streptavidin-FITC-conjugated core-shell Fe_3O_4-Au nanocrystals and their application for the purification of CD4^{+} lymphocytes. *Biomaterials* **2008**, *29*(29), 4003-4011.

[35] Armand, M.; Tarascon, J.-M. Building better batteries. *Nature* **2008**, *451*, 652-657.

[36] Pillai, U. R.; Sahle-Demessie, E.; Namboodiri, V. V.; Varma, R. S. An efficient and ecofriendly oxidation of alkenes using iron nitrate and molecular oxygen. *Green Chem.* **2002**, *4*(5), 495-497.

[37] Gonzalez-de-Castro, A.; Xiao, J. Green and efficient: Iron-catalyzed selective oxidation of olefins to carbonyls with O_2. *J. Am. Chem. Soc.* **2015**, *137*(25), 8206-8218.

[38] Tartaj, P.; Morales, M. P.; Gonzalez-Carreño, Veintemillas-Verdaguer, S.; Serna, C. J. The iron oxides strike back: From biomedical applications to energy storage devices and photoelectrochemical water splitting. *Adv. Mat.* **2011**, *23*(44), 5243-5249.

[39] Parkinson, G. S. Iron oxide surfaces. *Surf. Sci. Rep.* **2016**, *71*(1), 272-365.

[40] Pang, Y. L.; Lim, S.; Ong, H. C.; Chong, W. T. Research progress on iron oxide-based magnetic materials: Synthesis techniques and photocatalytic applications. *Ceramics Int.* **2016**, *42*(1A), 9-34.

[41] Arena, F.; Gatti, G.; Stievano, L.; Martra, G.; Coluccia, S.; Frusteri, F.; Spadaro, L.; Parmaliana, A. Activity pattern of low-loaded FeO_x/SiO_2 catalysts in the selective oxidation of C_1 and C_3 alkanes with oxygen. *Catal. Today* **2006**, *117*(1-3), 75-79.

[42] Shi, F.; Tse, M. K.; Pohl. M.-M.; Brückner, A.; Zhang, S.; Beller, M. Tuning catalytic activity between homogeneous and heterogeneous catalysis: Improved activity and selectivity of free nano-Fe_2O_3 in selective oxidations. *Angew. Chem. Int. Ed.* **2007**, *119*(46), 9022-9024.

[43] Schröder, K.; Junge, K.; Bitterlich, B.; Beller, M. Fe-catalyzed oxidation reactions of olefins, alkanes, and alcohols: Involvement of oxo- and peroxo complexes. In *Iron catalysis*; Plietker, B., Ed.; Springer: Berlin, 2011; pp 83-109.

[44] Rak, M. J.; Lerro, M.; Moores, A. Hollow iron oxide nanoshells are active and selective catalysts for the partial oxidation of styrene with molecular oxygen. *Chem. Commun.* **2014**, *50*(83), 12482-12485.

[45] Hong, H.; Hu, L.; Li, M.; Zheng, J.; Sun, X.; Lu, X.; Cao, X.; Lu, J.; Gu, H. Preparation of Pt@Fe_2O_3 nanowires and their catalysis of selective oxidation of olefins and alcohol. *Chem. Eur. J.* **2011**, *17*(31), 8726-8730.

[46] Perathoner, S.; Centi, G. Wet hydrogen peroxide catalytic oxidation (WHPCO) of organic waste in agro-food and industrial streams. *Top. Catal.* **2005**, *33*(1-4), 207-224.

[47] Rajabi, F.; Naresian, S.; Primo, A.; Luque, R. Efficient and highly selective aqueous oxidation of sulfides to sulfoxides at room temperature

catalysed by supported iron oxide nanoparticles on SBA-15. *Adv. Synth. Catal.* **2011**, *353*(11-12), 2060–2066.

[48] Pineda, A.; Balu, A. M.; Campelo, J. M.; Romero, A. A.; Carmona, D.; Balas, F.; Santamaria, J.; Luque, R. A dry milling approach for the synthesis of highly active nanoparticles supported on porous materials. *ChemSusChem* **2011**, *4*(11), 1561-1565.

[49] Shi, F.; Tse, M. K.; Pohl, M.-M.; Radnik, J.; Brückner, A.; Zhang, S.; Beller, M. Nano-iron oxide-catalyzed selective oxidations of alcohols and olefins with hydrogen peroxide. *J. Mol. Catal. A.* **2008**, *292*(1-2), 28-35.

[50] Rajabi, F.; Karimi, N.; Saidi, M. R.; Primo, A.; Varma, R. S.; Luque, R. Unprecedented selective oxidation of styrene derivatives using a supported iron oxide nanocatalyst in aqueous medium. *Adv. Synth. Catal.* **2012**, *354*(9), 1707-1711.

[51] Dignum, M. J. W.; Kerler, J.; Verpoorte, R. Vanilla production: Technological, chemical, and biosynthetic aspects. *Food Rev. Int.* **2001**, *17*(2), 119-120.

[52] Brazinha, C.; Barbosa, D. S.; Crespo, J. G. Sustainable recovery of pure natural vanillin from fermentation media in a single pervaporation step. *Green Chem.* **2011**, *13*(8), 2197-2203.

[53] Cavani, F.; Centi, G. Sustainable development and chemistry. In *Kirk-Othmer Encyclopedia of Chemical Technology*; Ley, C., Ed.; John Wiley & Sons: Chichester, 2011; Chapter 1, pp 1-61.

[54] Hocking, M. B. Vanillin: Synthetic flavoring from spent sulfite liquor. *J. Chem. Educ.* **1997**, *74*(9), 1055-1059.

[55] Hua, D.; Ma, C.; Lin, S.; Song, L.; Deng, Z.; Maomy, Z.; Zhang, Z.; Yu, B.; Xu, P. Biotransformation of isoeugenol to vanillin by a newly isolated bacillus pumilus strain: identification of major metabolites. *J. Biotechnol.* **2007**, *130*(4), 463-470.

[56] Sanchez, S.; Demain, A. l. Enzymes and bioconversions of industrial, pharmaceutical, and biotechnological significance. *Org. Process Res. Dev.* **2011**, *15*(1), 224-230.

[57] Li, K.; Frost, J. W. Synthesis of vanillin from glucose. *J. Am. Chem. Soc.* **1998**, *120*(40), 10545-10546.

[58] Lawless, J. *The Encyclopedia of Essential Oils*; HarperCollins: London, 2002; pp 48-168.

[59] Wangrangsimagul, N.; Klinsakul, K.; Vangnai, A. S.; Wongkongkatep, J.; Inprakhon, P.; Honda, K.; Ohtake, H.; Kato, J.; Pongtharangkul, T.

Bioproduction of vanillin using an organic solvent-tolerant Brevibacillus agri 13. *Appl. Microbiol. Biotechnol.* **2012**, *93*(2), 555-563.

[60] Tan, M. C.; Liew, S. L.; Maskat, M. Y.; Wan Aida, W. M.; Osman, H. Optimization of vanillin production using isoeugenol as substrate by *Aspergillus niger* I-1472. *Int. Food Res. J.* **2015**, *22*(4), 1651-1656.

[61] Kawamoto, H. Molecular mechanisms in the thermochemical conversion of lignins into bio-oil/chemicals and biofuels. In *Production of biofuels and chemicals from lignin*; Fang, Z., Smith, Jr., R. L., Eds.; Springer Science+Business Media Singapore: Singapore, 2016; Volume 6, pp 321-353.

[62] Herrmann, W. A.; Weskamp, T.; Zoller, J. P.; Fischer, R. W. Methyltrioxorhenium: oxidative cleavage of CC-double bonds and its application in a highly efficient synthesis of vanillin from biological waste. *J. Mol. Catal. A* **2000**, *153*(1-2), 49-52.

[63] Gusevskaya, E. V.; Menini, L.; Parreira, L. A.; Mesquita, R. A.; Kozlov, Y. N.; Shul'pin, G. B. Oxidation of isoeugenol to vanillin by the "H_2O_2-vanadate-pyrazine-2-carboxylic acid" reagent. *J. Mol. Catal. A* **2012**, *363-364*, 140-147.

[64] Adilina, I. B.; Hara, T.; Ichikuni, N.; Shimazu, S. Oxidative cleavage of isoeugenol to vanillin under molecular oxygen catalysed by cobalt porphyrin intercalated into lithium taeniolite clay. *J. Mol. Catal. A* **2012**, *361-362*, 72-79.

[65] Anastas, P. T.; Warner, J. C. Green chemistry: Theory and practice. Oxford University Press: New York, 1998; pp 10-55.

[66] Xu, C.; De, S.; Balu, A. M.; Ojeda, M.; Luque, R. Mechanochemical synthesis of advanced nanomaterials for catalytic applications. *Chem. Commun.* **2015**, *51*(31), 6698-6713.

[67] Mija, A. C.; de Jong, E.; van der Waal, J. C.; van Klink, G. P. M. Humins containing foam. WO Patent 2017074183A1, May 04, 2017.

[68] Ojeda, M.; Balu, A. M.; Barrón, V.; Pineda, A.; Coleto, A. G.; Romero, A. A.; Luque, R. Solventless mechnochemical synthesis of magnetic functionalized catalytically active mesoporous SBA-15 nanocomposites. *J. Mater. Chem. A* **2014**, *2*(2), 387-393.

[69] Zhang, Y.; Xu, P.; Han, S.; Yan, H.; Ma, C. Metabolism of isoeugenol via isoeugenol-diol by a newly isolated strain of *Bacillus subtilis* HS8. *Appl. Microbiol. Biotechnol.* **2006**, *73*, 771-779.

[70] Ribeiro, R. S.; Silva, A. T.; Figueiredo, J. L.; Faria, J. L.; Gomes, H. T. The influence of structure and surface chemistry of carbon materials on the decomposition of hydrogen peroxide. *Carbon* **2013**, *62*, 97-108.

[71] Hermanek, M.; Zboril, R.; Medrik, I.; Pechousek, J.; Gregor, C. Catalytic efficiency of iron(III) oxides in decomposition of hydrogen peroxide: Competition between the surface area and crystallinity of nanoparticles. *J. Am. Chem. Soc.* **2007**, *129*(35), 10929-10936.

[72] Gurol, M.; Lin, S.-S. Hydrogen peroxide/iron oxide-induced catalytic oxidation of organic compounds. *J. Adv. Oxid. Technol.* **2002**, *5*(2), 147-154.

Electronic Supplementary Information (ESI)

video-rt reaction ESI.mp4

Video 1. Spontaneous room temperature reaction at the 4th reuse of nanocomposite, H-TD-W.

Chapter 5

Conclusions & Future Outlooks

Conclusions & Future Outlook

It is time to fully understand the effects of our decisions in scientific development on present and especially future generations. By implementing true sustainability through improving resource efficiency, adopting a circular economy, and reducing the amount of energy used or waste generated of a chemical process, both economic and environmental benefits can be obtained. In particular, the use of renewable resources such as plants can reduce some of the alarming effects of pollution, *e.g.* climate change. However, lignocellulosic conversion strategies suffer from the occurrence of side-reactions which limits product yield and thus the resource efficiency of the process. In particular, the formation of polymeric by-products known as humins brings economic concerns in the implementation of biomass valorization strategies. Humins, furthermore, have an ill-defined structure and mechanism which complicates their understanding, minimization, and eventual valorization.

Future trends in the chemical industry need to focus on adding value to any possible (co-)product, residue or heat generated in a process. In this way, not only will valuable resources be conserved but new ways of embracing science into society and innovative products can be established. In this sense, humins can open new possibilities in the field of carbon-based materials. Even if not univocally defined in terms of how they are formed and how they can react, the general information and reactivity trends drawn from several studies can aid finding an application for these by-products. The aim of this thesis was to find orginal ways of identifying the

structural and mechanistic properties of humins, but also to give new lines of research for these polymeric compounds.

Knowing that humins present a conjugated furanic structure, the presence of fluorophoric activity was hypothesised and studied through photophysical studies. Indeed, it was found that humin by-products in solution present three distinct fluorophores depending on structural complexity, with one emitting in the UV region. In particular, longer wavelengths in the emission spectra can be attributed to an extended π-conjugated system which could be used as a signal of formation of complex polyfuranic structures. Simple organic/aqueous separations showed the possibility to separate the UV emitting species so that different applications can be envisioned. For instance, the conjugated system also implies a certain reactivity to electric currents, thus use in organic light-emitting diodes (OLED) could present an option for the valorization of humins. The extensive absorption range of humins can also be applied to the production of photovoltaics, either as is (organic solar cell) or in conjuction with semiconductors (dye-sensitized solar cell), upon study of the quantum yield. The easy separation of the UV emitting species with biphasic solvent systems can instead open new possibilities in the synthesis of carbon quantum dots, which in turn can find applications in bioimaging, sensing, catalysis, supercapacitors, and drug delivery if found safe to human health. Overall, a deeper understanding of the structure complexity of humins has been gained, presenting three species with different complexity in terms of conjugation and size.

To further elucidate the key species involved in the formation of humins, but also the possible reactivity of these molecules, we employed an innovative down-up approach to structural and

mechanistic identification of humins by employing thermal and catalytic conditions to decompose the polymeric structure. The identification of these small molecules shows the occurrence of a series of different mechanisms proposed in literature, and the incorporation of starting materials and (by-)products of the acid-catalyzed hydrolysis of lignocellulosic sugars including levulinates and aromatics. This work changes the perspective from humins being a completely HMF-based polymeric substance to a more heterogeneous structure with many oxygen functionalities, such as esters and acetals. Most importantly, the presence of aromatics not only hints to the formation of humins *via* ring-opening and aromatization to tri-substituted arenes, but also suggests the occurrence of Diels-Alder type reactions of the furanic moieties. Aromatic moieties, in particular, can lead to facilitated electron-transfer which can be correlated to catalytic activity. Nevertheless, the strong reaction conditions-structure depence of humins can generate a certain degree of structure uncertainty for humins. Differences between concentrations of functional groups may be observed, but the knowledge of reactivity of said functionalities can direct preference for certain valorization routes over others.

Thermal treatment of humins could yield aromatic-type systems with plausible catalytic activity, and the presence of reactive oxygen functionalities can act as anchoring points for metal ions towards the creation of organic-inorganic hybrid materials. Based on this supposition, the synthesis of catalytic nanocomposites of humins and metal precursors was studied. In particular, abundant and environmentally-friendly iron-based metal precursors were chosen for the preparation of catalytic systems. Based on the assumption that upon calcination of the humin-containing iron

oxides a series of oxygen functionalities would be present in the nanocomposites, the humin-based catalysts were tested in oxidation reactions, paticularly selective oxidative cleavage assisted by hydrogen peroxide. Remarkably, sole thermally-treated foams were found to be catalytically active although not stable in converting the desired reagent, isoeugenol. Low selectivity for the desired product, vanillin, hints to a different reaction mechanism of humins foams as catalysts, linkely favoring the formation of radicals which may be advantageous in polymerization or mineralization reactions. When combined with iron oxides, humins showed greatly improved catalytic activities of the bare oxides, indicating a synergistic effect between the metal oxide and the humins residue. This finding shows that oxygen-rich carbon residues can positively influence catalytic activities of transition metals. Further, higher stability in reusability tests was observed when already thermally treated humins (*i.e.* foams) were employed: when using reactive carbon materials, double thermal treatment may improve overall composite stability with respect to restructuring and leaching. By combing humins with different metals, a variety of catalytic nanocomposites could be produced with surprising catalytic activities.

Overall, new approaches can and must be applied to bio-derived products given their differences to traditional petroleum chemicals. Shifting from linear alkyl chemistries to cyclic carbonyl ones will open up new routes in product and application development. New strategies to better identify polymeric organic molecules through fluorescence and decomposition are herein proposed, and a route to valorize said compounds to catalytic materials is proved. Future research can take advantage of these results for the eventual production of a plethora of carbon-based materials with photoluminescent and/or catalytic properties. In this

sense, humins can contribute to a new chapter of carbon-based materials with improved properties to the traditional inorganic oxides. This potential is a sign that a circular economy can truly be implemented, and with further efforts sustainability can be achieved.

Appendices

Publications & More

Publications directly derived from the thesis

1. "Catalytic insights into the production of biomass-derived side products methyl levulinate, furfural and humins" by <u>Layla Filiciotto</u>, Alina M. Balu, Jan C. van der Waal, Rafael Luque. *Catal. Today* **2018**, *302*, 2-15.

   JCR Impact Factor
   Impact Factor (2018): 4.888
   Category: Chemistry, Applied
   Quartile (2018): 1   **Rank (2018):** 8/71

2. "Towards the photophysical studies of humin by-products" by <u>Layla Filiciotto</u>, Gustavo de Miguel, Alina M. Balu, Antonio A. Romero, Jan C. van der Waal, Rafael Luque. *Chem. Commun.* **2017**, *53*, 7015-7017.

   JCR Impact Factor
   Impact Factor (2017): 6.29
   Category: Chemistry, Multidisciplinary
   Quartile (2017): 1   **Rank (2017):** 32/172

3. "Benign-by-design preparation of humin-based iron oxide catalytic nanocomposites" by <u>Layla Filiciotto</u>, Alina M. Balu, Antonio A. Romero, Enrique Rodríguez-Castellón, Jan C. van der Waal, Rafael Luque. *Green Chem.* **2017**, *19*(18), 4423-4434.

   JCR Impact Factor
   Impact Factor (2017): 8.586
   Category: Chemistry, Multidisciplinary
   Quartile (2017): 1   **Rank (2017):** 20/172

4. "Biomass promises: A bumpy road to a renewable economy" by <u>Layla Filiciotto</u>, Rafael Luque. *Current Green Chem.* **2018**, *5*(1), 47-59.

   JCR Impact Factor
   Impact Factor (2018): N/A
   Category: Chemistry, Multidisciplinary
   Quartile (2018): N/A   **Rank (2018):** N/A

5. "Nanocatalysis for green chemistry" by <u>Layla Filiciotto</u>, Rafael Luque. In *Encyclopedia of Sustainability Science and Technology*; Meyers, R., Ed.; Springer: New York, 2018.

   JCR Impact Factor
   Impact Factor (2018): N/A
   Category: N/A
   Quartile (2018): N/A   **Rank (2018):** N/A

6. "Reconstruction of humins formation mechanism from decomposition products: A GC-MS study based on catalytic continuous flow depolymerizations" by <u>Layla Filiciotto</u>, Alina M. Balu, Antonio A. Romero, Carlo Angelici, Rafael Luque. *Mol. Catal.* **2019**, *479*, 110564.

   JCR Impact Factor
   Impact Factor (2018): 2.938
   Category: Chemistry, Physical
   Quartile (2018): 2   **Rank (2018):** 67/148

Publications not directly derived from the thesis

1. "Probing the functionality of *nanostructured* $MnCeO_x$ catalysts in the carbon monoxide oxidation: Part II. Reaction mechanism and kinetic modelling" by Francesco Arena, Roberto Di Chio, <u>Layla Filiciotto</u>, Giuseppe Trunfio, Claudia Espro, Alessandra Palella, Lorenzo Spadaro. *Appl. Catal. B* **2017**, *218*, 803-809.

   JCR Impact Factor
   Impact Factor (2017): 11.698
   Category: Chemistry, Physical
   Quartile (2017): 1   **Rank (2017):** 12/147

2. "Valorization of humins-extracted 5-methoxymethylfurfural: Toward high added value furanics via continuous flow catalytic hydrogenation" by Evan Pfab, <u>Layla Filiciotto</u>, Antonio A. Romero, Rafael Luque. *Ind. Eng. Chem. Res.* **2019**, *58*(35), 16065-16070.

   JCR Impact Factor
   Impact Factor (2018): 3.375
   Category: Engineering, Chemical
   Quartile (2018): 1   **Rank (2018):** 33/138

Prizes derived from the thesis

1. *Green Chemistry* Poster Prize at ISGC 2017, La Rochelle, France.

Conference communications

1. Poster "Ballmilling synthesis of iron-based redox catalyst with biorefinery waste template" at Encuentros sobre Nanociencia y Nanotecnología de investigadores y tecnólogos andaluces (NANOUCO VI), Córdoba, Spain, 25-26 January 2017.

2. Poster "Continuous flow hydrogenation of humins" at 4th MC meeting and 3rd Workshop of the FP1306 COST Action, Torremolinos, Spain, 27-28 March 2017.

3. Oral "Towards the hydrothermal carbonization of humins: A preliminary insight into the mechanism" at 1st International Symposium on Hydrothermal Carbon (HTC 2017), London, United Kingdom, 3-4 April 2017.

4. Poster "Partners in crime: Humins and iron as a new catalytic nanocomposites" at Internation Symposium on Green Chemistry (ISGC 2017), La Rochelle, France, 16-19 May 2017.

5. Poster "The humins challenge: Valorization through catalysis" at Amsterdam Chemical Innovation Day (ACID 2017), Amsterdam, The Netherlands, 20 October 2017.

6. Oral "The humins challenge: A catalytic approach" at the 19th Netherlands' Catalysis and Chemistry Conference (NCCC 2017), Noordwijkerhout, The Netherlands, 5-7 March 2018.

7. Poster "The humins challenge: A catalytic approach" at the RSC Twitter Poster Conference (Online), 6 March 2018. https://twitter.com/LaylaFiliciotto/status/971282913210888192

8. Oral "Catalytic approaches for biorefinery's waste valorization: The humins challenge" at 4th International Conference on Bioinspired and Biobased Chemistry and Materials (N.I.C.E. 2018), Nice, France, 14-17 October 2018.

9. Oral "El reto de las huminas: Un enfoque catalítico" at Encuentros sobre Nanociencia y Nanotecnología de investigadores

y tecnólogos andaluces (NANOUCO VII), Córdoba, Spain, 21-22 January 2019.

10. Poster "Hidrogenación en flujo continuo del metil levulinato" at VII Congreso Científico de Investigadores en Formación de la Universidad de Córdoba, Córdoba, Spain, 6-7 February 2019.

11. Poster "Hidrogenación en flujo continuo del levulinato de metilo" at Catálisis para el futuro: Avances en Estructuras, Procesos y Aplicaciones (SECAT '19), Córdoba, Spain, 24-26 June 2019.

12. Poster "Towards a bio-circular economy: Catalysis for humins valorization" at EuropaCat 2019, Aachen, Germany, 18-23 August 2019.

Public outreach activities

1. Participation at the European Researcher's Night 2018 in the *Feria de los Ingenios*, Córdoba, Spain, 28 September 2018.

2. Participation at the Café con Ciencia 2018, Córdoba, Spain, 05 November 2018.

3. Partecipation at the Pint of Science ES 2019, Córdoba, Spain, 22 May 2019.

4. Partecipation as event presenter at the European Researcher's Night 2019 in the *Microcharlas en el Bar*, Córdoba, Spain, 27 September 2019.

Copyright permission

Royal Society Of Chemistry

Author reusing their own work published by the Royal Society of Chemistry

You do not need to request permission to reuse your own figures, diagrams, etc, that were originally published in a Royal Society of Chemistry publication. However, permission should be requested for use of the whole article or chapter except if reusing it in a thesis. If you are including an article or book chapter published by us in your thesis please ensure that your co-authors are aware of this.

Reuse of material that was published originally by the Royal Society of Chemistry must be accompanied by the appropriate acknowledgement of the publication. The form of the acknowledgement is dependent on the journal in which it was published originally, as detailed in 'Acknowledgements'.

Elsevier

ELSEVIER   About Elsevier   Products & Solutions   Services   Shop & Discover   Search

Can I include/use my article in my thesis/dissertation? –

Yes. Authors can include their articles in full or in part in a thesis or dissertation for non-commercial purposes.

Can I use material from my Elsevier journal article within my thesis/dissertation? –

As an Elsevier journal author, you have the right to Include the article in a thesis or dissertation (provided that this is not to be published commercially) whether in full or in part, subject to proper acknowledgment; see the Copyright page for more information. No written permission from Elsevier is necessary.

This right extends to the posting of your thesis to your university's repository provided that if you include the published journal article, it is embedded in your thesis and not separately downloadable.

Acknowledgements

"Find a group of people who challenge and inspire you, spend a lot of time with them, and it will change your life forever"

Amy Poehler, Commencement Speech (Harvard Class of 2011)

Three years have passed by, and still, it feels like a dream. One of those dreams where you wish to never wake up from because no matter what disquieting moment you have experienced, the feelings of accomplishment, growth, and creating meaningful relationships leave you in a state of awe that could last forever.

This PhD has been an incredibly exciting journey: working with something new and barely defined, living in both an academic and an industrial world (and in two countries), travelling for learning and getting inspired from other professionals, continuously improving and mutating yourself into a self-asserted individual. But the reality is that no matter what is the level of independence that one has, we are nothing if not defined by the people around us, particularly the ones that have supported but also challenged you. I have been so lucky during my professional career that the list of the people I would like to thank might be a bit tedious; nonetheless, crucial to whom I am today.

First of all, I would like to thank my university supervisors, Prof. Rafael Luque and Prof. Alina Balu for having chosen little Sicilian me for this PhD position. I would like to thank them for having taught me to always keep trying with patience and without losing hope until your dreams are achieved, constantly improving and building confidence. It was always a great pleasure to be around at the University of Córdoba, with all the amazing visiting students from all over the world (you know who you are!!) and the pillars of the group. Of the research group in particular, I would like to thank Prof. Antonio Romero for being an incredible support to the lab activities, always available to give his advice and assistance, and share a laugh while doing so. At the same university, I would also like to thank Dr. Alfonso Yépez and Dr. Antonio Pineda for having helped me when I was particularly challenged in the lab, sharing their know-how and a series of tricks. Particular thanks also go to my mentee, Evan Pfab, who has courageously accepted the humins challenge and always lightened the mood with a joke or a song. Further, I would like to thank the other (PhD) students for the coffees, lunches, breaks, smiles, tears, and overall support in the department (in no particular order: Alessio, Weiyi, Esther, Daily, Ana,

185

Kenneth, Paloma, Soledad, Noelia, Paulette&Co.). I would like to especially thank Loles and Camilla for being more than colleagues and breakfast companions, building a relation of trust for our future days. Lastly, even if for a brief time, I thank also Prof. Mario Bautista and Dr. Alain Puente for sparking new ideas in the group.

When at the industrial site, I also had the chance to create a sense of association, affiliation and sodality, or, in other words, create a professional family. Out of all, the first man I NEED to thank is Dr. Jan C. "Kees" van der Waal for not only being the one recruiting me for this project but also being a wonderfully challenging manager during most of my time at Avantium. Although at times it might have seemed impossible to get something serious out of him, his outspoken and at the same time in-between-the-lines advice has been a tremendous support in difficult times and an extraordinary mentorship in good times. I want to thank also his "other half", Dr. Gerard van Klink for never backing down from opening more questions to a particular research topic, improving the quality of a publication or patent memo, even without public recognition. Particularly, I want to thank him also for the lunch shows that we have given to the company colleagues by the fast exchange of witty and sometimes politically incorrect observations. With Jan Kees as Statler, Gerard as Waldorf, and me as Miss Piggy, we have created an out of the ordinary trio which can only last a lifetime.

Also directly part of the project, I am incredibly grateful to Dr. Ed de Jong and Dr. Erica Ording for acting as coordinator, manager, and (scientific and non-) challenger. They have supported me greatly in intricate situations, even when it wasn't part of their job description. In particular, Erica has taken the time to help me in the transition from a student to a professional, strengthening my assertiveness and inspiring me to fully conquer the chemical world.

Avantium was also filled with inspiring professionals in all levels of the company, from management to the company-keepers, or even collaborators. Among them, I would like to particularly thank Dr. Carlo Angelici for becoming a friend in a professional setting, and always being available to give feedback and scientific insights. Also, special thanks to Dr. Erik-Jan Ras who has been more than a mentor and inspiration, even if only during a 5-minute break or our travels to EuropaCat. At the latter, I had the chance to bond with the members of the BD team of Catalysis, in particular, Jelle Blekxtoon, Markus Leuenberger (JP!!!) and even for a very brief time Math Lambalk, with whom we have shared wonderful moments and career brainstorms. I am deeply grateful to all of them for having

treated me as part of the team and shared numerous insights and advice. In this category, I would like to thank also Dr. Francesco Acquasanta, Bart vdB, Timothy, Merande, Jorge, Pablo, Rens, Qiaona, Imko, David, Davide (x2), Jagdeep, Lucas etc. for a great time spent together inside and outside the company. Also, big thanks go to Tom Huizinga who has been incredibly open and willing to give career advice to a young professional, but also share his extensive knowledge in the renewable chemical market and classical music. Finally, enormous thanks go to the colleague that became way more than a trusted friend, but also a brainstorming master and sarcastic bomb, future Dr. Matthew Phillips.

As a miscellaneous part of my acknowledgements, I would like to thank the people that have rooted for me during these years, believing I would be where I am today when I had developed some insecurities and doubts. Especially, I want to thank my family who has always demonstrated me that no matter the challenges we are facing, integrity, strength and honesty will take us far and beyond, and together we can only go even farther. You have been essential to who I am today. Also, I will always be grateful to Prof. Francesco Arena, Dr. Giuseppe Trunfio and Dr. Roberto Di Chio for having originally sparked my passion for green chemistry and catalysis. On another note, I would like to thank Simona Consoletti for her kind heart and patience which I could experience both in Spain and the Netherlands. I would then like to thank my forever friends from Cardiff (Regan, Shyam, Nico, Tomas) and Sicily (Esther&Co., Francesca & Teresa, Rosita), but above all Patrycja who is always and will always be there for any aspect of life, but also inspires me to be an exceptionally strong woman who can do anything she wants in life. Also, I would like to thank my personal "truth potato" and mi arbol de la vida (mi familia córdobesa!!) for having helped me in remembering that there is more to life than work, and that being serious is not always a necessity. Further, I would like to thank all the invited participants of the HUGS symposium at the N.I.C.E. conference in 2018, particularly Dr. Rajender Varma for becoming a trusted advisor and friend. Also, I would like to thank Prof. Francesco Mauriello, Prof. Luis Serrano Cantandor, Prof. Juan Carlos Colmenares, Prof. María del Camino Gonzaléz Arellano, and Prof. Clemente Alvarado for their help and support at the end of this PhD programme.

Finally, I want to thank those 4 people who truly understood what I was going through and have supported me but also allowed me to support them during this journey: the HUGS PhD students. Anna with her amazing organisational skills and determination, Anitha with her kindness and

affability, Fatima with her incredible strength and scientific rigour, and Pierluigi with his laid-back attitude and over-the-top availability (hence, tirelessness), they all have represented something more than colleagues and friends, but a true HUGS family (including Rosario, Shelly, Vicky and Ludwig). We have lived and travelled together like a pack of wolves in a "fiery winter", and we have shared undeletable memories. Along with them came all the HUGS supervisors, Prof. Hans de Vries, Prof. Nicolas Sbirrazzuoli, Prof. Alice Mija, Dr. Guy Marlair and Dr. Nathanael Guigo (& Co.) with whom we have created a wonderful network, with a lot of excitement and scientific curiosity, and the aim to grow together while also enjoying lunches and dinners during our schools and meetings. Because, overall, it wasn't only my PhD that needed to be successful but also this beautiful Marie Skłodowska Curie Actions (MSCA) project, HUGS, where we truly wanted to do science for the sake of science itself, curiosity, the environment, and the world. For this, we can only thank the European Commission for believing in innovation, research, and exceptional individuals who can shape the world to be a better place for the coming generations; because, in reality, this is the dream that we will keep on dreaming and making a reality for how much we can.

Grazie, Tack, Gracias, Bedankt, Dziękuję, Dhanyavaad, Ačiū, Merci, Danke, Xie Xie, Shukran, Moteshakeram, Teşekkürler

MSCA-ITN-2015-EID
ID: 675325